IN VIVO MODELLING OF MYELOID HEMATOLOGICAL MALIGNANCIES

WITH COMPLEX KARYOTYPES

My mother Maria who is the biggest blessing in my life, for her restless love and support.

My brother Iakovos for his faith in my skills, constant love and ability to mitigate every problem.

My father who passed away in November 2015 and who would have been proud of this.

IN VIVO MODELLING OF MYELOID HEMATOLOGICAL MALIGNANCIES WITH COMPLEX KARYOTYPES

In acute myeloid leukemia (AML), *TP53* mutations are associated with a subtype known as complex karyotype AML (CK-AML), which is defined by the presence of 3 or more cytogenetic abnormalities and a dismal 5-year survival rate of less than 2% (Papaemmanuil et al., 2016b; Rucker et al., 2012). Functional studies in mice indicate that *p53* inactivation in the hematopoietic compartment can produce chemoresistant malignancies with increased leukemia initiating potential, mirroring key features linked to *TP53* mutations in AML patients (Chen et al., 2014; Zhao et al., 2010; Zuber et al., 2009). However not all *TP53* mutations are created equal, as some mutations have been termed *gain-of-function* (GOF) and have been shown to promote chemoresistance, invasiveness, and/or an epithelial-to-mesenchymal transition and other diverse mechanisms in solid tumors (Freed-Pastor et al., 2012; Olive et al., 2004; Weissmueller et al., 2014).

Here, we identified a gain-of-function (GOF) *p53* mutation that accelerates leukemia initiation beyond p53 loss and, surprisingly, is required for disease maintenance. The $p53^{R172H}$ mutation ($TP53^{R175H}$ in humans) exhibits a neomorphic function by promoting aberrant self-renewal in leukemic cells, a phenotype that is present in hematopoietic stem and progenitor cells (HSPCs) even prior to their transformation. We identified the Forkhead box H1 transcription factor (Foxh1) as a critical mediator of mutant p53

function that binds to and regulates stem cell-associated genes and transcriptional programs. Our results describe a context where mutant p53 acts as a *bona fide* oncogene that contributes to the pathogenesis of CK-AML and suggests a common biological theme for *TP53* gain-of-function in cancer.

CK-AML is also characterized by recurring deletions of chromosomes 7 and 17 (7/del(7q) and 17/del(17p)) which are associated with poor prognosis. However, the presence of functionally relevant tumor suppressors at these chromosomal sites is largely unexplored. Using RNAi we show that reduction in gene dosage of *Ezh2* and *Suz12*, located on 7q36.1 and 17q11.2 respectively, cooperate with loss of p53 and Mll3, a previously shown tumor suppressive gene on chromosome 7q36.1, to promote leukemogenesis. Ezh2 and Suz12 suppression enhance self-renewal of HSPCs, and similarly to the human 7/del(7q) and 17/del(17p) AMLs, the derived leukemias are refractory to conventional chemotherapy. Hence, our mouse model suggests that Ezh2 and Suz12 are putative tumor suppressive genes in p53-deficient AML and can contribute to leukemia without being mutated but rather lost via chromosomal aberrations.

Altogether we have developed models of CK-AML in mice that were not available in the past. We propose to use these leukemias, which faithfully recapitulate the human disease, to better understand the complexity and molecular composition of AML as well as to use this as a preclinical platform for drug discovery.

BIOGRAPHICAL SKETCH

X grew up in Cyprus and attended the National and Kapodistrian University of Athens in Greece where she did her undergraduate dissertation project on the Familial British and Danish Dementias. There she worked in the laboratory of Dr. Spyros Efthimiopoulos elucidating the mechanism underlying the homodimerization of BRI2, a cell surface protein associated with these diseases.

Following the completion of her undergraduate degree she obtained her Masters in Science (MSc) from the University College London (UCL). There she completed her thesis work on a form of targeted therapy called antibody-directed enzyme prodrug therapy (ADEPT) applied in pancreatic cancer under the supervision of Dr. Barbara Padley.

With her Masters completed she decided to move to the United States where she joined the laboratory of Dr. Iannis Aifantis at NYU as a research technician where she co-authored several scientific papers.

In 2013 X was accepted by the Weill Cornell Graduate School of Medical Sciences and joined the laboratory of Dr. Scott W. Lowe the following year. She has been supported by the Dorris J. Hutchison Fellowship Award during her studies.

ACKNOWLEDGMENTS

I thank my thesis mentor Dr. Scott W. Lowe for giving me the opportunity to be part of his laboratory where numerous great scientists have trained from around the world. I want to thank him for his guidance, patience and kindness throughout the five years I spent in his lab. He let me fail and succeed so that I would become a stronger and more independent woman and scientist than I was when I walked into his lab. He allowed me to learn not only from him but also from the extraordinarily enriching environment he has cultivated inside the lab.

He has encouraged me to be critical of my scientific discoveries and taught be to be rigorous, yet he was always the first to remind me of all that I had accomplished at difficult moments. He fostered my enthusiasm to talk about my science and invited me to the p53 workshop (Singapore, 2017), an HHMI Science Meeting (Washington DC, 2016) and gave me numerous opportunities to present my work at other local meetings with collaborators.

The most precious gift he has given me though is meeting the extraordinary people from his lab, current or past:
Cory Rillahan for being my first mentor in the lab, Lukas Dow for making me feel part of the Lowe lab when I joined, Darjus Tschaharganeh for being my friend, Ana Banito for being an invaluable advisor and the best roommate, Geulah Livshits for her invaluable help on the project during the early years of my PhD and for being a great friend, Direna Alonso-Curbelo for her enthusiasm about science which is contagious, all the technicians in the Lowe lab but mostly May Chalarca, Wei Luan, Anahi Tehuitzil, Sha Tian, Sarah Ackerman, and Janelle Simon, Katerina Chatzi who was an amazing friend, fellow Greek and an excellent collaborator, Chi-Chao Chen for being funny at difficult moments and sharing the PhD experience together, Sean Chen, Timour Baslan, Grace Xiang Li for all the chocolate at key moments, Amanda Kim, Ted Kastenhuber for sharing the PhD experience and enthusiasm for p53 biology, Mei-Ling Li for being a great listener and friend, Riccardo Mezzadra for pushing me to run longer and faster, Scott Millman for being together in the blood group, Paul Romesser, Stella Paffenholz for sharing the PhD experience together, Marcus Ruscetti, Pancho Barriga for being an excellent friend, Francisco Sanchez-Rivera who advised me, supported me and became one of my closest friends, Kaloyan Tsanov for being the best bay mate and made me laugh on a daily basis, Corina Amor Vegas, Leah Zamechek, Zhen Zhao, Kiki Liu for sharing her leukemia expertise, Eusebio (Chebi) Manchado for advising me and helping me when I started, Allison Mayle, Kevin O'Rourke, Jose Reyes for being an excellent bay mate, John P. Morris IV for always making time to help me and give me advice, Anne Trumble and Lynn Boss for always having our back

in the lab. Lastly I want to thank Ray (Jui-Yu) Ho who listened, helped and fixed everything bioinformatically related with love and patience.

I appreciate the consistent insight that I have been receiving from my thesis committee members Ross Levine, Scott Armstrong and Omar Abdel-Wahab, as well as the additional newer members Lukas Dow and Carol Prives. Their comments, criticism and advice always pushed me one step further.

I would also like to thank additional people that have taken the time to share their knowledge on a subject or technique, provided me with useful reagents, tools and methods, edited my work and gave me critical advice that shaped my project. I have greatly enjoyed our interactions in these years. These people are: Charles Sherr for believing in me, constructively criticized my science and helped me to write my paper, Yadira Soto-Feliciano, Viraj Sangvi, Yilong Zou, Maria Skamagki, Javier Carmona, Olga Guryonova, Gina DeNicola, Bryan King, Richard Koche, Benjamin Durham, Shannon Buckley, Chun-Hao Chen, Wouter Karhaus, Eunhee Kim, Akihide Yoshimi, Jiajun Zhu and Alejandra Mendoza.

I especially want to thank Andy Koff for believing in my abilities and allowing me to be part of the BCMB program. A special thanks to Denisse Jenkins for her effort to ensure the completion of the PhD.

From beginning to end, I am very grateful to all of the Weill Cornell Medicine Graduate School, BCMB program and the Sloan Kettering Institute for the recourses, support and the amazing opportunity to train in this phenomenal academic environment. I consider this to be my biggest achievement so far and I will always be a proud alumnus.

I would thank to thank all of my supportive and loyal friends, but mostly Josef Leibold who has been one of the best friends I have made in the 8 years I have lived in NY and who loved and supported me like very few other people in my life. Last but not least I would like to thank Maria Ruano-Guillamot who was always there with love and understanding no matter the circumstances and kept me happy at difficult times.
Lastly, I would to thank Iannis Aifantis who gave me the opportunity to work in his lab where I learned to do science. He encouraged and fostered my love for research and he kept his promise of continuous and increasing support through the years.

I would also like to thank my boyfriend Jhimmy Talbot for loving me and believing in me and for inspiring me with his work ethic to want to be better day after day.

TABLE OF CONTENTS

LIST OF FIGURES

Figures were created with BioRender

LIST OF TABLES

LIST OF ABBREVIATIONS

AML: Acute Myeloid Leukemia

CNV: Copy Number Variation

CK-AML: Complex Karyotype Acute Myeloid Leukemia

DNMT3a*:* DNA-Methyltransferase 3A

FLT3-ITD: Fms-Like Tyrosine Kinase 3

NPM1: Nucleophosmin 1

TET2: Tet Methylcytosine Dioxygenase 2

IDH1/2: Isocitrate Dehydrogenase

CEBPA: CCAAT/enhancer-binding protein alpha

TSG: Tumor Suppressor Gene

LOH: Loss of heterozygosity

m/hESCs: mouse and human Embryonic Stem Cells

PRC2: Polycomb Repressive Complex 2

EZH1/2: Enhancer of Zeste Homolog 1/2

SUZ12: Suppressor of Zeste Homolog 12

MDS: Myelodysplastic Syndrome

PMF: Primary Myelofibrosis

INTRODUCTION

Genetics, Treatment, and Classification of Acute Myeloid Leukemia

Acute Myeloid Leukemia (AML) is a type of hematological malignancy that leads to the uncontrolled expansion of abnormally differentiated cells called blasts that infiltrate the bone marrow, peripheral blood and other organs of patients (Dohner et al., 2015). Despite the fact it has been more than two hundred years since the disease was first described by Peter Cullen as a disease that gave rise to “milky blood” (Cullen, 1811) the cure for patients over 60 years of age is still very low (5-15%) (Dohner et al., 2010).

The gold standard for patients with AML is to undergo induction therapy with the goal of achieving complete remission (CR). Unfortunately, relapse because of minimal residual disease (MRD) is very common and will lead to discontinuation of the treatment. For this reason, treatment of AML begins with induction therapy, that upon a positive outcome is then followed by a consolidation therapy in order to eliminate MRD and achieve long lasting remission. Induction therapy consists of the ‘7+3’ regimen, which combines 7 days of continuous infusion cytarabine with 3 days of anthracycline (De Kouchkovsky and Abdul-Hay, 2016). This is normally given to patients with an intermediate or favorable prognosis (Estey, 2014). Induction regimens use daunorubicin (60 or 90 mg/m^2), or idarubicin (12 mg/m^2) with similar responses (Estey, 2014; Gong et al., 2015; Li et al., 2015). Cytarabine is normally given at 100–200 mg/m^2 daily. Some studies have shown increased efficacy of cytarabine at higher doses, yet this is generally given to patients with refractory disease since at induction the therapeutic benefit is small and presents with increased toxicity (De Kouchkovsky

and Abdul-Hay, 2016). Other drugs such as combination of fludarabine, cytarabine, G-CSF and idarubicin (FLAG-IDA), have also been used as alternative to standard induction regimens and lead to similar CR rates and OS overall but more patients achieve CR after a single course (Burnett et al., 2013).

Despite the advances in treating AML, there is a lack of optimal treatment options for elderly patients (> 65 years old), which account for more than half of the patients with AML (Thein et al., 2013). These patients are also more likely to present a disease profile with an adverse cytogenetic-risk, lack of response to chemotherapy which often also leads to increased treatment-related toxicities. In 2012, a randomized trial of the hypomethylating agent decitabine compared to supportive care or low-dose cytarabine in elderly patients showed a significant improvement in OS (Kantarjian et al., 2012), yet similar studies have observed conflicting results (Dombret et al., 2015). The use of hypomethylating agents in older individuals is promising, but it fails to achieve durable responses especially in those patients with cytogenetic abnormalities and with mutations in *TP53* discussed in more detailed below.

Patients with AML used to be diagnosed and classified based on conventional morphologic and cytochemical features (Bennett et al., 1976). However, with the advent of high throughput sequencing we now recognize the enormous molecular heterogeneity of the disease in addition to the cytogenetic one that had been recognized many years prior (Dohner et al., 2010). Although these molecular markers are important because of their clinical relevance, they have also been insightful for the pathogenesis of the disease

and have led to the development of novel targeted therapies, albeit not to a satisfactory degree.

In 2010, the European LeukemiaNet (ELN) developed a system that combined genetic abnormalities with cytogenetics and mutation analyses together with prognostic outcomes (Dohner et al., 2010). This system led to the creation of four genetic groups: favorable, intermediate-I, intermediate-II, and adverse (Dohner et al., 2010). For example, sole NPM1 mutations or CEBPA mutations are classified as favorable as well as patients that have t(8;21)(q22;q22) or RUNX1-RUNX1T1 related chromosomal aberrations. All other FLT3-ITD/NPM1 mutation combinations are considered to have intermediate-1 genetic risk (Rollig et al., 2011).

The group with the adverse prognosis in AML is the group that exhibits more than three acquired chromosomal aberrations and it is called complex-karyotype AML (CK-AML) (Papaemmanuil et al., 2016b) (Table 1). These patients are almost exclusively characterized by mutations in the *TP53* gene (Rucker et al., 2012), which when presented together with a complex-karyotype confer an even worse prognosis (Papaemmanuil et al., 2016b).

Table 1 Prognostic Groups in AML (Papaemmanuil et al., 2016a)

Genomic Subgroup	Frequency in the Stud Cohort (N = 1540)	Most Frequently Mutated Genes* no. of patients (%) gene (%)
AML with NPM1 mutation 418 (27)	418 (27)	NPM1 (100), DNMT3A (54), FLT3ITD (39), NRAS (19), TET2 (16), PTPN11 (15)
AML with mutated chromatin, RNA-splicing genes, or both† 275 (18)	275 (18)	RUNX1 (39), MLLPTD (25), SRSF2 (22), DNMT3A (20), ASXL1 (17), STAG2 (16), NRAS (16), TET2 (15), FLT3ITD (15)
AML with TP53 mutations, chromosomal aneuploidy, or both‡	199 (13)	Complex karyotype (68), −5/5q (47), −7/7q (44), TP53 (44), −17/17p (31), −12/12p (17), +8/8q (16)
AML inv(16)(p13.1q22) or t(16;16)(p13.1;q22); CBFB–MYH11	81 (5)	inv(16) (100), NRAS (53), +8/8q (16), +22 (16), KIT (15), FLT3TKD (15)
AML with biallelic CEBPA mutations	66 (4)	CEBPA biallelic (100), NRAS (30), WT1 (21), GATA2 (20)
AML t(15;17)(q22;q12); PML–RARA	60 (4)	t(15;17) (100), FLT3ITD (35), WT1 (17)
AML with t(8;21)(q22;q22); RUNX1–RUNX1T1	60 (4)	t(8;21) (100), KIT (38), −Y (33), −9q (18)
AML with MLL fusion genes; t(x;11)(x;q23)	44 (3)	t(x;11q23) (100), NRAS (23)
AML with inv(3)(q21q26.2) ort(3;3)(q21;q26.2);GATA2, MECOM(EVI1)	20 (1)	inv(3) (100), −7 (85), KRAS (30), NRAS (30), PTPN11 (30), ETV6 (15), PHF6 (15), SF3B1 (15)
AML with IDH2R172 mutations and no other class-defining lesions	18 (1)	$IDH2^{R172}$ (100), DNMT3A (67), +8/8q (17)
AML with t(6;9)(p23;q34); DEK–NUP214	15 (1)	t(6;9) (100), FLT3ITD (80), KRAS (20)
AML with driver mutations but no detected class-defining lesions	166 (11)	$FLT3^{ITD}$ (39), DNMT3A (16)
AML with no detected driver mutations	62 (4)	
AML meeting criteria for ≥2 genomic subgroups	56 (4)	

* Genes with a frequency of 15% or higher are shown in descending order of frequency. Key contributing genes in each class are shown in boldface type.
† Classification in this subgroup requires one or more driver mutations in RUNX1, ASXL1, BCOR, STAG2, EZH2, SRSF2, SF3B1, U2AF1, ZRSR2, or MLLPTD. In the presence of other class-defining lesions, namely, inv(16), t(15;17), t(8;21), t(6;9), MLL fusion genes, or complex karyotype or driver mutations in TP53, NPM1, or CEBPA biallelic, two or more chromatin spliceosome mutations are required.
‡ Classification in this subgroup requires TP53 mutation, complex karyotype, or in the absence of other class-defining lesions, one or more of the following: −7/7q, −5/5q, −4/4q, −9q, −12/12p, −17/−17p, −18/18q, −20/20q, +11/11q, +13, +21, or +22.
Multiple fusion partners for MLL were found, clinical implications depended on the specific partner.

Complex-Karyotype AML

From studies analyzing the impact of cytogenetics on clinical outcome in AML it became obvious that certain chromosomal abnormalities were associated with this disease and predicted a poor survival. These abnormalities mostly affected in decreasing order of occurrence, chromosome arms 5q, 17p, 7q, 18q, 16q, 17q, 12p, 20q, 18p and 3p, and also the less frequent chromosomal gains of 8q, 11q, 21q, 22q, 1p, 9p, and 13q (Mrozek, 2008). Overall, the molecular consequences of these recurrent chromosomal losses and gains of specific chromosomes in AML patients with complex karyotypes are poorly understood. However, some genes that reside on these regions have been identified as genes that might have a role in the disease. Beyond *TP53* that has been long recognized as a TSG, other putative tumor suppressors such as α-catenin (*CTNNA1*) on 5q31 (Liu et al., 2007), *NF1* on 17q11 (Rucker et al., 2006), *SPRY4* on 5q31.3 (Zhao et al., 2015), *MLL3 (KMT2C)* on 7q36.1 (Chen et al., 2014) and *EGR1* on 5q31.2 (Joslin et al., 2007) have been described to contribute to leukemogenesis when they are decreased in expression.

The Lowe laboratory has used some of these genes in combination as a proxy to the chromosomal deletions that happen in patients and has shown that some of these genes are bona fide tumor suppressor genes. In the absence of *p53* and *Nf1*, both *Mll3* (Chen et al., 2014) and *Spry4* (Zhao et al., 2015) down regulation by shRNAs cooperate *in vivo* (Figure 1A) and give rise to AML that exhibits complex karyotype unlike leukemias that are $p53^{WT}$ (Figure 1B).

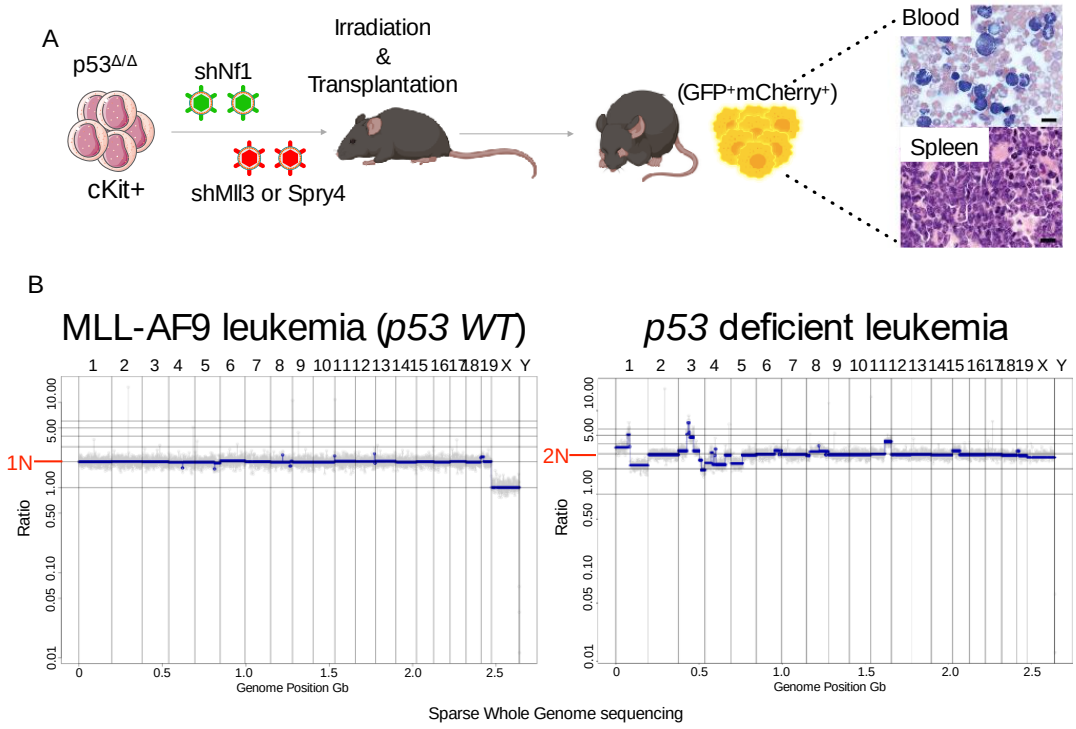

Figure 1 Murine Complex Karyotype AML (CK-AML) model.

(A) Schematic representation of generating murine CK-AML by co-transduction of cKIT+ p53Δ/Δ cells with shRNAs against Nf1 (GFP) and Mll3 or Spry4 (mCherry). The cells are transplanted in lethally irradiated mice and the disease that arises is double positive (DP) GFP+mCherry+ that infiltrates the spleen and the peripheral blood of the mice (Adapted from (Chen et al., 2014)). (B) Low-pass genome sequencing of MLL-AF9 driven murine leukemia (left) and p53 deficient murine leukemia (right).

These two mouse models are currently the only CK-AML murine models and despite their caveats, one being the fluorescence on the hairpins that renders them immunogenic to some extent, they are still essential for understanding molecularly the pathogenesis

of this disease. Creating better tools and models in the lab would be essential in developing effective drugs for these patients.

The tumor suppressor gene TP53

The renowned developmental biologist Artavanis-Tsakonas of Harvard Medical School, once said: ‘There are two types of scientists; the ones that work on Notch and the other ones that don’t know they work on Notch yet’. He was referring to the highly conserved signaling pathway that controls a bewildering number of biological functions in animals. The same however could be said about p53. *TP53* is by far the most studied gene in cancer biology not only because it controls a plethora of tumor suppressive functions but also because it is the most highly mutated gene in cancer.

p53 is a sequence-specific transcription factor which contains two N-terminal transactivation domains, a proline rich domain, a central DNA binding domain, and a C-terminus that includes its nuclear localization signals and an oligomerization domain needed for transcriptional activity (Laptenko and Prives, 2006). The most well characterized functions of p53 include its ability to promote cell cycle arrest and apoptosis by transcriptional transactivation of genes such as *p21 (CDKN1A)* and *Bax* respectively (el-Deiry et al., 1994; Marzo et al., 1998) (Figure 2). Upon different types of stresses such as oncogene activation, p53 has also been shown to induce cellular senescence, which is considered to be a more stable cell cycle arrest program that involves the cell cycle inhibitor p16 (Serrano et al., 1997) (Figure 2). The quality or quantity of the stress is thought to dictate these differential responses, but this is still an active field of investigation.

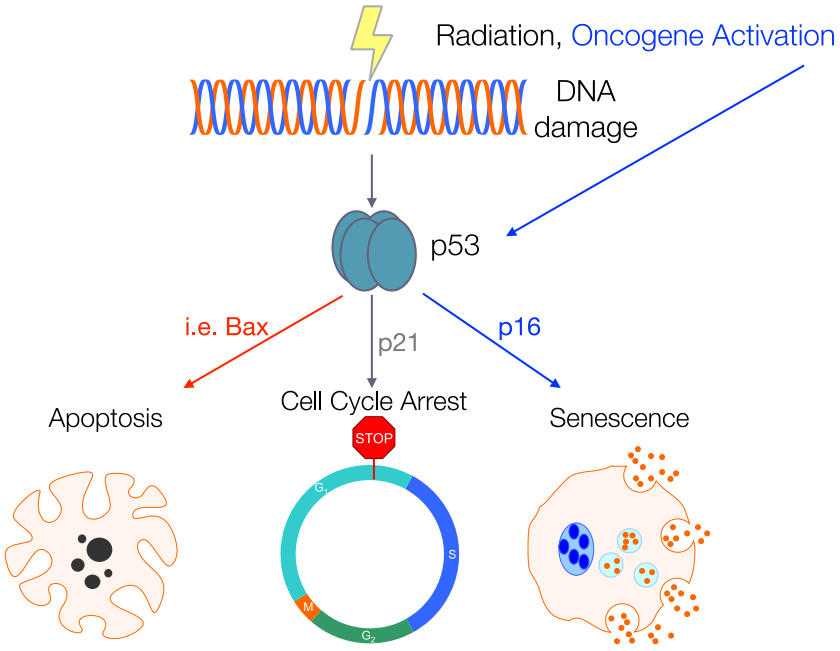

Figure 2 The TP53 tumor suppressive pathway.

Upon DNA damage that can be induced by different stimuli such as irradiation or oncogene activation, p53 gets stabilized and it can transcriptionally activate different targets that can lead to apoptosis (i.e. Bax), cell cycle arrest (i.e. p21) or senescence (i.e. Rb).

The protein was initially discovered in 1979 as a 53 kD host protein bound to the large T antigen of the simian virus 40 (SV40) transformed cells (Lane and Crawford, 1979; Linzer and Levine, 1979). It was also observed that many tumors accumulated high levels of p53, something that is not observed in normal tissues, suggesting that p53 might be an oncogene or have pro-oncogenic effects (Bartek et al., 1990b; DeLeo et al., 1979; Rotter, 1983) (Figure 3A). This idea was reinforced when ectopic expression of

a p53 cDNA was shown to cooperate with oncogenic RAS to transform primary cells in culture (Eliyahu et al., 1984; Parada et al., 1984) (Figure 3B). Furthermore, overexpression of p53 was demonstrated to increase tumorigenicity in otherwise p53-null cells (Wolf et al., 1984). And therefore, because of the erroneous utilization of a cancer cell line expressing a mutant form of p53, the gene was thought to be a proto oncogene for the first decade of its discovery (Freed-Pastor and Prives, 2012).

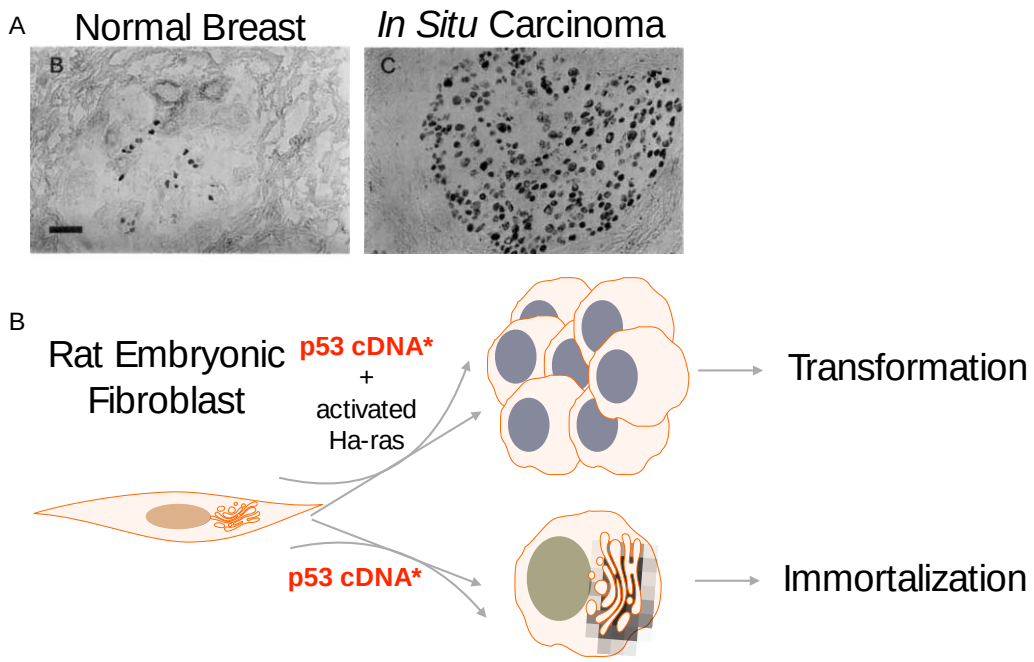

Figure 3 Mutant p53 as an oncogene

A. Expression of p53 in normal tissue of the breast (left) and in in situ Carcinoma (right) (Bartek et al., 1990a). B. Overexpression of p53 in rat embryonic fibroblasts lead to transformation in cooperation with Ha-ras and immortalizations of the cells when overexpressed alone

Subsequent work corrected the initial classification of p53 as an oncogene and showed that wild-type p53 suppresses growth and oncogenic transformation (Baker et al., 1990a; Finlay et al., 1989) and, very importantly, inactivating mutations targeting both *TP53* alleles are a very frequent event in human tumors (Baker et al., 1990b). Some of the strongest data to support the tumor suppressive functions of p53 were generated when the *Trp53* knockout mice were shown to develop tumors with very high penetrance (Donehower et al., 1992).

TP53 mutations occur in their majority on the DNA binding domain and the overwhelming majority of these are missense mutations (Figure 4). Some mutations occur in an extraordinary frequency and can vary to some extent from tissue to tissue (reviewed by (Kastenhuber and Lowe, 2017). These so-called "hotspot" mutations have been shown to exert a dominant-negative effect when they occur in cells with a wild-type allele by inhibiting the canonical p53 functions such as cell cycle arrest and apoptosis (Willis et al., 2004). However, these mutations are more commonly presented in the absence of a wild-type allele (hemizygous mutations). The loss of the wild-type allele (LOH) has been shown to occur very frequently after chromosomal aberrations that lead to loss of 17p where *TP53* resides (Tamada et al., 1994; Tomita et al., 2004).

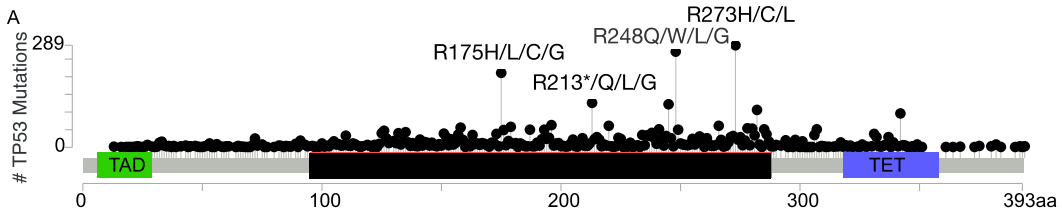

Figure 4 TP53 mutations in cancer patients.

Missense Mutations, Truncating Mutations: Nonsense, Nonstop, Frameshift deletion, Frameshift insertion, Splice site, Inframe Mutations: Inframe deletion, Inframe insertion, Other Mutations: All other types of mutations. MSK-IMPACT (Zehir et al., 2017))

In the 1990s it was shown that some missense *TP53* mutations have gain-of-function (GOF) properties. For example, patients with Li-Fraumeni syndrome that are predisposed to a hereditary cancer syndrome because of *TP53* germline mutations, they would develop tumors even nine years prior to patients that had loss of function (LOF) (i.e. truncating mutations) p53 mutations (Bougeard et al., 2008). Experimentally several groups, including Arnold Levine's group, showed that overexpressing murine or human mutant p53 proteins, in cells lacking endogenous p53 protein, increased tumorigenic potential in nude mice and enhanced plating efficiency in agar cell culture (Dittmer et al., 1993).

Moreover, it was shown that only mice expressing a *p53* mutant allele developed metastases in a model of rhabdomyosarcoma, in line with other models such as pancreatic ductal adenocarcinoma (Morton et al., 2010) and squamous cell carcinoma (Caulin et al., 2007) where the incidence of metastasis was much higher in the presence of the mutant protein compared to the tumors that did not express p53. Furthermore, mouse models engineered to express two of the most common hotspot mutations observed in human tumors (R172H and R270H corresponding to R175H and R273H in

patients) developed a higher incidence of carcinomas compared to *p53* deficient mice (Olive et al., 2004).

Mutant p53 has also been shown to cooperate with EGFR to enhance EMT in human esophageal cells and overcomes EGFR-mediated senescence (Ohashi et al., 2010). Not surprisingly and in addition to all other functions attributed to mutant p53 and its GOF effects, it can also augment cell proliferation, which has been shown both *in vitro* as well as in vivo (Duan et al., 2008) as well as induce chemoresistance (Do et al., 2012). Furthermore several groups have also shown that these mutant proteins rewire the metabolic output of tumor cells and therefore alter their adaptation and survival abilities (Freed-Pastor et al., 2012; Humpton et al., 2018) (Figure 5).

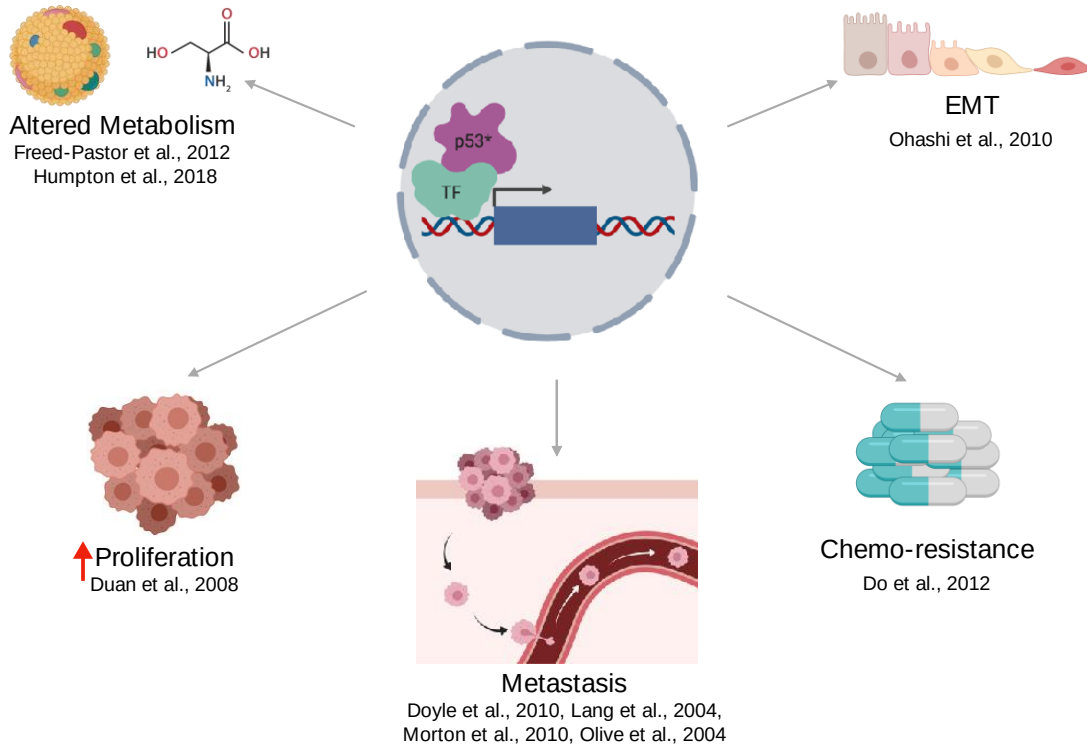

Figure 5 Functions of mutant p53

The molecular mechanisms that have been proposed for the GOF are various and include interaction of mutant p53 with other transcription factors such as ETS1/2, NF-Y, and the p53 family members p63 and p73 (Di Agostino et al., 2006; Weissmueller et al., 2014; Zhu et al., 2015). While the precise nature of how p53 alters transcription remains open for debate, multiple lines of evidence indicate it can augment the metastatic potential of tumors.

TP53 in stem cells and development

Interestingly, mice with genetic loss of p53 develop normally despite the evidence for a role of p53 in the regulation of stem cells (Donehower et al., 1992). Currently there is little knowledge on how p53 is mediating these effects in stem cells and whether it is through its transcriptional function or through another activity.

John Gurdon in the ‘70s tried to transplant nuclei from differentiated cells of a tadpole into the egg of Xenopus laevis, an experiment that failed many times until they passaged the nuclei through the egg and early embryo and only then they succeeded in producing a normal tadpole (Gurdon, 1973). As suggested in these early studies this preconditioning of the nuclei might have been an “epigenetic” priming that allowed the developmental program necessary for this process to occur. Based on those experiments and many that followed, including the legendary Yamanaka experiment in which mouse embryonic fibroblasts were infected to overexpress four transcription factors (Oct-4. Sox2, Klf-4 and c-Myc), we now know that “induced pluripotency” exists (Takahashi and Yamanaka, 2006). Since 2006, these induced pluripotent stem (iPS) cells have

become the subject of interest for a plethora of laboratories across the world because of their clinical potential in regenerative medicine.

The role of p53 in iPS formation was examined and in 2009 five papers were published in *Nature* showing that loss of p53 enhances re-programming from 0.01% to 80% while expediting the process that normally takes 2 weeks to just 3 days (Banito et al., 2009; Hong et al., 2009; Kawamura et al., 2009; Marion et al., 2009; Utikal et al., 2009). Their findings had huge implications on the understanding of stem cell biology as it showed clearly the antagonistic relationship between stemness and tumor suppression. These papers suggested that the p53 pathway existed in stem cells to inhibit their formation from their differentiated counterparts and to ensure a unidirectional program during development. Interestingly GOF p53 mutants have been shown to enhance further the efficiency of the reprogramming process compared with p53 deficiency albeit leading to the formation of aggressive tumors and once again suggesting the differential roles of the hotspot mutants compared to the loss-of-function ones (Sarig et al., 2010).

Even though this idea was new, it was in line with the tumor suppressive roles that p53 was already known to have. p53 is not essential for survival, as loss of the gene does not cause embryonic lethality. However, this comes at a cost: both mice and humans with these genetic lesions are highly prone to developing tumors. Thus, the concept that p53 restricts self-renewal in stem cells is in line with the observation that stem and progenitor cells have many more programmed cell divisions and are largely long-lived, which makes them ideal candidates for transformation. These findings were supported by earlier studies showing that p53 was highly expressed in the early mouse embryo

(12-14 days old) but not at later stages during development (16 days old) (Sabapathy et al., 1997). Another example of p53's role in stem cell biology is seen in the hematopoietic system. Hematopoietic stem and Progenitor cells (HSPCs) express the highest levels of p53 and as cells differentiate its expression declines with them (Pant et al., 2012) (Figure 6). In addition it was also shown that p53 is highly abundant in mESCs and its expression declines when the cells differentiate (Sabapathy et al., 1997). Importantly though, studies have shown that despite the fact that p53 is highly expressed in mESCs it is localized in the cytoplasm where it is thought to be inactive (Qin et al., 2007). Similarly, in hESCs even though p53 seems to be in the nucleus, it exists in its inactive deacetylated form (Jain et al., 2012). This presents a paradox and raises the following question: how are these cells ensuring their genome integrity under stress conditions? Are they able to transiently induce p53 upon demand or is there an unknown player involved in these processes?

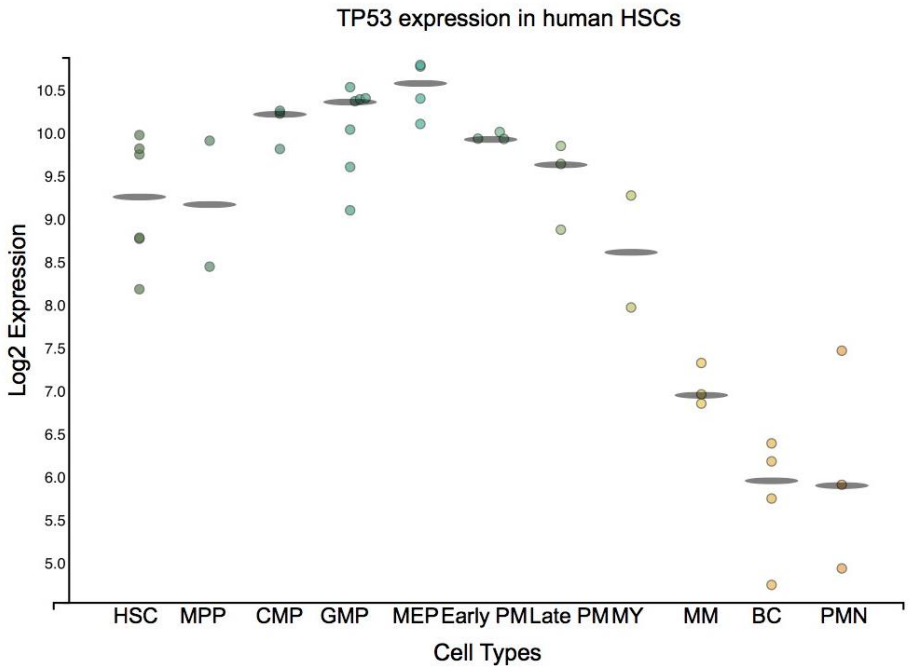

Figure 6 Expression of TP53 in human hematopoietic cells.

Hematopoietic stem cells (HSC) and different types of progenitors (MPP: multipotent progenitors, CMP: Common myeloid progenitors, GMP: Granulocyte and Monocyte progenitors, MEP: megakaryocyte progenitors) express the highest level of TP53 which is gradually declining with differentiation in the myeloid lineage.

Hence, p53 seems to mediate the balance between genome stability and plasticity, which is pivotal in maintaining tissue homeostasis. In a somatic cell, p53 has a major role in translating stress signals into classic processes such as apoptosis, cell cycle arrest and senescence, but in stem cells an imbalance between genomic integrity and plasticity can have detrimental consequences. In this regard, increased senescence or apoptosis can result in a severe depletion of the functional stem cell reservoir leading to early aging. This dilemma emphasizes the important relationship between the quantity and quality

of stem cells and puts p53 at the epicenter ensuring a balance between maintaining an intact genome and allowing stem cell plasticity.

The hematopoietic system has long served as a model system to understand the functions and properties of stem cells. In the last couple of years there has been a series of studies describing the presence of leukemia-related mutations in elderly individuals leading to clonal hematopoiesis (Genovese et al., 2015). Some of these mutations include *DNMT3A, TET2, ASXL1* as well as *TP53*, all of which when mutated have been shown to enhance self-renewal and induce leukemia with or without other lesions (Abdel-Wahab et al., 2013; Moran-Crusio et al., 2011; Tadokoro et al., 2007; Zhao et al., 2010). With increasing age, stem cell function declines so it has been hypothesized that these mutations evolved to counteract this in the expense of enhanced risk of developing cancer. All of the genes mentioned above are epigenetic modifying enzymes and are thought to mediate enhanced self-renewal by altering the chromatin. Is it perhaps possible that p53 is controlling self-renewal by doing the same? Due to the fact that p53 is phosphorylated, acetylated, methylated and ubiquitinylated – modifications also found on histones – it has been suggested by Arnold Levine and colleagues that p53 may monitor the epigenetic changes that take place during reprogramming by these same post-translational alterations (Yi et al., 2012).

When a differentiated cell acquires epigenetic changes that confer aberrant self-renewal (i.e. formation of a cancer stem cell), p53 might be involved in recognizing these epigenetic changes in a cell as stress signals and prevent them from happening, which is in absolute accordance with its tumor suppressive nature. We are only beginning to understand the role of p53 in stem cells and the underlying mechanisms are even less

clear. It is of particular interest to understand how p53 hotspot mutations that arise so frequently in patients perturb this tumor suppressive function that normally inhibits the formation of genomic alterations but also maintains the ability of stem cells to properly self-renew. Loss of either of these functions is detrimental to life, hence understanding how this is mediated is of paramount importance.

Epigenetic Modifiers in cancer

It has been long appreciated that epigenetic dysregulation is common in cancer and various studies have shown that genes controlling epigenetic processes are mutated in different types of cancer.

Epigenetics historically referred to heritable processes that regulate gene expression without leading to changes in the sequence of the DNA. In recent years the field of epigenetics has focused on studying – but not limited – to DNA cytosine methylation and hydroxymethylation as well as histone methylation, acetylation, ubiquitylation and phosphorylation. Unlike the irreversible changes that occur from mutations on the DNA, an altered epigenetic state is thought to be amenable to change and thus it has been proposed to be a potential therapeutic target (Goldberg et al., 2007).

Emerging sequencing studies from patients with AML identified recurring mutations in genes that are epigenetic modifiers (Cancer Genome Atlas Research et al., 2013), which when modelled in mice significantly contributed to hematopoietic transformation (Woods and Levine, 2015). These data suggest that these somatic alterations in epigenetic regulators contribute to leukemia initiation and support what it had already

been suggested by the finding of recurrent translocations involving histone lysine acetyltransferases like lysine acetyltransferase 6A (KAT6A/CREBBP) and the very common mixed-lineage leukemia (MLL) translocations.

In AML the most common mutations in epigenetic modifiers involve DNA methyltransferase 3A (*DNMT3A*), tet methylcytosine dioxyge-nase 2 (*TET2*), isocitrate dehydrogenase 1 and 2 (*IDH1/2*), additional sex combs-like 1 (*ASXL1*) and in the enhancer of zeste homologue 2 (*EZH2*), which beyond their biological significance have clinical and future therapeutic relevance in myeloid malignancies (Shih et al., 2012) (Patel et al., 2012).

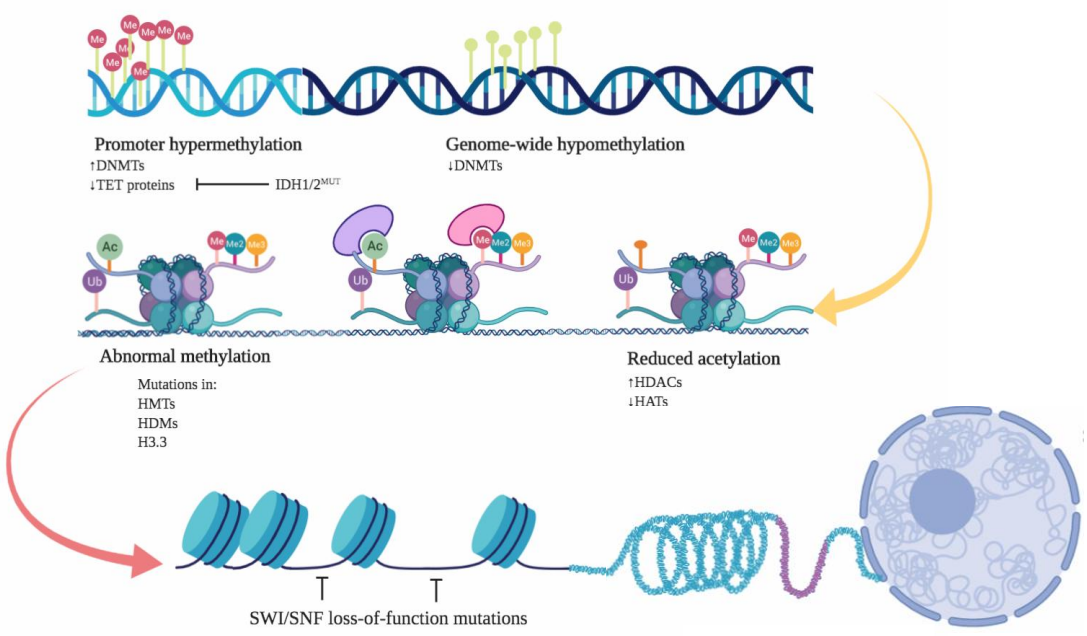

Figure 7 Illustration of the organization of genomic DNA and how mutations in epigenetic modifiers can affect this.

Tumors exhibit mutations in (i) DNA methyltransferase/demethylases (DNMT3a and TET2), which can alter cytosine methylation on DNA. In addition, mutated enzymes can generate oncometabolites that block the activity of other enzymes, such as 2-hydroxyglutarate production blocking TET2 activity in IDH1/2-mutated tumors. ; (ii) histone tail modifiers (HMT: histone methyl-transferase, HDM: histone demethylase, HDAC: histone deacetylase, HAT: histone acetyl-transferase), which can modify histone tails to insert or remove methyl and acetyl groups; and (iii) the SWI/SNF complex, which can alter the position of nucleosomes along the DNA

One chromatin modifying complex whose subunits are targeted by mutations in different tumor types is the PRC2 complex. The Polycomb group (PcG) proteins repress transcription and regulate cell identity to maintain tissue homeostasis. There are two distinct PRC complexes, PRC1 and PRC2, with a third PcG complex identified in Drosophila melanogaster (Margueron and Reinberg, 2011). These complexes initiate and maintain transcriptional silencing through specific post-translational histone modifications. The PRC2 complex consists of four core members: EZH1 or EZH2, the embryonic ectoderm development (EED), the suppressor of zeste 12 homologue (SUZ12) and RBAP48 (also known as RBBP4) (Margueron and Reinberg, 2011) (Figure 8).

The PcG member that has been most studied in cancer is EZH2, which has the catalytic activity to deposit methyl groups onto histone 3 at lysine 27 (H3K27) (Vire et al., 2006). EZH1 has similar enzymatic activity, and it has been proposed that they have some

redundant roles but also distinct ones that become more apparent when one enzyme is compensating for the absence of the other (Shen et al., 2008). Interestingly, the overexpression of wild-type EZH2 is commonly observed in various epithelial malignancies, and somatic, heterozygous activating mutations of *EZH2* that affect residue Y641 have been identified in germinal-center diffuse large-B-cell (DLBC) lymphomas where these mutations lead to increased di- and tri-methylation of H3K27 (Sneeringer et al., 2010).

EZH2 mutations have also been reported in myeloid diseases such as MDS, chronic myelomonocytic leukemia (CMML), and primary myelofibrosis (PMF) but are rare in other chronic or acute myeloid malignancies (Ernst et al., 2010; Nikoloski et al., 2010).

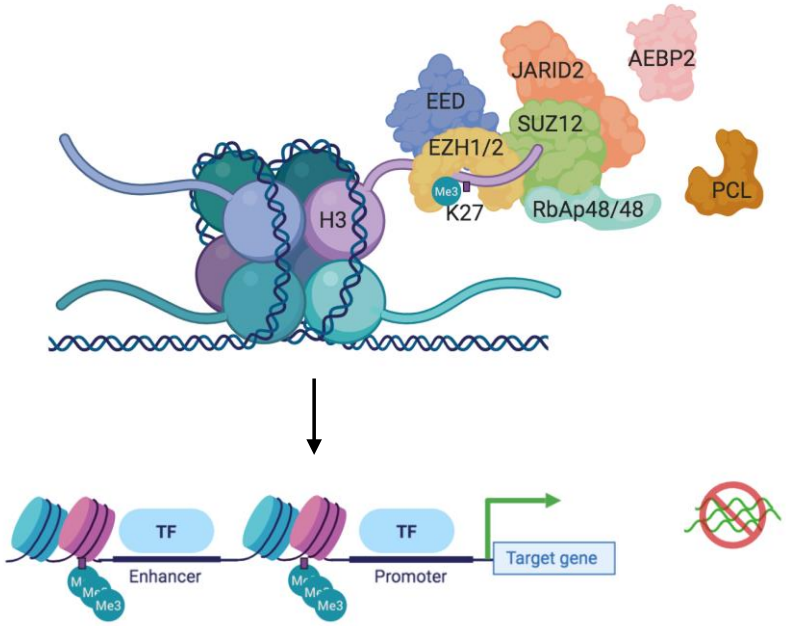

Figure 8 The PRC2 complex.

The complex consists of several members that include the proteins EZH1 and EZH2 that have the catalytic activity to catalyze H3K27me3. Other proteins such as EED, SUZ12, JARID2, RbAp48/48, AEBP2 and PCL have an important auxiliary role that helps mediate the repressive histone mark at enhancers and promoters that is associated with decreased transcription.

Efforts trying to understand the role of the PRC2 complex in hematological malignancies utilized mouse models with conditional deletion of *Ezh2* in the hematopoietic compartment of mice that resulted in defects in B-cells without overt effects in stem or progenitor functions (Su et al., 2003). Whereas $Eed^{+/-}$ mice develop severe, lethal myeloid and lymphoid proliferation (Lessard et al., 1999). Despite the fact that other mutations in PRC2 components are less frequent than EZH2 they do occur in myeloid malignancies with 1.4% of patients with MDS/MPN exhibiting *SUZ12* mutations and less than 1% having *EED* deletions or mutations (Brecqueville et al., 2011; Score et al., 2012). Mutations in PRC2 components do not seem to be mutually exclusive at least in patients with T cell acute lymphoblastic leukemia (T-ALL), in which mutations in PRC2 components are more frequent than in myeloid malignancies (Zhang et al., 2012). This suggests that perhaps these mutations go beyond inactivating the complex and some of these proteins might have functions not yet understood that contribute to these diseases.

Interestingly both at the single nucleotide variant and copy-number level it appears that PRC2 alterations are loss-of-function and frequently heterozygous, suggesting that these genes might be haploinsufficient tumor suppressors involved in the pathogenesis

of myeloid malignancies. Recent work demonstrated that EZH1/2 also pose a dependency in myeloid leukemias evident from the prolonged survival that was achieved in mice treated with a selective inhibitor against these proteins (Xu et al., 2015). This work, as well as an shRNA screen that identified Eed and Suz12 (Shi et al., 2013) as dependencies in a murine model of AML, suggest that components of the PRC2 complex may serve both as oncogenes and tumor suppressor genes in the myeloid compartment.

Despite the possible complex biology that *EZH2* mutations might have in myeloid malignancies, it has been apparent that these mutations confer an adverse outcome in MDS and PMF but also might be contributing to the poor outcome associated with loss of chromosome 7q where EZH2 is located (Guglielmelli et al., 2011; Le Beau et al., 1996). In what way *EZH2* mutations contribute to poor patient survival is still not well understood and needs to be studied further as remarkably these mutations do not increase the risk of transformation to AML from MDS (Sashida et al., 2014) and are rare in de novo AML.

Understanding the functions of PRC2 components *in vivo* would be important to elucidate how many of these genes that reside within the segmental deletions occurring in CK-AML contribute to the pathogenesis of the disease and will perhaps show that even partial impairment of these members is sufficient.

I joined the Lowe lab with an initial interest in understanding more this type of leukemia with dismal prognosis and wanted to study whether mutant p53, which had been linked primarily to metastasis, might have a gain of function effect in the hematopoietic

compartment. In addition, as several chromatin modifying factors that reside in segmental deletions in CK-AML genetically co-occurred with p53 and have been extensively linked to other types of leukemia we decided in collaboration with Katerina Hatzi to study their role in this disease.

CHAPTER I: A gain-of-function p53 mutant oncogene promotes cell fate plasticity and myeloid leukemia through the pluripotency factor Foxh1

ABSTRACT

Mutations in the *TP53* tumor suppressor gene are common in many cancer types, including the acute myeloid leukemia (AML) subtype known as complex karyotype (CK) AML. Here, we identify a gain-of-function (GOF) *p53* mutation that accelerates CK-AML initiation beyond p53 loss and, surprisingly, is required for disease maintenance. The $p53^{R172H}$ mutation ($TP53^{R175H}$ in humans) exhibits a neomorphic function by promoting aberrant self-renewal in leukemic cells, a phenotype that is present in hematopoietic stem and progenitor cells (HSPCs) even prior to their transformation. We identify the Forkhead box H1 transcription factor (Foxh1) as a critical mediator of mutant p53 function that binds to and regulates stem cell-associated genes and transcriptional programs. Our results identify a context where mutant p53 acts as a *bona fide* oncogene that contributes to the pathogenesis of CK-AML and suggests a common biological theme for *TP53* gain-of-function in cancer.

SIGNIFICANCE

Our study demonstrates how a gain-of-function p53 mutant can hijack an embryonic transcription factor to promote aberrant self-renewal. In this context mutant *p53* functions as an oncogene to both initiate and sustain myeloid leukemia and suggests a potential convergent activity of mutant *p53* across cancer types.

INTRODUCTION

TP53 mutations occur in the majority of human cancers and are often associated with poor outcomes (Kandoth et al., 2013; Olivier et al., 2010). *TP53* encodes a sequence-specific transcription factor (Kern et al, 1991) that is normally maintained at low levels through strict post-translational control (Laptenko and Prives, 2006). In response to DNA damage, activated oncogenes, or other forms of cellular stress, p53 is stabilized and promotes cell cycle arrest, apoptosis, senescence, or other anti-proliferative programs depending on cellular context (Kastan et al., 1991; Kastenhuber and Lowe, 2017; Lowe et al., 1993; Serrano et al., 1997). Most *TP53* mutations occur in the DNA binding domain and disrupt its transcriptional activity, thereby preventing these stress responses and enabling aberrant proliferation and survival of mutated cells (Bouaoun et al., 2016).

Cancer-associated mutations typically inactivate p53 through a two-hit mechanism, whereby one allele acquires a missense mutation and the other undergoes "loss-of-heterozygosity" (LOH) via chromosomal deletion (Kastenhuber and Lowe, 2017). Missense *TP53* mutations encode proteins that have attenuated capacity to transactivate wild-type target genes, despite being frequently stabilized owing to reduced interaction with negative regulators (Prives and Hall, 1999). These mutant proteins can instill neomorphic gain-of-function (GOF) activities that contribute to cancer phenotypes beyond p53 loss (Muller and Vousden, 2014). At the organismal level, mice harboring certain germline missense mutations in *Trp53* (hereafter referred to as *p53*) develop an altered tumor spectrum compared to *p53* null mice, including a larger fraction of

epithelial cancers with increased metastatic potential (Olive et al., 2004; Weissmueller et al., 2014). At the cellular level, some GOF p53 mutants promote chemoresistance, invasiveness, and/or an epithelial-to-mesenchymal transition through diverse mechanisms (Freed-Pastor et al., 2012; Olive et al., 2004; Weissmueller et al., 2014). Another neomorphic function of mutant p53 involves its ability to facilitate the formation of induced pluripotent stem cells (iPSCs) more so than p53 loss (Sarig et al., 2010; Yi et al., 2012), though the extent to which this GOF activity is relevant to cancer is poorly understood.

In contrast to their high prevalence in most solid tumors, *TP53* mutations occur in around 10% of blood cancers though, when they occur, are associated with poor prognosis (Papaemmanuil et al., 2016b; Rucker et al., 2012). In acute myeloid leukemia (AML), *TP53* mutations are associated with a subtype known as complex karyotype AML (CK-AML), which is defined by the presence of 3 or more cytogenetic abnormalities and a dismal 5-year survival rate of less than 2% (Papaemmanuil et al., 2016b; Rucker et al., 2012). Functional studies in mice indicate that *p53* inactivation in the hematopoietic compartment can produce chemoresistant malignancies with increased leukemia initiating potential, mirroring key features linked to *TP53* mutations in AML patients (Chen et al., 2014; Zhao et al., 2010; Zuber et al., 2009). Still, whether and how *TP53* missense mutations confer GOF activities to p53 in AML is not known.

In this study, we set out to test whether mutant p53 has GOF activity in AML and, if so, to determine the underlying mechanisms behind this effect. We chose to study $p53^{R172H}$

(*R175H* in humans), a mutant form of *p53* that has been shown to confer GOF activity in solid tumors and is the most common allele in AML patients (Elli Papaemmanuil, personal communication). Several complementary *in vitro* and *in vivo* systems were used to compare the biological features of wild-type, *p53* null, or *p53* mutant alleles, leading us to identify a neomorphic function of mutant p53 in hematopoietic stem and progenitor cells that exerts its effect by enhancing cellular self-renewal beyond that produced by p53 inactivation. We also identify a novel mediator of mutant p53 function, Foxh1, which contributes to the aberrant self-renewal phenotype. As such, suppression of either mutant p53 or Foxh1 ablates this stemness capacity by triggering differentiation. These observations illustrate how mutant p53 can acquire a pro-oncogenic activity that magnifies loss of its tumor suppressive functions and creates a previously unappreciated molecular dependency in AML.

RESULTS

$p53^{R172H}$ accelerates the onset of hematological malignancies beyond effects of p53 deficiency.

We first compared the ability of a mutant or null *p53* allele to promote leukemogenesis in a well-defined genetic model. Because of its previously defined GOF activity in other settings, we used a conditional mutant *p53* allele harboring a *R172H* mutation downstream of a "lox-stop-lox" cassette (*LSL-*$p53^{R172H}$) (Olive et al., 2004), which corresponds to $TP53^{R175H}$, one of the most frequent mutations in clinical cases of AML (Papaemmanuil et al., 2016b). Mouse cohorts were produced to harbor one $p53^{R172H}$ allele and a *p53 floxed* allele ($p53^{LSL\text{-}R172H/F}$), or were homozygous for the *floxed p53* allele ($p53^{F/F}$), such that all hematopoietic cells would become $p53^{R172H/\Delta}$ and $p53^{\Delta/\Delta}$,

respectively, in the presence of the hematopoietic-specific *Vav1-cre* transgene (Ogilvy et al., 1998). While both the $p53^{R172H/\Delta}$ and $p53^{\Delta/\Delta}$ cohorts eventually succumbed to disease with full penetrance, mice harboring the $p53^{R172H}$ allele became moribund significantly faster (Figure 1A). As commonly observed in $p53^{-/-}$ mice (Donehower et al., 1995), most animals developed thymic lymphoma, although some had leukemias and rarely a mixed disease (leukemia and lymphoma) (Figure 1B).

The above observations are consistent with those previously obtained using mice harboring a humanized $p53^{R248Q}$ allele expressed in the whole body of mice, which also develop T cell lymphoma faster than *p53* null mice (Hanel et al., 2013). However, neither model addresses the biology of mutant p53 action in the clinically-relevant context of AML, likely due to the high penetrance of lymphomas that arise in the mouse. Therefore, to bias the model against T cell lymphoma development, we transplanted bone marrow cells from *Mx1-Cre;*$p53^{R172H/F}$ and *Mx1-Cre;*$p53^{F/F}$ mice into thymectomized recipients. Three weeks post-transplantation, intraperitoneal injection of PolyI:C was used to activate the interferon-inducible Mx1-Cre, triggering the recombination of floxed alleles in transplanted cells (Kuhn et al., 1995). Of note, the use of the inducible Mx1-Cre recombinase enabled transplantation of functionally wild type whole bone marrow (WBM) cells, avoiding biases in engraftment efficiency that might occur upon p53 alteration. As in the autochthonous model, $p53^{R172H/\Delta}$ mice succumbed to disease faster than their *p53-null* counterparts (Figure 1C), though, in this instance, the disease was immunophenotypically and histologically characterized as AML based on the expression of Cd11b and Gr1 on the surface of infiltrating leukemic

cells (Figure 1D, E). Thus, $p53^{R172H}$ gives rise to an aggressive leukemia that significantly shortens overall survival as compared to the disease arising from p53 deficient bone marrow cells, providing functional evidence that a *p53* mutant allele can contribute to AML beyond effects of p53 loss.

Figure 1. $p53^{R172H}$ Leads to Accelerated Onset of Hematological Malignancies. (**A**) Kaplan-Meier survival curves of native mice with $p53^{\Delta/\Delta}$ and $p53^{R172H/\Delta}$ hematopoietic cells recombined using Vav1-Cre. (**B**) Spectrum of hematological malignancies arising in $p53^{\Delta/\Delta}$ (n=15) and $p53^{R172H/\Delta}$ (n=11 native mice. (**C**) Kaplan-Meier survival curves of thymectomized mice transplanted with $p53^{f/f}$, $p53^{f/f}$;Mx1-Cre and $p53^{R172H/F}$;Mx1-Cre bone marrow (BM) (**D**) Expression of CD11b and Gr1 in the peripheral blood of moribund mice from (C) (**E**) Representative H&E image of mice with acute myeloid leukemia arising after transplant in thymectomized recipients. ** $p < 0.005$, **** $p < 0.0001$, Log-rank (Mantel-Cox) test.

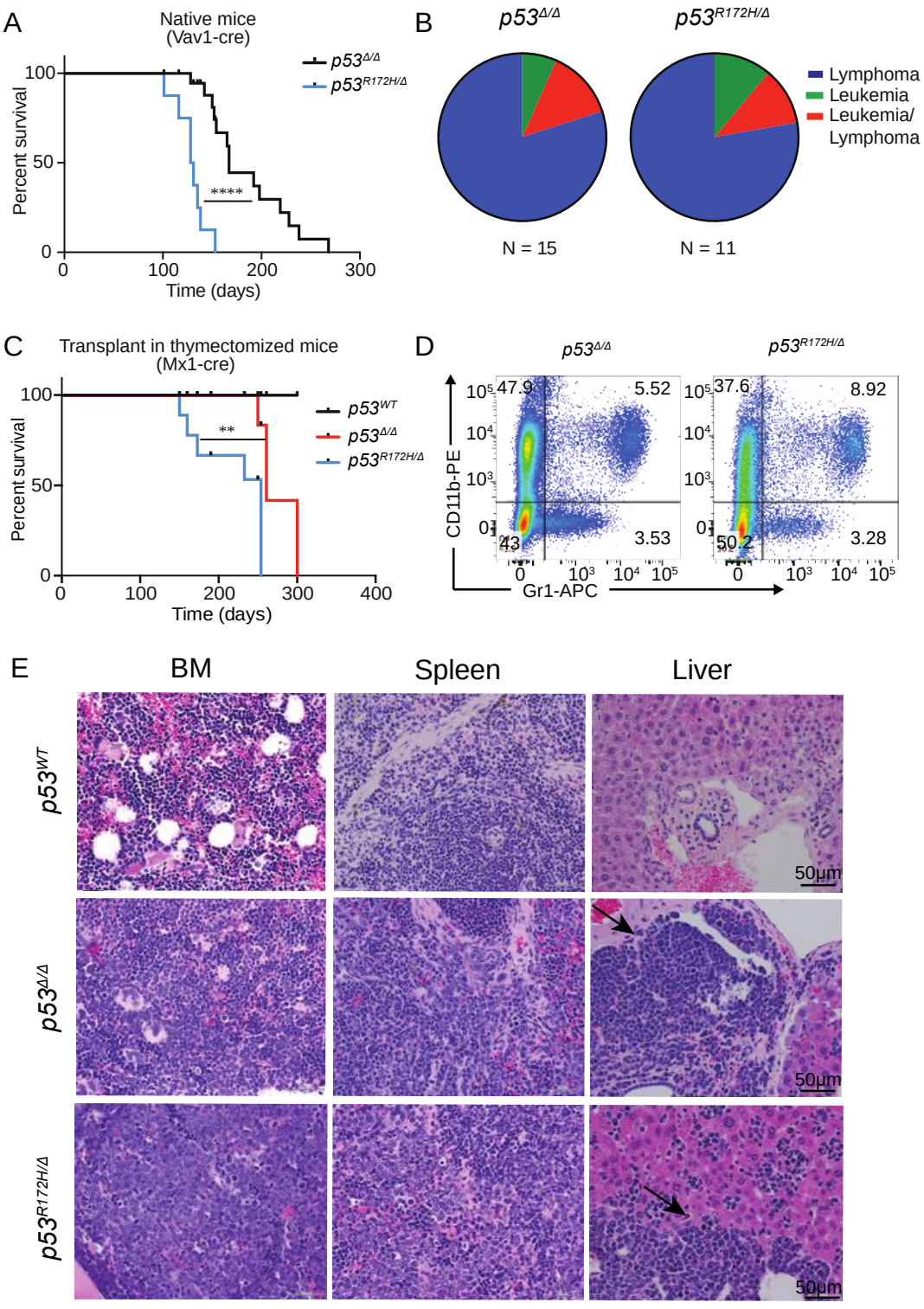
A
Native mice
(Vav1-cre)
Percent survival
Time (days)
p53Δ/Δ
p53R172H/Δ
****
B
p53Δ/Δ
p53R172H/Δ
Lymphoma
Leukemia
Leukemia/
Lymphoma
N = 15
N = 11
C
Transplant in thymectomized mice
(Mx1-cre)
Percent survival
Time (days)
p53WT
p53Δ/Δ
p53R172H/Δ
**
D
p53Δ/Δ
p53R172H/Δ
CD11b-PE
Gr1-APC
47.9
5.52
43
3.53
37.6
8.92
50.2
3.28
E
BM
Spleen
Liver
p53WT
p53Δ/Δ
p53R172H/Δ
50μm
50μm
50μm

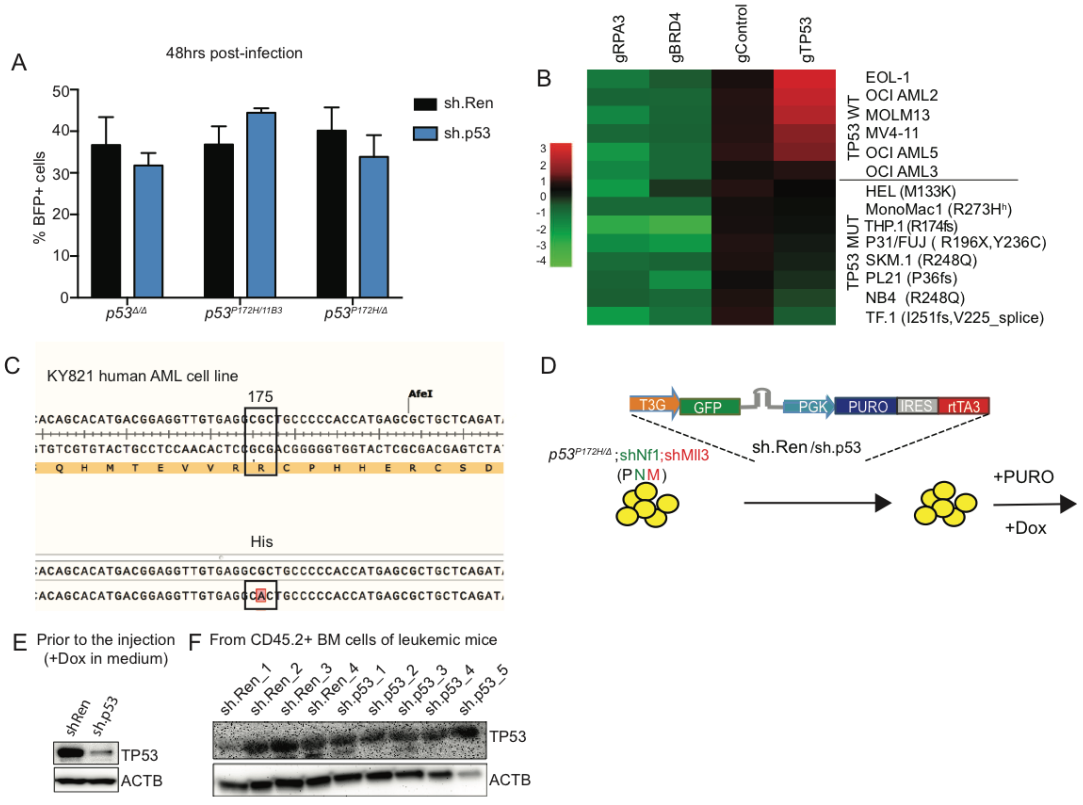

Figure S1. Mutant p53 is necessary to sustain leukemic cells *in vitro and in vivo*. Related to figure 2. (**A**) Percentage of BFP+ cells 48hrs post-infection as assessed by FACS in the three cell lines. (**B**) Genome-wide CRISPR screen was used to visualize the proliferation of 14 human AML cell lines with different *TP53* status after the use of a gRNA against *TP53* (gRPA3 and gBrd4 were used as positive controls) (Wang et al., 2017) (**C**) Sanger sequencing results confirming the presence of the R175H *TP53* mutation in KY821 cells. (**D**) Schematic representation of transplanting $p53^{R172H/\Delta}$ sh.Ren or sh.p53 doxycyclin-inducible containing cells in CD45.1 mice. (**E**) Western-Blotting confirming knock-down of TP53 in $p53^{R172H/\Delta}$ sh.p53 cells *in*

vitro upon doxycyclin addition to the medium of the cells. (**F**) Western-Blotting for TP53 (BM).

Sustained expression of mutant p53 is required for the maintenance of p53^{R172H} leukemic cells

We next examined whether the p53^{R172H} mutant protein was required for survival of p53 mutant leukemic cells. We utilized previously characterized *p53$^{\Delta/\Delta}$* or *p53$^{R172H/\Delta}$* and *p53$^{R172H/11B3}$* CK-AML murine cell lines that were created by co-transduction of short hairpin RNAs (shRNAs) targeting *Nf1* (GFP-labeled) and *Mll3* (mCherry-labeled), hereafter referred to as PNM (Chen et al., 2014; Liu et al., 2016). These cell lines were generated to reflect the most common genetic configurations found in patients, including *p53* loss alone (*p53$^{\Delta/\Delta}$*), *p53^{R172H}* over a focal *p53* deletion (*p53$^{R172H/\Delta}$*) or *p53^{R172H}* over a larger genomic deletion that encompasses *p53* (*p53$^{R172H/11B3}$*) (Liu et al., 2016). Control shRNAs against Renilla luciferase (shRen) or p53 (sh.p53) were co-expressed with a blue fluorescent protein (BFP) reporter (Figure S1A) (Zuber et al., 2011a). The percentage of BFP+ cells was monitored over time as a measurement of fitness under the two shRNA-containing conditions.

We observed a significant reduction in the relative number of sh.p53 BFP+ cells compared to sh.Ren BFP+ cells over time (Figure 2A light blue and dark blue lines), indicating negative selection against cells in which the mutant protein is depleted. By contrast, sh.p53 had no effect on *p53$^{\Delta/\Delta}$* AML cells, ruling out potential off target effects of the p53 shRNA (Figure 2A black line). p53 depletion in cells harboring *p53^{R172H}* promoted differentiation and triggered apoptosis as assessed by flow cytometry for

CD11b and Annexin V, respectively (Figure 2B,C). Thus, AML cells expressing $p53^{R172H}$ acquire a molecular dependency on mutant p53 that contributes to a differentiation block that sustains leukemogenesis.

To determine whether human AML can also depend on sustained expression of mutant p53, we first examined publicly available CRISPR/Cas9 genome-wide screening data (Wang et al., 2017). In these studies, sgRNAs were introduced into human AML lines expressing Cas9 followed by assessment of their enrichment or depletion over time using next generation sequencing. Interestingly, sgRNAs targeting p53 were invariably enriched in AML lines harboring wild-type *TP53* but depleted to varying degrees in those expressing mutant *TP53* genes (e.g. *R248Q* – another hotspot *TP53* mutation), suggesting that a subset of the latter group might depend on sustained expression of the mutant protein for their proliferation and/or survival (Figure S1B).

None of the AML cell lines used in the aforementioned CRISPR/Cas9 screen harbored an *R175H* mutation (corresponding to the mutation we studied in mice). However, we identified a human AML cell line (KY821) that harbored this mutation in the absence of a *WT p53* allele (Figure S1C) and used it to functionally test the requirement for this mutant form of *TP53 in vitro* and *in vivo*. Cells were transduced with a validated shRNA targeting human p53 (sh.TP53) (Brummelkamp et al., 2002) or empty vector control (Ctrl) and examined for their ability to form colonies in methylcellulose culture *in vitro* or give rise to leukemia upon transplantation into sub-lethally irradiated NOD-scid IL-$2R^{-/-}$ (NSG) immune-deficient mice. Similar to observations from murine AML,

suppression of mutant *TP53* in KY821 cells significantly reduced their colony-forming ability (Figure 2D,E) and led to the up-regulation of the myeloid differentiation marker CD16 (Figure 2F), again suggesting that this p53 mutant contributes to a differentiation block.

To test whether $TP53^{R175H}$ mutant cells transduced with sh.TP53 exhibited reduced fitness *in vivo*, we analyzed peripheral blood for the presence of human CD45-positive leukocytes in recipient mice 5 weeks post-transplantation. Remarkably, this analysis revealed a significant reduction of cells containing sh.TP53 versus control cells (Figure 2G), confirming the suppressive effect of mutant p53 knock-down in p53 mutant-expressing human leukemias. In addition, knockdown of mutant p53 significantly increased the survival of transplanted mice compared to controls (Figure 2H). At the time of death, the resulting leukemias invariably selected against expression of the p53-targeting shRNA and restored the expression of mutant p53, consistent with our observations from murine models (Figure 2I and S1D-F). Therefore, KY821 cells require mutant p53 protein to sustain leukemia. Collectively, these results reveal an oncogenic function for mutant p53 in murine and human AML.

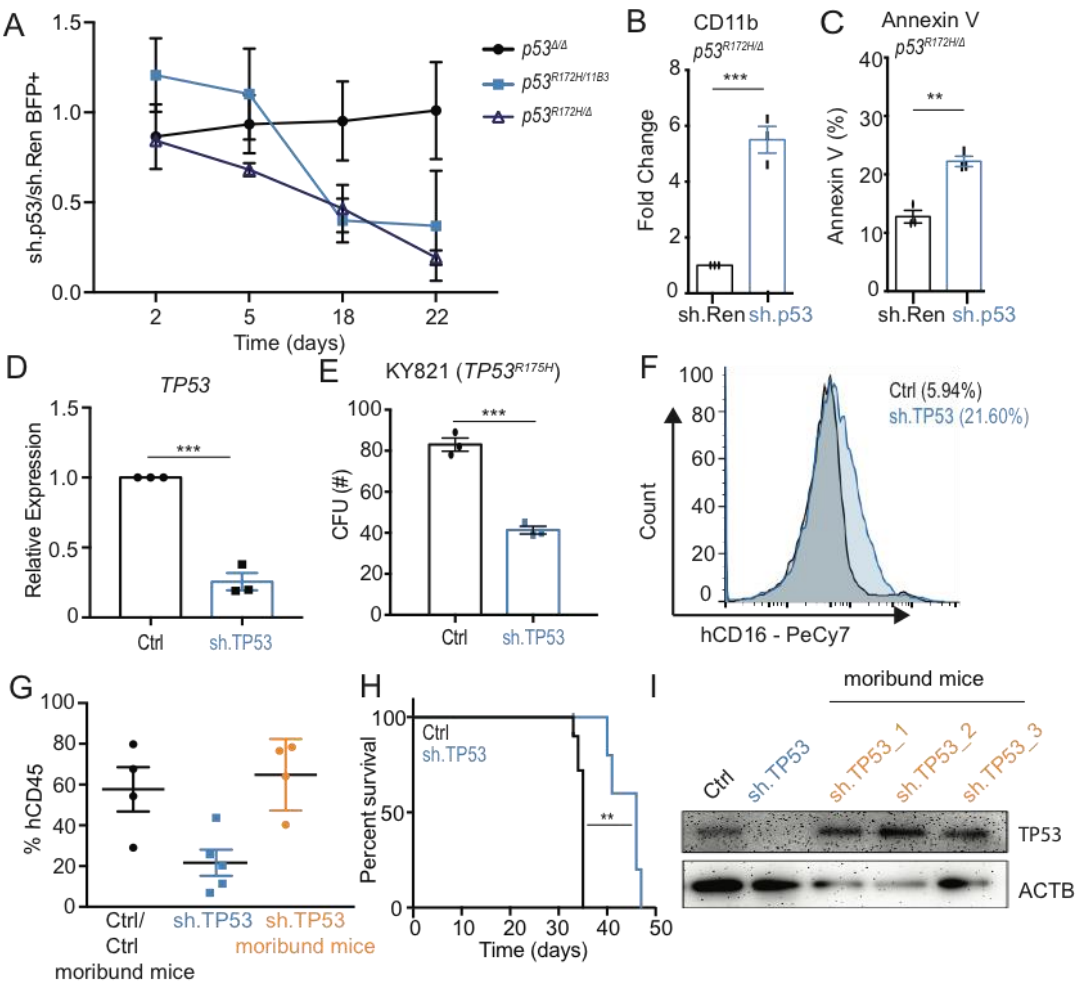

Figure 2. Depletion of mutant p53 impairs the growth of p53 mutant leukemias. (**A**) The ratio of sh.p53 BFP+ cells compared to sh.Ren BFP+ cells over time in leukemic lines. **(B)** CD11b expression in the shRNA BFP+ containing cells ($n = 3$) and (**C**) Annexin V shown by FACS 7 days after infection. Data presented as mean ± s.e.m (**D**) Relative expression of *TP53* 7 days post infection with pRS sh.TP53 in human KY821 cells. (**E**) CFU in human AML cells with sh.Ren or sh.TP53. Data presented as mean ± s.e.m ($n = 3$) (**F**) hCD16 expression by FACS in pRS Ctrl or pRS

TP53 cells from growing in CFU assay (**G**) Percentage of hCD45 in the peripheral blood of mice 5 weeks post transplant in shCntr and shCntr moribund mice (black), shTP53 (blue) and shTP53 moribund mice (orange). Data are represented as mean ± s.e.m (n=5 and n=5) (**H**) Kaplan-Meier curve from NSG mice transplanted with equal numbers of KY821 cells transduced with wither shCntr or shTP53 (*n=5 and n=5)*. (**I**) Western blot for human TP53 in cells before injection and in sorted hCD45 cells from the peripheral blood of 3 independent moribund shTP53 mice. *p <0.05, **p <0.005 ***p <0.0005. **B.** Kruskal-Wallis 1-way ANOVA. C, D, F, J, unpaired t-test.

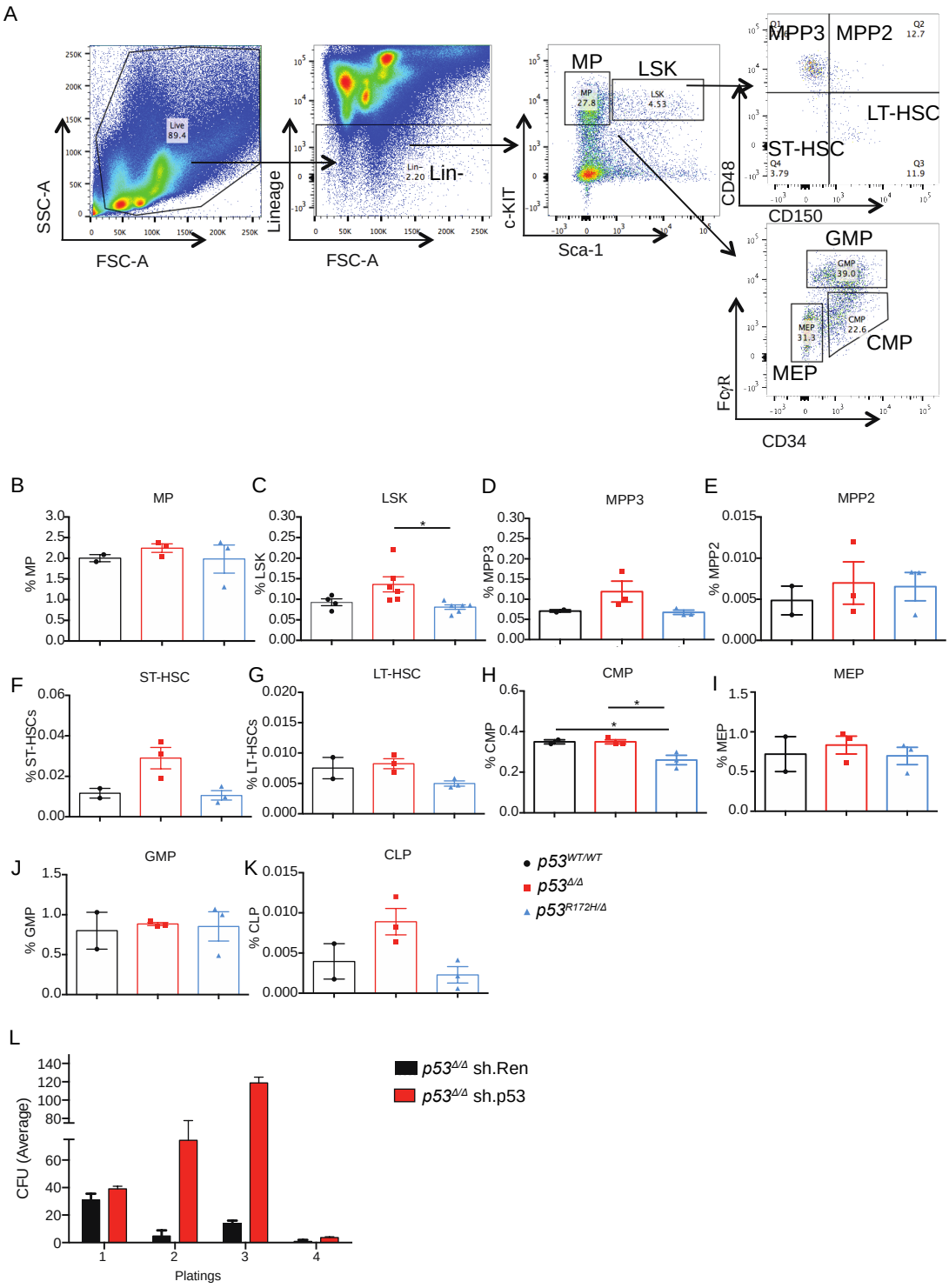
A
SSC-A
FSC-A
Live
89.4
Lineage
Lin-
2.20
Lin-
FSC-A
c-KIT
Sca-1
MP
27.8
LSK
4.53
MP
LSK
CD48
CD150
MPP3
MPP2
LT-HSC
ST-HSC
Q1
Q2
12.7
Q4
3.79
Q3
11.9
GMP
CMP
MEP
GMP
39.0
CMP
22.6
MEP
31.3
FcγR
CD34
B
MP
% MP
C
LSK
% LSK
D
MPP3
% MPP3
E
MPP2
% MPP2
F
ST-HSC
% ST-HSCs
G
LT-HSC
% LT-HSCs
H
CMP
% CMP
I
MEP
% MEP
J
GMP
% GMP
K
CLP
% CLP
p53WT/WT
p53Δ/Δ
p53R172H/Δ
L
CFU (Average)
Platings
p53Δ/Δ sh.Ren
p53Δ/Δ sh.p53

Figure S2. Immunophenotyping 7-week old *p53*$^{WT/WT}$, *p53*$^{\Delta/\Delta}$ and *p53*$^{R172H/\Delta}$ mice. **Related to figure 4.** (**A**) FACS gating strategy for mouse HSPCs. Percentage of different types of cells in the BM of 7-week old *p53*$^{WT/WT}$, *p53*$^{\Delta/\Delta}$, and *p53*$^{R172H/\Delta}$ mice (**B**) Myeloid Progenitors (MP), (**C**) Lineage- cKIT+ Sca-1+ (LSK), (**D**) Multipotent Progenitors 3 (MPP3), (**E**) Multipotent Progenitors 2 (MPP2), (**F**) Short-term hematopoietic stem cells (ST-HSC), (**G**) Long-term hematopoietic stem cells (LT-HSC), (**H**) Common Myeloid Progenitors (CMP), (**I**) Megakaryocyte-Erythrocyte Progenitors (MEP), (**J**) Granulocyte and Monocyte Progenitors (GMP), (**K**) Common Lymphoid Progenitors (CLP), (**L**) Total number of colony-forming units (CFU) generated by *p53*$^{\Delta/\Delta}$ HSPCs containing sh.Ren or sh.p53. Data are representative of three experiments. Error bars correspond to mean ± s.e.m (n=3) * $p < 0.05$, ** $p < 0.005$, *** $p < 0.0005$.

p53^{R172H}-derived leukemia is associated with stem cell transcriptional signatures. Most studies suggest that the GOF activities of mutant p53 proteins arise from their ability to alter transcription in a manner that is distinct from effects due to p53 loss (Weisz et al., 2007). Therefore, to examine how mutant p53 altered the transcriptome of CK-AML cells, we performed gene expression profiling of PNM *p53*-null and *p53*-mutant leukemias via RNA sequencing (RNA-seq) and identified 252 significantly differentially expressed genes (Figure 3A and Table S1). A systematic and unbiased analysis of the data using gene ontology (GO) pathway analysis revealed Tgf-β and stem cell pathways to be positively correlated with the top upregulated genes in our p53^{R172H} murine leukemias (Figure 3B). Notably, these same signatures were enriched in the

transcriptional profiles of leukemias obtained from CK-AML patients – the AML subtype in which missense *TP53* mutations most commonly occur – compared to other leukemia subtypes or normal hematopoietic cells (www.bloodspot.eu) (Bagger et al., 2019) (Figure 3C). Beyond general stem cell signatures, gene set enrichment analysis indicated that p53 mutant AML was enriched for genes linked to hematopoietic stem cells (HSC) and long term-HSCs (LT-HSCs) (Pietras et al., 2015) (Figure 3D). Therefore, both murine and human mutant p53-expressing (but not p53-deficient) leukemias converge on similar transcriptional pathways, some of which are linked to stemness and inhibition of myeloid differentiation.

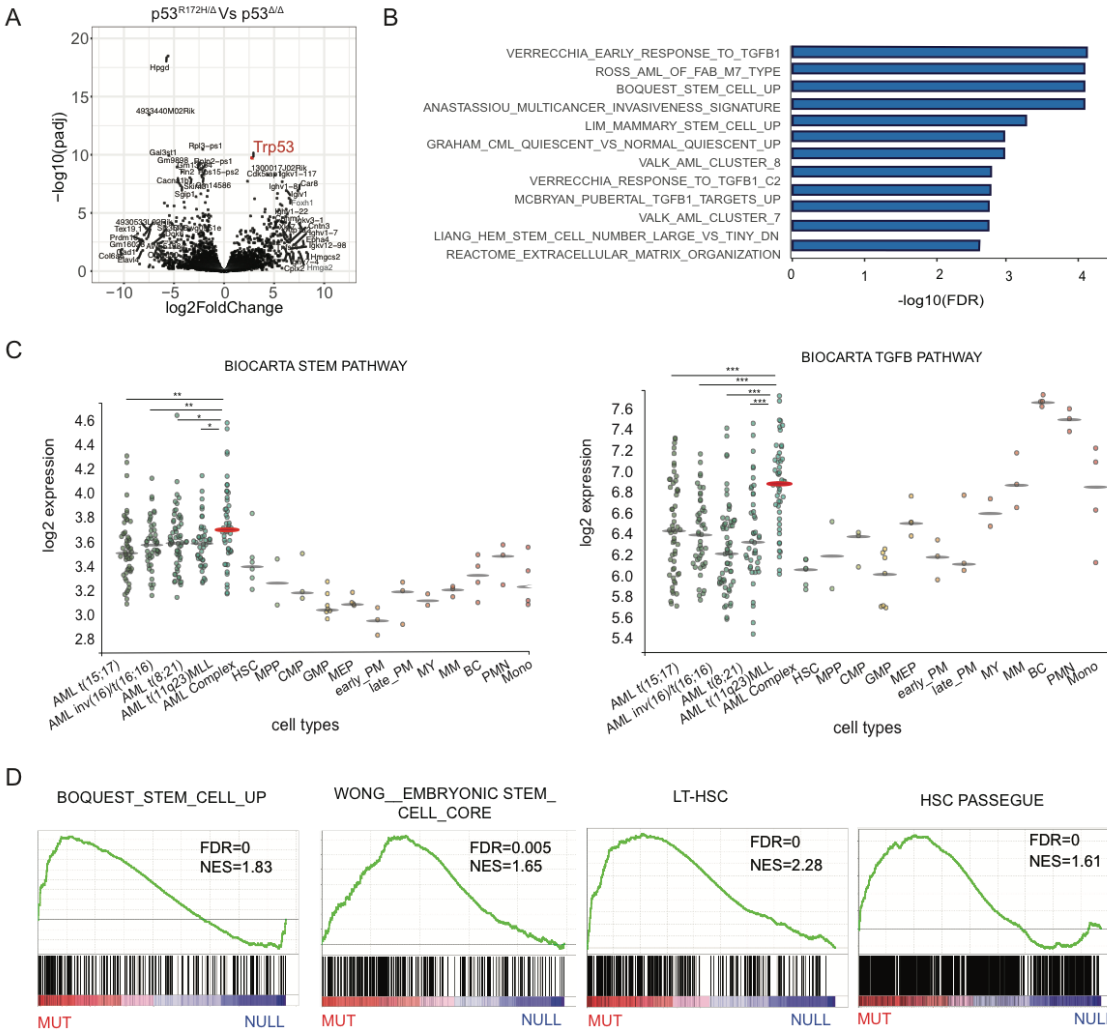

Figure 3. Gene expression profile of *p53*$^{R172H/\Delta}$ leukemias.

(**A**) Volcano plot from RNA-seq comparing *p53*$^{R172H/\Delta}$ leukemias to *p53*$^{\Delta/\Delta}$ showing *p53* as the most highly expressed gene between the two groups. (**B**) Gene ontology analysis of pathways associated with genes up-regulated in *p53*$^{R172H/\Delta}$ leukemias. (**C**) Expression of Gene Ontology-associated pathways in human AML samples and normal human hematopoietic cells (www.bloodspot.eu). (**D**) Gene Set Enrichment Analysis (GSEA) comparing gene expression between *p53*$^{R172H/\Delta}$ leukemias to *p53*$^{\Delta/\Delta}$

and other known signatures related to stem cells and hematopoietic stem cells. Two-tailed t-test * $p < 0.05$, ** $p < 0.005$, *** $p < 0.0005$. HSC: Hematopoietic stem cell, MPP: Multipotential progenitors, CMP: Common myeloid progenitor cell, GMP: Granulocyte monocyte progenitors, MEP: Megakaryocyte-erythroid progenitor cell, early_PM: Early Promyelocyte, late_PM: Late Promyelocyte, MY: Myelocyte, MM: Metamyelocytes, BC: Band cell, PMN: Polymorphonuclear cells, Mono: Monocytes.

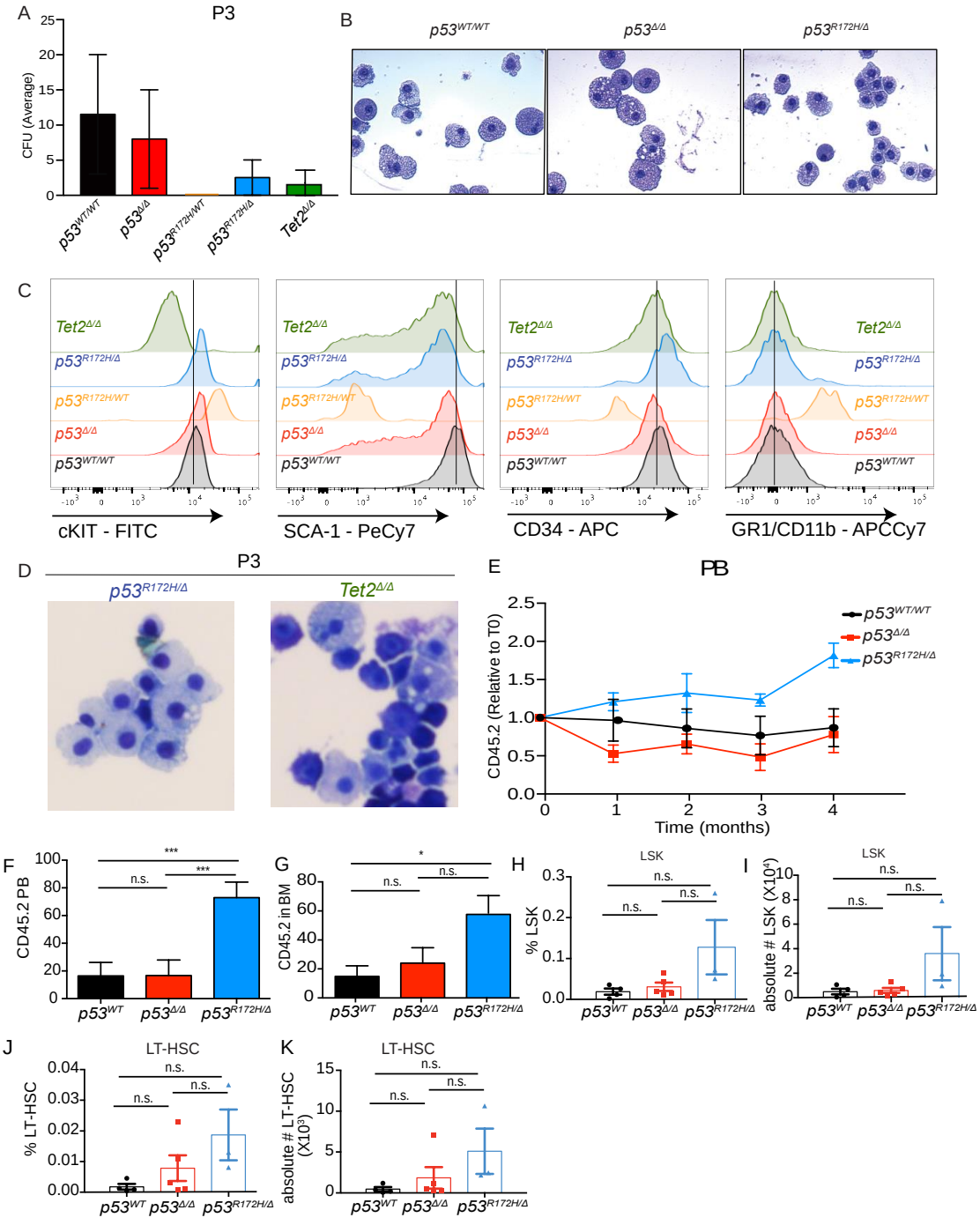

Figure S3. Mutant p53 increases self-renewal *in vitro and vivo*. Related to Figure 4. (**A**) Number of colonies from $p53^{WT/WT}$, $p53^{\Delta/\Delta}$, $p53^{R172H/WT}$, $Tet2^{\Delta/\Delta}$ and $p53^{R172H/\Delta}$

HSPCs. (**B**) Cytospins from $p53^{WT/WT}$, $p53^{\Delta/\Delta}$ and $p53^{R172H/\Delta}$ cells growing in CFUs at P3. (**C**) FACS analysis of cKIT, SCA-1, CD34, GR1 and CD11b expression in cells from CFUs. (**D**) Cytospins from P3 of $p53^{R172H/\Delta}$ and $Tet2^{\Delta/\Delta}$ cells growing in CFUs. (**E**) CD45.2 in the PB relative to time 0 (T0) as assessed by FACS, (**F**) Percentage of CD45.2 in the PB of mice, (**G**) Percentage of CD45.2 in the BM of mice. From secondary competitive transplant four months post-transplant (**H**) Percentage of LSKs, (**I**) Absolute number of LSKs, (**J**) Percentage of LT-HSCs, (**K**) Absolute number of LT-HSCs. Data are representative of three experiments. Error bars correspond to mean ± s.e.m (n=3) * pvalue <0.05, ** pvalue <0.005, *** pvalue <0.0005.

$p53^{R172H}$ enhances self-renewal in hematopoietic cells in vitro and *in vivo*

AML arises from alterations (e.g. mutations) that promote proliferation or enhance the self-renewal of myeloid progenitor cells (Nowak et al., 2009; Passegue et al., 2003). To directly examine the functional consequences of mutant p53 expression in the normal hematopoietic compartment, we isolated adult whole bone marrow (WBM) cells from $p53^{WT/WT}$, $p53^{\Delta/\Delta}$ and $p53^{R172H/\Delta}$ mice and performed limiting dilution cultures in methylcellulose medium followed by serial replating. Under these cytokine-rich culture conditions, wild-type cells lose their replating capacity after three sequential passages (Nakahata and Ogawa, 1982). As previously described (Liu et al., 2009), loss of p53 modestly increased the replating capacity of hematopoietic cells as compared to those expressing wild-type p53 (Figure 4A). In stark contrast, hematopoietic cells expressing

p53$^{R172H/\Delta}$ not only replated more frequently than *p53*$^{\Delta/\Delta}$ and *WT* controls, but also could replate indefinitely (Figure 4A).

This enhanced capability could not be explained by differences in the pre-existing frequency of stem and progenitor cells in the bone marrow, since immunophenotyping of 7 week-old mice (the time of bone marrow collection) did not show an increase in any type of stem or progenitor cell (Figure S2A-K). This increase in self-renewal was observed in *p53*$^{R172H/\Delta}$ but not *p53*$^{R172H/WT}$ cells, suggesting that loss of the residual *WT* allele is a prerequisite for this GOF effect (Figure S3A). Furthermore, *p53*$^{R172H/\Delta}$ cells exhibited higher nuclear to cytoplasmic ratio when compared to *p53*$^{\Delta/\Delta}$ and *WT cells* at the same passage (P3) (Figure S3B) and expressed the highest levels of CD34 (Figure S3C), an important marker of long-term repopulation of HSCs (Matsuoka et al., 2001). The replating phenotype produced by mutant *p53* was similar to that produced by disruption of *Tet2*, a well-characterized leukemia tumor suppressor gene whose loss promotes enhanced self-renewal (Figure S3C) (Challen et al., 2011; Moran-Crusio et al., 2011). Nevertheless, the *p53*$^{R172H/\Delta}$ cells were different than *Tet2*$^{\Delta/\Delta}$ cells at the immunophenotypic and morphological levels (Figure S3C, D), suggesting subtle differences between how these alterations act.

To further explore the relationship between mutant p53 and self-renewal potential, we isolated cKit+ bone marrow cells from the *p53*$^{R172H/\Delta}$ mice and transduced them with viral vectors co-expressing an shRNA targeting mutant p53 (sh.p53) or a Renilla control (sh.Ren). These vectors encoded puromycin resistance, allowing us to select and maintain pure shRNA-expressing cells in culture. This isogenic comparison validated

our previous observation: p53 knockdown in *p53* mutant cells halted replating capacity after the fourth passage (comparable to $p53^{\Delta/\Delta}$ WBM), whereas sh.Ren cells (which retain expression of mutant p53) were able to replate indefinitely (Figure 4B and 4C). We confirmed that the normalization of self-renewal potential by sh.p53 was not due to an off target effect of RNAi, as the same shRNA had no effect on the fitness of $p53^{\Delta/\Delta}$ hematopoietic cells (Figure S2L).

Consistent with these findings, competitive transplantation studies using $p53^{WT/WT}$, $p53^{\Delta/\Delta}$ and $p53^{R172H/\Delta}$ BM (Figure 4D) demonstrated that $p53^{R172H/\Delta}$ cells outcompeted wild-type cells to a greater extent than $p53^{\Delta/\Delta}$ cells (Figure S3E-G), a phenotype that was further exacerbated in secondary transplants (Figure 4E). Analysis of peripheral blood (Figure 4F) and BM (Figure 4G) demonstrated that $p53^{R172H/\Delta}$ cells were significantly enriched with respect to $p53^{WT}$ cells. Furthermore, within the BM of $p53^{R172H/\Delta}$ mice, HSCs were expanded in relative and absolute number compared to $p53^{\Delta/\Delta}$ mice (Figure S3H-K). All downstream progenitors, including megakaryocyte/erythroid progenitors (MEPs), granulocyte/macrophage progenitors (GMPs) and common myeloid progenitors (CMPs), were significantly increased in $p53^{R172H/\Delta}$ mice (Figure 4H-J).

For further validation, we examined the consequences of inhibiting mutant p53 in normal mouse HSCs. For these experiments, we used the bone marrow of $p53^{R172H/\Delta}$ mice to isolate lineage negative (Lin-)/Sca-1^{+}/cKit^{+} cells (LSKs), a cell population capable of maintaining long-term hematopoiesis in mice (Seita and Weissman, 2010).

To suppress p53, these cells were infected with retroviruses encoding an shRNA (targeting mutant p53 or Renilla control) linked to blue fluorescent protein (BFP) (Figure 4K). Equal numbers of either sh.Ren or sh.p53 cells were mixed with non shRNA expressing $p53^{R172H}$ BFP^{-} cells and transplanted into CD45.1 lethally irradiated mice in an *in vivo* competition format. The fraction of BFP^{+} cells in the peripheral blood was monitored for four months. $p53^{R172H/\Delta}$ BM cells transduced with the p53 shRNA were progressively depleted from peripheral blood, becoming nearly undetectable by the end of the experiment (Figure 4L).

Analysis of bone marrow at the final time point revealed that fewer cells expressing sh.p53 remained as compared with those expressing control sh.Ren (Figure 4M). Moreover, the proportion of LSKs within the sh.p53 population was lower than in the control sh.Ren population (Figure 4N). Altogether, these observations establish a role for $p53^{R172H}$ in promoting aberrant self-renewal in adult hematopoietic cells in a manner that renders these cells dependent on its action for their maintenance in a pre-malignant setting. Hence, phenotypes linked to p53 mutant GOF can emerge in the hematopoietic system prior to neoplastic transformation.

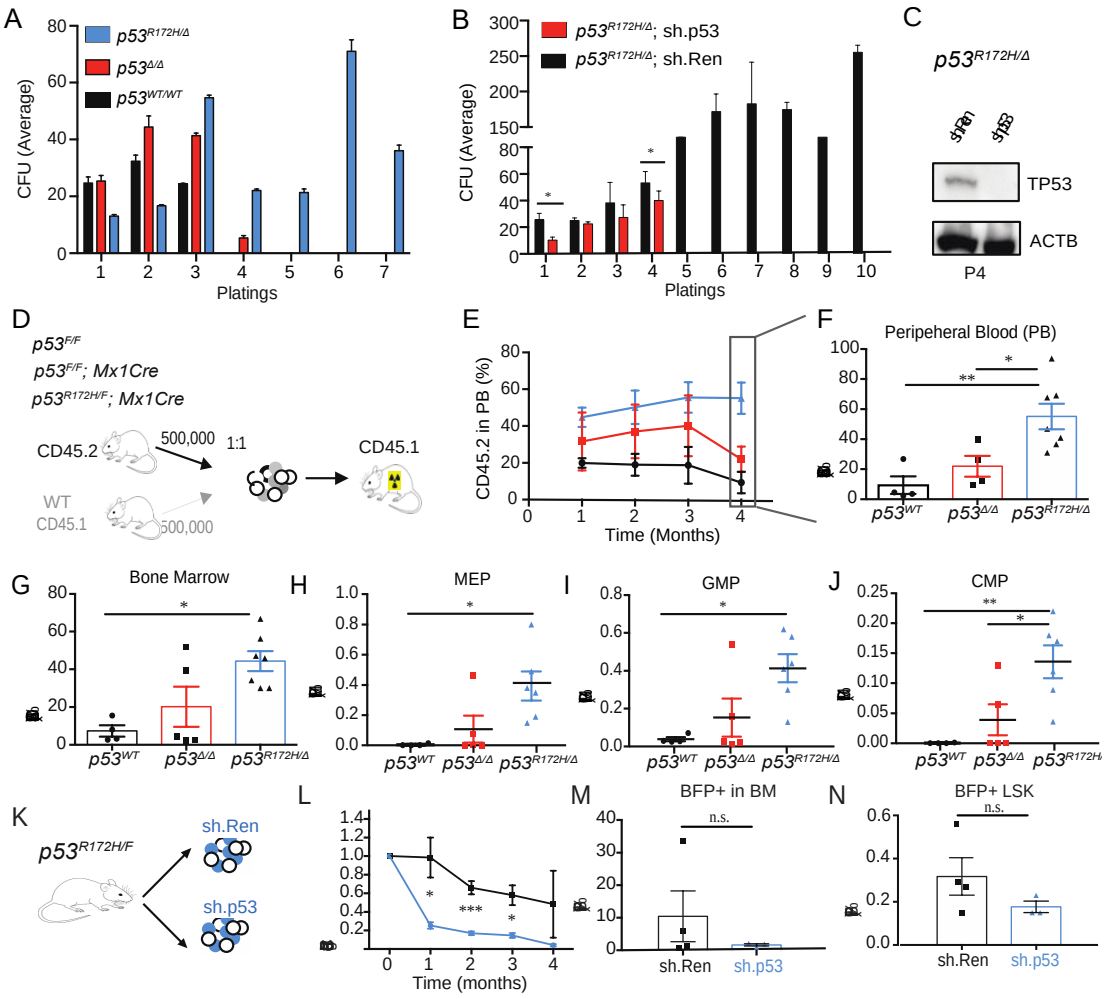

Figure 4. p53^{R172H} induces aberrant self-renewal *in vitro and in vivo.*

(**A**) Total number of colony-forming units (CFU) generated by *p53^{WT}* (black), *p53$^{Δ/Δ}$* (red) and *p53$^{R172H/Δ}$* (blue) cells. Data are representative from four independent experiments. Error bars correspond to mean ± s.e.m (n=3). **(B)** Total number of colony-forming units (CFU) generated by *p53$^{R172H/Δ}$* cKIT+ cells containing sh.Ren or sh.p53. Data are representative from three independent experiments. Error bars correspond to mean ± s.e.m (n=3). (**C**) Western-blotting for TP53 and B-ACTIN at passage 4 (P4). (**D**) Schematic representation of the competitive transplantation

protocol. (**E**) Percentage of CD45.2 cells during the secondary competitive transplant in the PB of mice monitored monthly by bleeding (*n=5* per group). (**F**) Percentage of CD45.2 cells in the PB four months after transplant (*n=4-7)*. (**G**) Percentage of CD45.2 cells in the BM four months after transplant (n=4-7), **(H)** Percentage of Megakaryocyte Erythrocyte Progenitors (MEP), **(I)** Granulocyte Monocyte Progenitors (GMP) and **(J)** Common Myeloid Progenitors (CMP) in the BM of mice four months after transplant (*n=4-7)*. (**K**) Schematic representation of the transplant layout. LSKs were sorted from $p53^{R172H/\Delta}$ mice and were infected with an sh.Ren or sh.p53 conjugated to BFP fluorescence. Two days after infection equal numbers of cells were transplanted in lethally irradiated CD45.1 mice. (**L**) BFP fluorescence over time as assessed by monthly bleeds in recipient mice (*n=5*). (**M**) Percentage of BFP+ cells in the BM of mice with sh.Ren or sh.p53 four months after transplant (*n=3-5*). (**N**) Percentage of BFP+ LSKs in the BM of mice with sh.Ren or sh.p53 four months after transplant (*n=3-5*). **B**, **C**, and **D**. Two-tailed t-test * $p < 0.05$, ** $p < 0.005$, *** $p < 0.0005$. Error bars correspond to mean ± s.e.m.

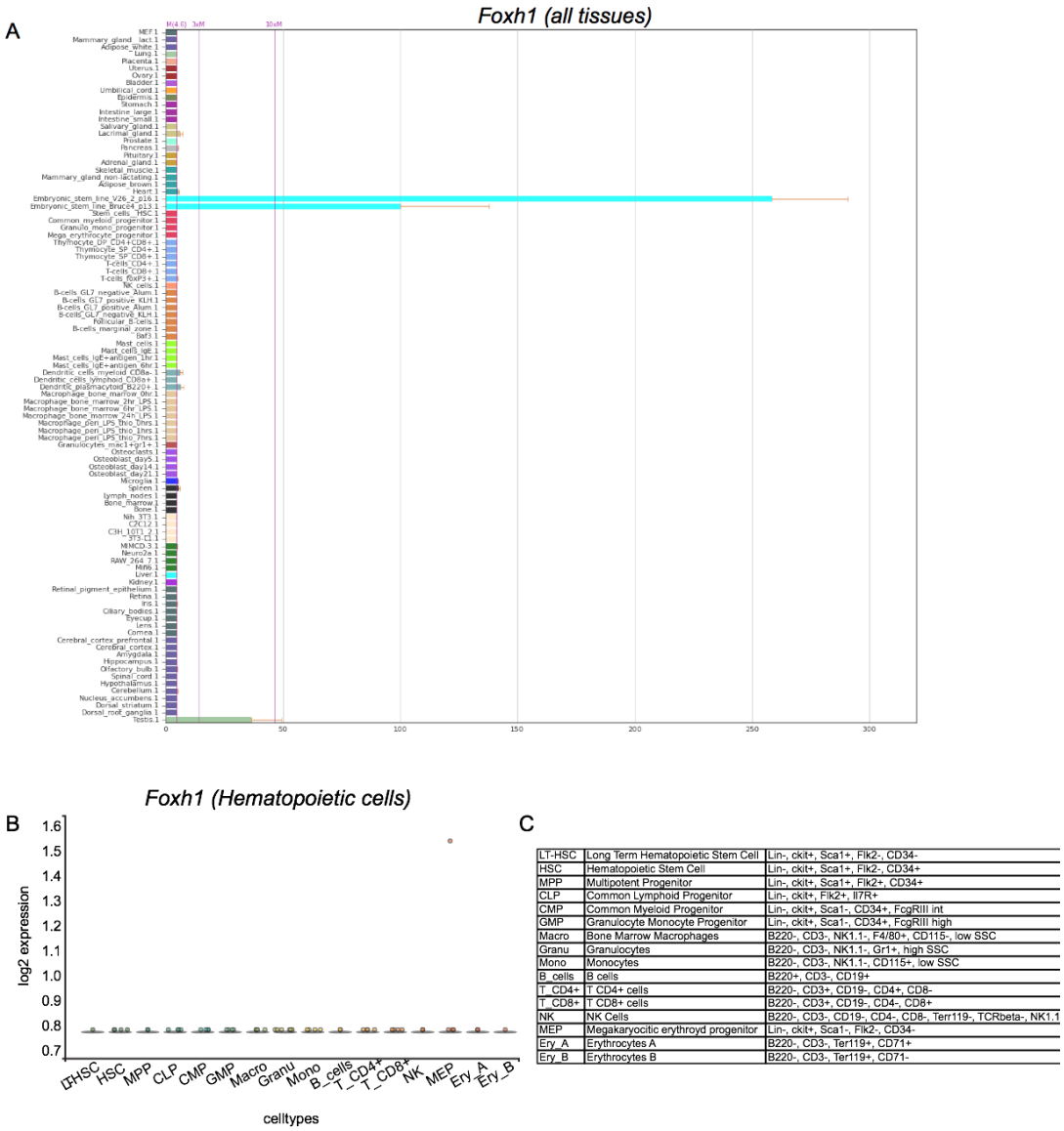

LT-HSC	Long Term Hematopoietic Stem Cell	Lin-, ckit+, Sca1+, Flk2-, CD34-
HSC	Hematopoietic Stem Cell	Lin-, ckit+, Sca1+, Flk2-, CD34+
MPP	Multipotent Progenitor	Lin-, ckit+, Sca1+, Flk2+, CD34+
CLP	Common Lymphoid Progenitor	Lin-, ckit+, Flk2+, Il7R+
CMP	Common Myeloid Progenitor	Lin-, ckit+, Sca1-, CD34+, FcgRIII int
GMP	Granulocyte Monocyte Progenitor	Lin-, ckit+, Sca1-, CD34+, FcgRIII high
Macro	Bone Marrow Macrophages	B220-, CD3-, NK1.1-, F4/80+, CD115-, low SSC
Granu	Granulocytes	B220-, CD3-, NK1.1-, Gr1+, high SSC
Mono	Monocytes	B220-, CD3-, NK1.1-, CD115+, low SSC
B_cells	B cells	B220+, CD3-, CD19+
T_CD4+	T CD4+ cells	B220-, CD3+, CD19-, CD4+, CD8-
T_CD8+	T CD8+ cells	B220-, CD3+, CD19-, CD4-, CD8+
NK	NK Cells	B220-, CD3-, CD19-, CD4-, CD8-, Terr119-, TCRbeta-, NK1.1
MEP	Megakaryocitic erythroyd progenitor	Lin-, ckit+, Sca1-, Flk2-, CD34-
Ery_A	Erythrocytes A	B220-, CD3-, Ter119+, CD71+
Ery_B	Erythrocytes B	B220-, CD3-, Ter119+, CD71-

Figure S4. Foxh1 expression in mouse cells. Related to Figure 5. (**A**) Foxh1 expression in different types of mouse cells (http://ds.biogps.org/?dataset=GSE10246&gene=14106) (**B**) Foxh1 expression in normal mouse hematopoietic cells (bloodspot – Mouse Normal RNA-seq)

(http://servers.binf.ku.dk/bloodspot/?gene=Foxh1&dataset=mouse_nl_rna_seq). (**C**) Names for each abbreviation and immunophenotyping used per cell type.

Foxh1 is required for mutant p53 induced self-renewal in both normal and leukemic cells.

To explore the mechanism by which mutant p53 enhances cellular self-renewal, we surveyed the genes that were expressed at higher levels in $p53^{R172H/\Delta}$ leukemias compared to $p53^{\Delta/\Delta}$ leukemias. One of the most significantly up-regulated genes in our analysis was *forkhead box H1* (*Foxh1*) (Supplementary Table 1), which encodes a key transcription factor that is known to mediate Nodal/Tgf-β signaling during embryogenesis but is not expressed at appreciable levels in the adult hematopoietic compartment or any other mouse tissue (Figure S4A and S4B-C). Like mutant p53 (Muller and Vousden, 2013), Foxh1 has been linked to EMT (Attisano et al., 2001; Chiu et al., 2014) and can facilitate the reprogramming of fibroblasts into induced pluripotent stem cells (iPSCs) (Takahashi et al., 2014). Furthermore, many of the top upregulated genes in $p53^{R172H/\Delta}$ leukemias were known Foxh1 targets (Charney et al., 2017) (Figure 5A). Taken together, these observations led us to hypothesize that Foxh1 might be a key mediator of the $p53^{R172H}$ GOF activity in leukemia.

In agreement, analysis of publicly available expression data from normal human hematopoietic cells and different leukemia subtypes revealed that FOXH1 expression was significantly higher in all AMLs (particularly in CK-AML patients, the majority of which harbor *TP53* mutations) compared to any type of normal cell (Figure 5B and

S5A-B). In addition, like mutant *TP53*, *FOXH1* upregulation correlated with poor survival in AML patients (Cerami et al., 2012; Gao et al., 2013) (Figure 5C). Consistent with the RNA-seq results, Foxh1 expression was also higher in $p53^{R172H/\Delta}$ hematopoietic stem and progenitor cells (HSPCs) compared to $p53^{\Delta/\Delta}$ cells growing in colonies (Figure 5D), and knockdown of mutant p53 reduced Foxh1 levels in murine HSPCs (Figure 5E) as well as murine and human leukemic cells (Figures 5F and 5G, respectively). Thus, mutant p53 expression leads to higher levels of Foxh1 in both normal and leukemic cells from mouse and human leukemias.

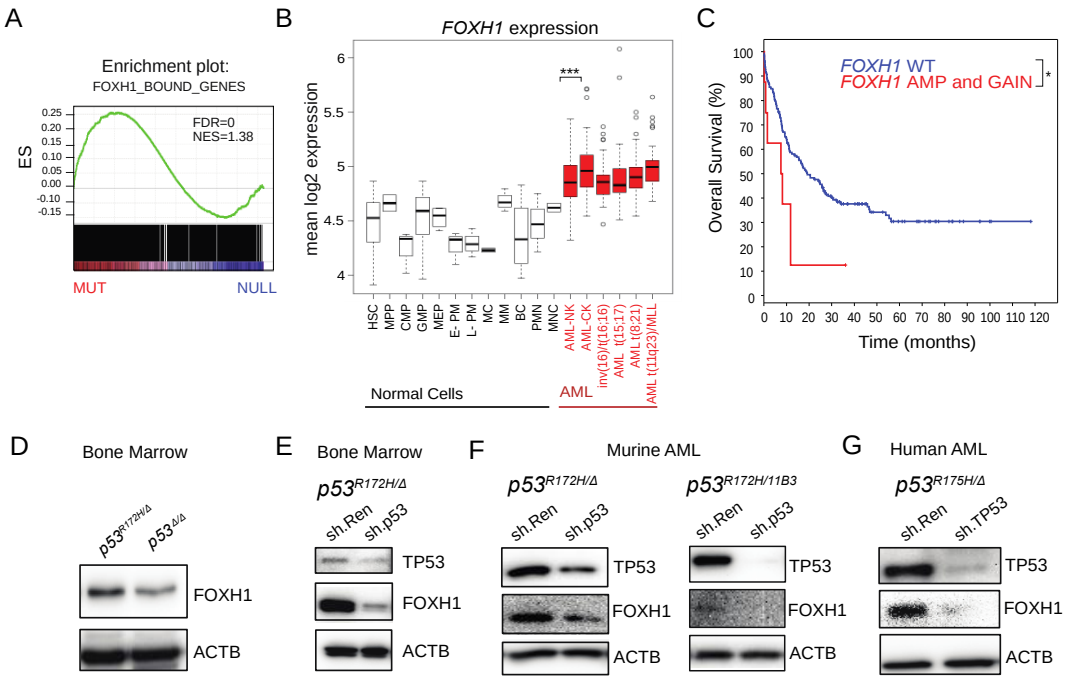

Figure 5. Identification of Foxh1 as a p53 mutant mediator.

(A) GSEA comparing the expression of genes associated with genomic regions occupied by Foxh1 when compared to the genes differentially expressed in $p53^{R172H}$

and *p53*$^{\Delta/\Delta}$ leukemias. (**B**) Microarray data showing the expression of FoxH1 across normal human hematopoietic cells and different types of leukemias. **(C)** Overall Survival in patients with AML that have FoxH1 mRNA upregulation or genetic amplification compared to patients without (cbioportal –TCGA). **(D)** Western-blotting for FOXH1 in HSPCs from p53^{R172H} and p53$^{\Delta/\Delta}$ cells at Passage 4. **(E)** Western-Blotting for TP53 and FOXH1 in p53^{R172H} HSPCs transduced with sh.Ren or sh.p53. **(F)** Western-Blotting for TP53 and FOXH1 in two independent p53^{R172H} murine leukemic cells transduced with sh.Ren or sh.p53. **(G)** Western-Blotting for TP53 and FOXH1 in p53^{R175H} human leukemic cells transduced with sh.Ren or sh.TP53. * $p < 0.05$, ** $p < 0.005$, *** $p < 0.0005$. Hematopoietic stem cell, MPP: Multipotential progenitors, CMP: Common myeloid progenitor cell, GMP: Granulocyte monocyte progenitors, MEP: Megakaryocyte-erythroid progenitor cell, early_PM: Early Promyelocyte, late_PM: Late Promyelocyte, MY: Myelocyte, MM: Metamyelocytes, BC: Band cell, PMN: Polymorphonuclear cells, Mono: Monocytes.

A

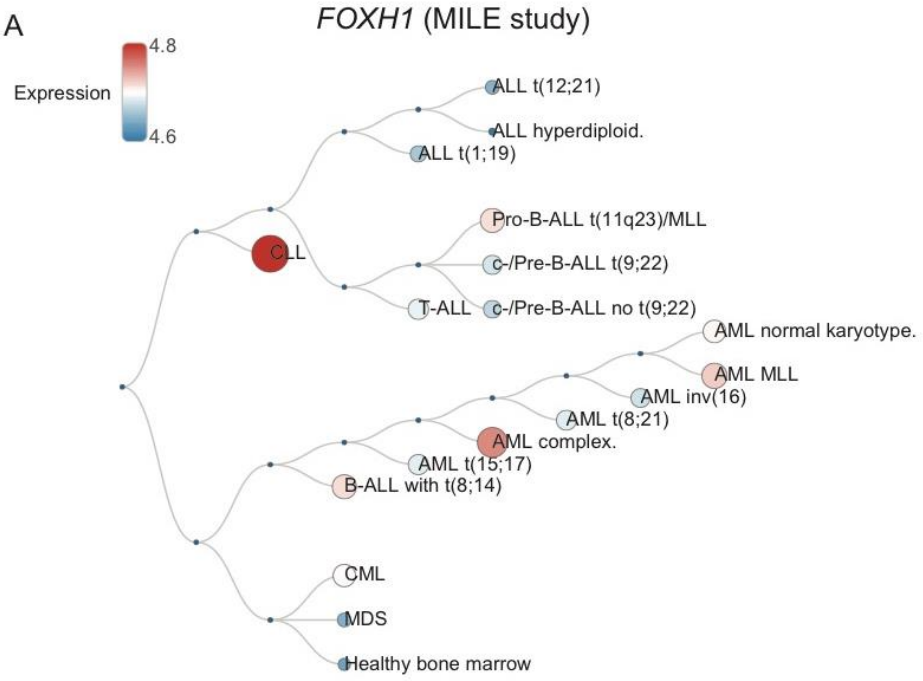

B

ALL hyperdiploid	ALL with hyperdiploid karyotype
ALL t(12;21)	ALL with t(12;21)
ALL t(1;19)	ALL with t(1;19)
AML complex.	AML complex aberrant karyotype
AML inv(16)	AML with inv(16)/t(16;16)
AML normal karyotype	AML with normal karyotype + other abnormalities
AML MLL	AML with t(11q23)/MLL
AML t(15;17)	AML with t(15;17)
AML t(8;21)	AML with t(8;21)
CLL	Chronic Lymphoid Leukemia
CML	Chronic Myeloid Leukemia
MDS	Myelodysplastic syndrome
Healthy bone marrow	Non-leukemia and healthy bone marrow
Pro-B-ALL t(11q23)/MLL	Pro-B-Aacute Lymphoid Leukemia with t(11q23)/MLL
T-ALL	T-Acute Lymphoid Leukemia
c-/Pre-B-ALL t(9;22)	c-ALL/Pre-B-ALL with t(9;22)
c-/Pre-B-ALL no t(9;22)	c-ALL/Pre-B-ALL without t(9;22)
B-ALL with t(8;14)	mature B-ALL with t(8;14)

Figure S5. FOXH1 expression in human leukemias. Related to Figure 5. (**A**) FOXH1 expression in different types of human leukemias and normal cells. (**B**) List

of names for each abbreviation used in figures derived from bloodspot (http://servers.binf.ku.dk/bloodspot/?gene=FOXH1&dataset=all_mile).

Foxh1 is a critical effector of p53^{R172H} via its ability to bind and regulate stem cell genes

Since Foxh1 is a transcription factor and its role in cells of hematopoietic origin is not known, we performed chromatin immunoprecipitation with an anti-Foxh1 antibody followed by high-throughput sequencing (ChIP-Seq) in order to identify the genome-wide Foxh1 binding sites in p53 mutant murine leukemic cells (Figure 6A). Sites bound by Foxh1 correlated with the presence of canonical Foxh1 binding motifs (*p<1e-1915)* as well as with other Tgf-β mediators (Lee et al., 2000; Spittau and Krieglstein, 2012) (Figure 6B). GO pathway analysis indicated that genes associated with Foxh1 peaks are involved in BMP and Tgf-β signaling pathways, as well as myeloid leukemia (Figure 6C).

To investigate how many of the genes bound by Foxh1 are dynamically regulated, we suppressed Foxh1 and compared the downregulated genes (green circle) to those physically bound by Foxh1 (orange circle) (Figure 6D). Consistent with a molecular relationship between mutant p53 and Foxh1 expression, there was a significant overlap between the genes that were decreased upon knockdown of mutant p53 (blue circle) or Foxh1 (green circle), with over 50% of genes showing evidence of co-regulation (Fisher Exact Test p-value < 2.2e-16). Gene set enrichment analysis (GSEA) confirmed that genes that were downregulated upon Foxh1 knockdown significantly overlapped with those downregulated upon mutant p53 knockdown (NES=-14.5, FDR=0) (Figure 6E).

In line with these results, many of the transcriptional signatures related to hematopoietic stem cells and leukemia (previously shown to be up-regulated in $p53^{R172H/\Delta}$ cells) were conversely enriched upon suppression of either Foxh1 (Figure 6E) or p53 (Figure S6A). As examples two genes involved in leukemia and hematopoietic cell differentiation, *Runx2* (Kuo et al., 2009) and *Mef2c* (Schuler et al., 2008) are both bound by Foxh1 and their expression is reduced by either Foxh1 or p53 knockdown (Figure 6F). Hence, our data show that mutant p53 induces Foxh1, which can directly bind to and control genes linked to the differentiation status and self-renewal properties of AML.

To confirm that these Foxh1-dependent transcripts were also observed in human AML, we derived a transcriptional signature composed of differentially up-regulated genes in $p53^{R172H/\Delta}$ versus $p53^{\Delta/\Delta}$ murine leukemias and compared it to expression data from different karyotypes of human AML as well as normal hematopoietic cells (Bagger et al., 2019). We observed a significant up-regulation of $p53^{R172H/\Delta}$ murine leukemia-derived transcriptional signature in CK-AML patients (dark red) compared to all other leukemia types (light red) or normal hematopoietic cells (black) (Figure 6G), suggesting our model transcriptionally resembles CK-AML harboring *TP53* mutations. A similar increase in Foxh1-dependent transcripts (sh.Foxh1 vs sh.Ren) was also observed in CK-AML patients (Figure 6H). These results reveal a FOXH1 signature in human AML harboring *TP53* mutations, further supporting the existence of a functional mutant p53-Foxh1 axis in this disease.

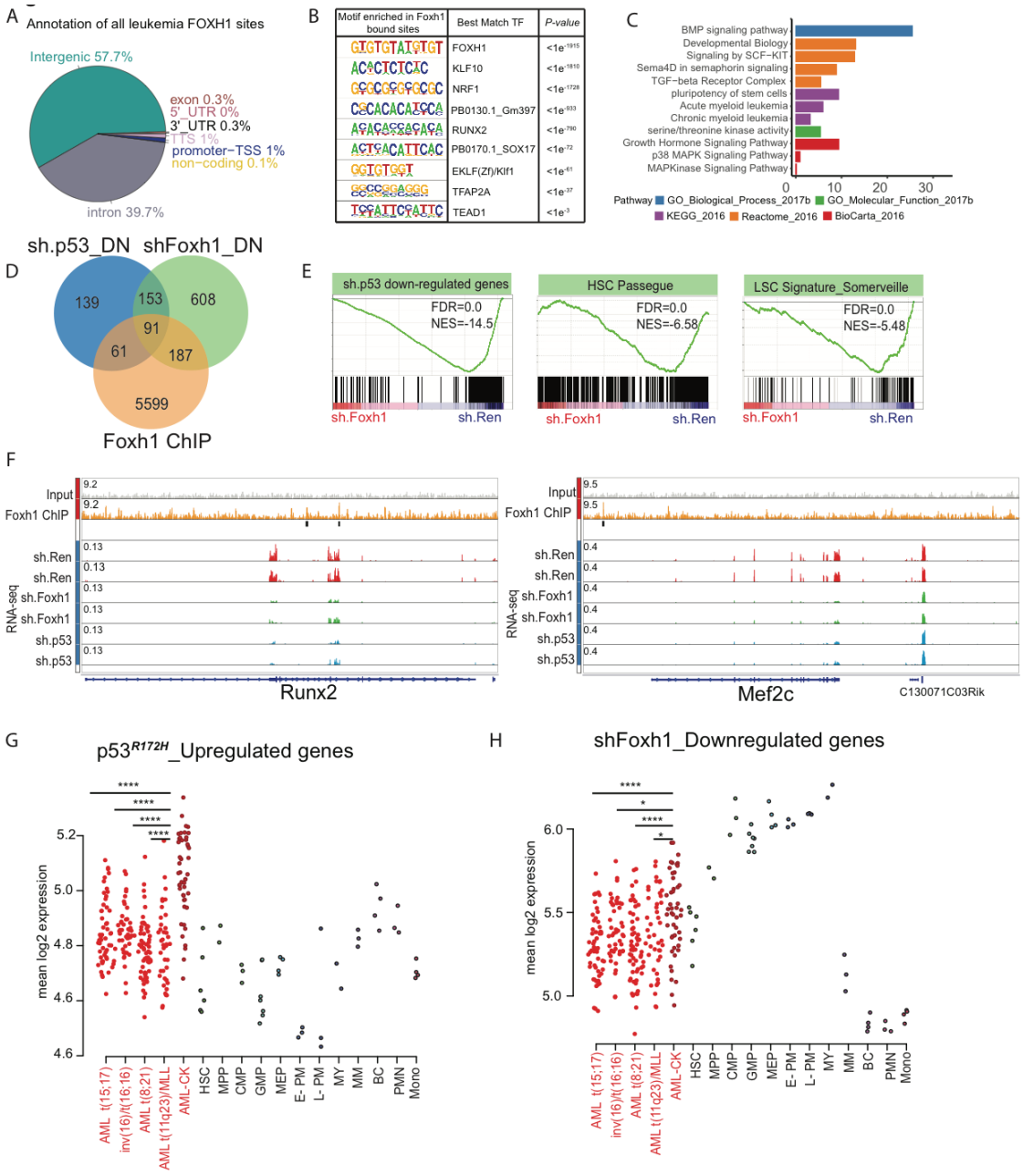

Figure 6. Foxh1 directly binds genes involved in leukemia and stem cell properties.

(A) Pie charts depicting the genome-wide distribution of Foxh1 binding in murine leukemic cells. **(B)** Motif enrichment analysis for the Foxh1 bound genomic regions in leukemic cells. **(C)** Gene ontology analysis of genes bound by Foxh1 in murine leukemic cells **(D)** Venn Diagram depicting the overlap between the genes down regulated upon p53 KD (blue circle, Foxh1 KD (green circle) and Foxh1 ChIP (orange circle). (**E**) GSEA from transcriptional profile of cells upon Foxh1 KD. (**F**) Gene tracks for Foxh1 ChIP-seq at the *Runx2* and *Mef2c* loci together with RNA-seq tracks from either sh.Ren (Red), sh. Foxh1 (green) or sh.p53 (blue). (**G**) Mean log2 expression of transcriptional signature composed of significantly up-regulated genes in $p53^{R172H/\Delta}$ versus $p53^{\Delta/\Delta}$ murine leukemias across AML and normal cells, as well as (**H**) same comparison for genes downregulated following Foxh1 KD. Student's t-test between CK- AML and other AML types: * p <0.05, ** p <0.005, *** p <0.0005, **** p <0.00005..

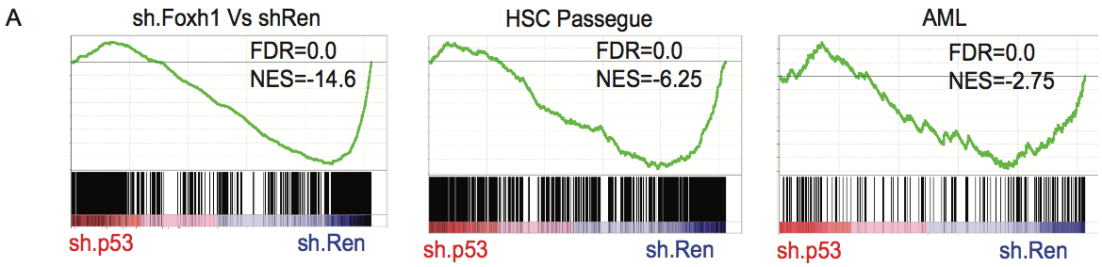

Figure S6. Elimination of mutant p53 in $p53^{R172H/\Delta}$ leukemic cells leads to differentiation. Related to Figure 6. (**A**) GSEA analysis from RNA-seq data in $p53^{R172H/\Delta}$ cells where mutant p53 was depleted with an shRNA.

Foxh1 is necessary and sufficient for the enhanced self-renewal phenotype produced by mutant p53.

To further explore the links between mutant p53, Foxh1, and aberrant self-renewal, we knocked-down mutant p53 or Foxh1 in *p53*$^{R172H/\Delta}$ HSPCs and performed CFU and immunophenotyping assays. Knockdown of Foxh1 ablated the replating capacity of these cells (Figure 7A), phenocopying in large part the effects observed upon mutant p53 knockdown. Furthermore, similar to mutant p53 ablation, Foxh1 suppression leads to the downregulation of the stem cell factor receptor cKit and the stem cell antigen 1 (Sca-1) in *p53*$^{R172H/\Delta}$ HSPCs (but not in p53 deficient cells), which is functionally accompanied by coarsening of chromatin and nuclear segmentation, morphological changes indicative of differentiation (Figure 7B and Figure S7A and S7B). Conversely, over-expression of Foxh1 in both p53$^{WT/WT}$ and p53$^{\Delta/\Delta}$ HSPCs endowed these cells with increased colony forming ability (Figure 7C) and also led to the up-regulation of cKit and Sca-1 along with concomitant down-regulation of Gr1/Cd11b (Figure 7D and Figure S7C). Analogous results were also observed in leukemia cells, where suppression of either mutant p53 or Foxh1 in two *p53* mutant AML lines reduced cKit expression (Figure S8A-D) and led to cellular differentiation determined by morphological criteria (Figure S8E and S8F) and transcriptional profiling (Figure S8G). Finally, to determine whether Foxh1 could phenocopy mutant p53 effects, we performed an epistasis experiment using *p53*$^{R172H/\Delta}$ HSPCs where mutant p53 was suppressed and cells were co-transduced to overexpress either a Foxh1 cDNA or control vector and examined for self-renewal capacity in serial replating assays. Enforced Foxh1 expression partially

reversed the loss of replating potential produced by suppressing mutant p53 (Figure 7E), suggesting that Foxh1 functions downstream of mutant p53 to enforce aberrant self-renewal. Collectively, these data demonstrate that Foxh1 is necessary and sufficient to support an aberrant self-renewal phenotype in both pre-malignant and malignant p53 mutant cells.

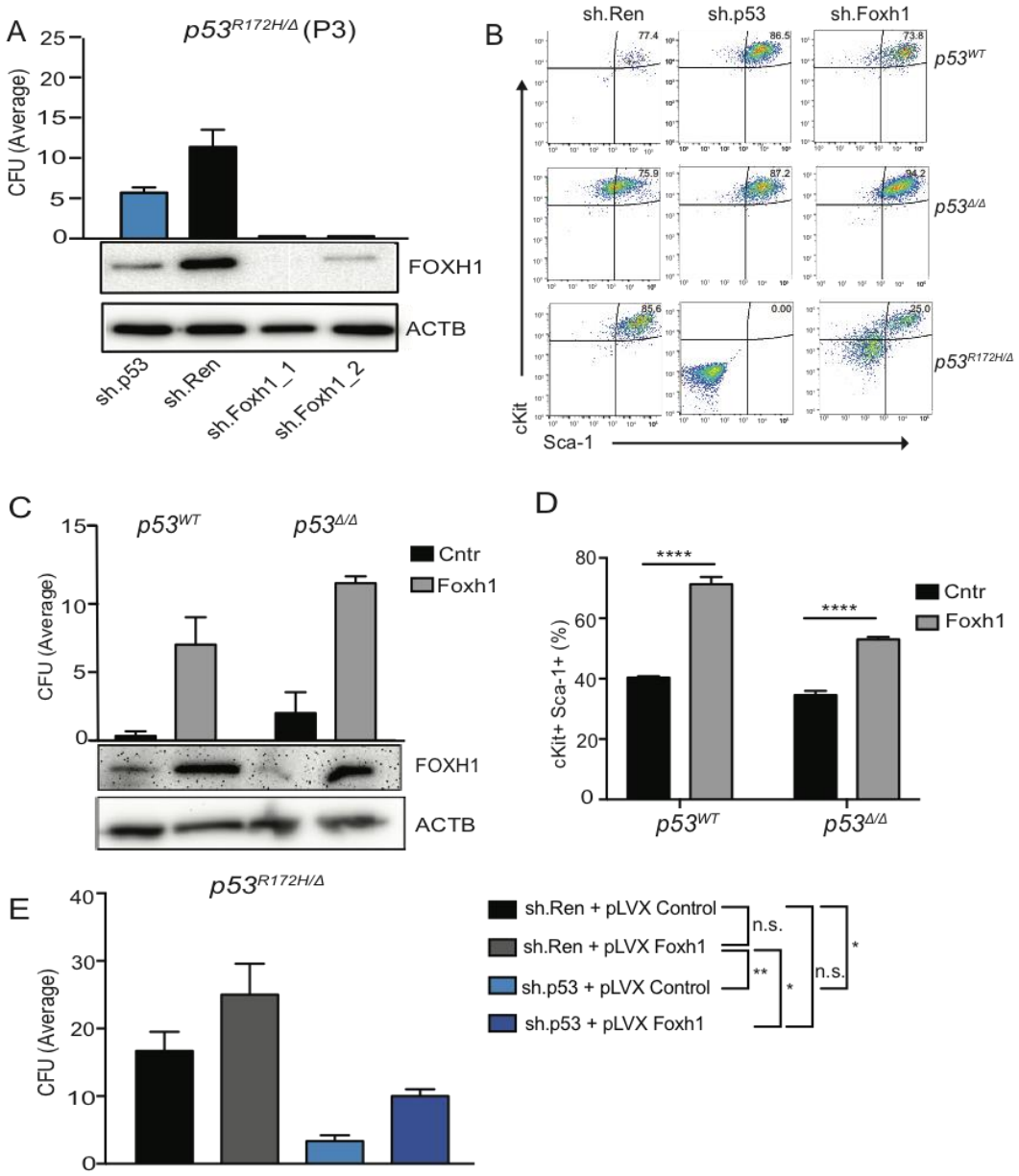

Figure 7. ***Foxh1 is necessary and sufficient for the enhanced self-renewal phenotype produced by mutant p53.*** **(A)** Total number of colony-forming units (CFU) generated by $p53^{R172H/\Delta}$ HSPCs containing sh.p53 (blue), sh.Ren (black), shFoxH1.1072 (1) (plum), shFoxH1.1116 (2) (maroon). Data are representative of three experiments. Error bars correspond to mean ±s.e.m (n=3). Lower panels: Western-blotting intensities for FOXH1 for the different conditions. **(B)** $cKit^+$ and $Sca\text{-}1^+$ expression analyzed by FACS in sh.Ren, sh.p53 and sh.FoxH1 containing HSPCs from $p53^{WT}$, $p53^{\Delta/\Delta}$ and $p53^{R172H/\Delta}$ mice. Data are representative of three experiments. **(C)** Total number of colony-forming units (CFU) generated by $p53^{\Delta/\Delta}$ and $p53^{WT}$ HSPCs containing pLVX Control (black) or pLVX Foxh1 cDNA (grey). Data are representative of three experiments. Error bars correspond to mean ±s.e.m (n=3). Lower panel: Western-blotting for FOXH1 for the different conditions. **(D)** Percentage of $cKit^+Sca\text{-}1^+$ HSPCs analyzed by FACS in $p53^{\Delta/\Delta}$ and $p53^{WT}$ cells containing pLVX Control or pLVX Foxh1 cDNA. Data are representative of three experiments. Error bars correspond to mean ±s.e.m (n=3). **(E)** Total number of colony-forming units (CFU) generated by $p53^{R172H/\Delta}$ HSPCs containing sh.Ren+pLVX Control (black), sh.Ren+pLVX Foxh1 cDNA (grey), sh.p53+ LVX Control (light blue), sh.p53+pLVX Foxh1 cDNA (dark blue). Data are representative of three experiments. Error bars correspond to mean± s.e.m(n=3)*$p<0.05$,**$p<0.005$,***$p<0.0005$

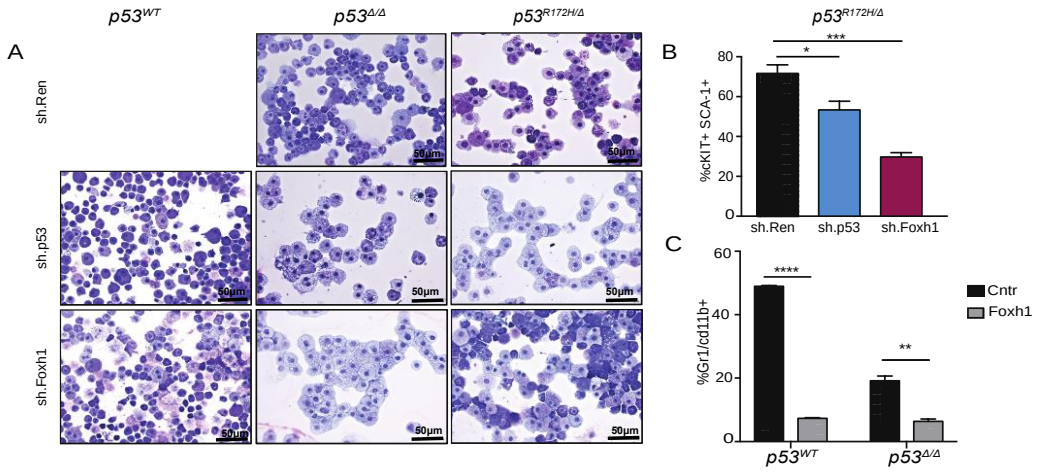

Figure S7. Foxh1 loss in *p53*$^{R172H/\Delta}$ HSPCs leads to differentiation. Related to Figure 7. (**A**) Cytospins from cells growing in CFU from *p53*$^{WT/WT}$, *p53*$^{\Delta/\Delta}$, and *p53*$^{R172H/\Delta}$ cKIT+ cells with either an sh.Ren, sh.p53 or sh.Foxh1. (**B**) Percentage of cKIT and Sca-1 expression in sh.p53 *p53*$^{R172H/\Delta}$ cKIT+ cells as assessed by FACS. (**C**) Percentage of Gr1 and Cd11b+ expression in *p53*$^{WT/WT}$ and *p53*$^{\Delta/\Delta}$ cKIT+ cells with pLVX control or pLVX Foxh1 cDNA overexpression. Data are representative of three experiments. Error bars correspond to mean ± s.e.m (n=3) * p <0.05, ** p <0.005, *** p <0.0005.

DISCUSSION

While mutations in the *TP53* tumor suppressor gene ablate its anti-proliferative functions, some mutant *p53* alleles also appear to produce "gain-of-function" phenotypes that display more profound phenotypes than those produced by complete p53 loss. Nonetheless, studies investigating the basis for these effects have failed to

coalesce around a common biological or molecular mechanism and, indeed, a recent comprehensive analysis of DNA sequence and functional genomics data suggested that the primary selective pressure for the appearance of p53 mutation in cancer arises from their purely inactivating and/or dominant-negative effects (Giacomelli et al., 2018). Here we studied the action of the most common *p53* mutant allele in the initiation and maintenance of acute myeloid leukemia, a well characterized liquid tumor where p53 loss is linked to aggressive and chemoresistant disease and one in which the potential GOF effects of mutant p53 have not been previously examined. We show that this p53 mutant accelerates leukemia onset and, strikingly, is required for leukemia maintenance, such that suppression of mutant p53 eliminates leukemia initiating potential.

The biological basis of AML involves the emergence of leukemic blasts that have acquired mutations that drive increased proliferation of stem and progenitor cells, block their maturation, and promote their aberrant self-renewal (Kelly and Gilliland, 2002; Takahashi, 2011). In our models, the murine $p53^{R172H}$ mutant contributes to the latter activity, such that its elimination in leukemic cells releases the differentiation block. Similar results are observed with human AML cells harboring the equivalent *R175H* allele and likely explain the apparent requirement of certain other leukemia cells to additional mutant p53 alleles (e.g. *R248Q*; see Figure S1B – (Wang et al., 2017)). Taking advantage of well-validated assays of self-renewal in the hematopoietic system, we show that $p53^{R172H}$ acts in non-transformed hematopoietic cells to promote self-renewal to a substantially greater degree than does p53 loss, and that suppression of mutant p53 reverses these effects. Thus, in AML, *mutant p53* can produce phenotypes

analogous to *bone fide* oncogenes, such as the MLL-AF9 fusion oncoprotein, which also contributes to leukemia by enforcing aberrant self-renewal and exerts a continuous dependency for disease maintenance (Armstrong et al., 2002; Somervaille and Cleary, 2006; Zuber et al., 2011b).

While most *TP53* mutations disrupt its DNA binding capabilities, the resulting proteins are frequently stable and retain an intact transcriptional activation domain (Laptenko and Prives, 2006; Weisz et al., 2007). Some studies suggest that mutant p53 can be recruited to chromatin to induce gene expression via interaction with other transcriptional regulators, such as NF-Y and ETS2 (Di Agostino et al., 2006; Do et al., 2012; Weisz et al., 2007; Zhu et al., 2015). Others studies support a model where mutant p53 proteins can directly bind to and perturb the function of other transcription factors, including p63, p73, and SREBP (Di Agostino et al., 2006; Do et al., 2012; Freed-Pastor et al., 2012; Weissmueller et al., 2014; Zhu et al., 2015). In the AML system studied herein, mutant p53 increases the expression of the Foxh1 transcription factor, leading to its significant upregulation compared to $p53^{\Delta/\Delta}$ leukemias. Functional studies revealed that $p53^{R172H}$ is necessary and sufficient to induce Foxh1 which, in turn, binds stem cell-associated genes and contributes to enhanced self-renewal. The precise details of how mutant p53 induces Foxh1 remain to be determined and, to date, we have been unable to detect a robust ChIP signal for mutant p53 on DNA or validate an interaction with other p53 family members. Nevertheless, the importance of this molecular axis is supported by the conserved ability of mutant p53 to increase Foxh1 expression cross

species and by the significant upregulation Foxh1 expression in CK-AML, a leukemia subtype characterized by a high frequency of *TP53* mutations.

Foxh1 is expressed in embryonic stem cells and during early embryonic development. There, it is induced by the TGF-β family member Nodal (Brennan et al., 2001) and acts to promote an epithelial to mesenchymal transition that takes place during gastrulation (Attisano et al., 2001; Yamamoto et al., 2001). Foxh1 is not normally expressed in the adult hematopoietic system and, as such, mutant p53 appears to hijack Foxh1-driven programs to promote leukemia by enforcing the expression of genes normally involved in promoting stemness and cell plasticity during hematopoiesis. Like the $p53^{R172H}$ allele, p53-deficiency – as produced by two homozygous null *p53* alleles – can also accelerate AML development by promoting aberrant self-renewal and enhancing leukemia initiating potential (Zhao et al., 2010). However, the aberrant program produced by the p53 null state is not as potent as that produced by $p53^{R172H}$ and does not depend on elevated levels of Foxh1. Presumably, this distinct rewiring of self-renewal programs explains why cells differentiate and lose leukemia initiating capacity upon mutant p53 elimination to produce a p53 null state, the latter event being known to promote leukemogenesis if present as an initiating event. Thus, in this context, mutant p53 GOF produces a more profound phenotype than p53 loss while concomitantly creating unique molecular dependencies.

Our results may also have relevance to the pathogenesis of human AML. Specifically, beyond the GOF effect of $p53^{R172H}$ in leukemogenesis, this work reveals that mutant

p53 can exert its phenotypes even prior to leukemia onset, leading to the continuous self-renewal of HSPCs *in vitro* and *in vivo*. Most previous GOF studies of mutant p53 have been in the context of established cancer and, to our knowledge, this is the first study to reveal that a GOF activity can produce molecular dependencies *prior* to neoplastic transformation. The effect is such that elimination of the mutant protein in pre-malignant cells promotes differentiation, impairs colony-forming ability, and reduces competitive fitness during long-term hematopoiesis *in vivo.* While *TP53* mutations are considered a later event during the progression of many solid tumors (Vogelstein et al., 2013), they are present as "truncal" mutations with a high variant allele frequency in human AML such that we identified 35 AML cases with the *R175H* mutation and a median variant allele frequency (VAF) of 36% that showed evidence of clonal or sub-clonal presentation. (Wong et al., 2015). Indeed, *TP53* mutations are often observed in clonal hematopoiesis (CH), a phenomenon where stem cells harboring leukemia-associated mutations expand in the peripheral blood of individuals in more than 0.02 VAF without an overt disease (Abelson et al., 2018; Steensma et al., 2015; Xie et al., 2014). We identified 9 cases of CH that harbored *TP53 R175H* mutations with a high VAF that ranged from 2-9%. Strikingly, 3 out of 9 cases (~33%) only harbored a single mutation - *TP53 R175H* - strongly suggesting that this is an early event. Of the remaining 6 cases, 2 individuals harbored clonal *TP53* R175H mutations while the remaining 4 contained sub-clonal mutations. Furthermore, individuals presenting with clonal hematopoiesis involving a *TP53* mutation have the highest risk for progressing to AML (Abelson et al., 2018). Taken together, these observations strongly suggest that $TP53^{R175H}$ mutation is an early, "first-hit" event in the pathogenesis

of human AML.

Our data predict that some cancers might depend on continuous expression of mutant *TP53* and are consistent with studies on the $p53^{R248Q}$ mutant protein in mouse models of lymphoma, colon cancer, and others (Alexandrova et al., 2015; Schulz-Heddergott et al., 2018). Nevertheless, it seems unlikely that all mutant *TP53* alleles have GOF activity, and even those that do may impinge on distinct molecular mechanisms depending on context. For example, while $p53^{R172H}$ can display GOF effects by promoting invasion and metastasis in a pancreas cancer model, it is not required for the sustained proliferation of pancreatic cancer cells, at least *in vitro* (Weissmueller et al., 2014). Moreover, a recent report analyzing broad functional genomic datasets concluded that mutant *TP53* was generally dispensable for the proliferation of human cell lines in culture (Giacomelli et al., 2018). However, this study only assessed the effects of gene disruption on proliferation under *in vitro* conditions and did not examine signals associated with allele specificity or cellular context that are highly prevalent in the biology of p53 (Kastenhuber and Lowe, 2017), whereas studies *in vivo* have confirmed a greater advantage of some of the hotspot mutations (Kotler et al., 2018). Indeed, our functional experiments show a requirement for $p53^{R175H}$ in the leukemia initiating potential of a human AML line, which could have been missed by performing a different type of analysis. Additionally, upon detailed inspection of publicly available CRISPR screening data, we note that some *TP53* mutant lines appear to depend on mutant *TP53* for their survival (Figure S1B) (Wang et al., 2017). Dissecting the underlying mechanism of this context specificity will be important to determine when

and where mutant p53 proteins and their associated molecular programs may represent therapeutic targets.

Still, despite the perplexing range of molecular and biological mechanisms that have been attributed to GOF *p53* mutations, our studies reveal convergent features between mutant p53 GOF action in solid and liquid tumors, as well as in experimental models of induced pluripotency (Takahashi et al., 2014). In solid tumors, the best characterized phenotype associated with *TP53* GOF mutations involves their ability to drive invasion and metastasis (Lang et al., 2004; Morton et al., 2010; Olive et al., 2004; Schulz-Heddergott et al., 2018; Weissmueller et al., 2014), which is often associated with an EMT and cellular plasticity that enables the acquisition of a more stem cell like state. Consistent with this, the transcriptional profiles of p53 mutant tumors are enriched for gene signatures expressed in embryonic stem cells (Ben-Porath et al., 2008; Mizuno et al., 2010; Shibue and Weinberg, 2017). In AML, $p53^{R172H}$ promotes self-renewal, as well as a transcriptional landscape enriched for gene signatures linked to stemness and, intriguingly, EMT. One such gene is *Foxh1*, which is known to promote EMT during embryonic development, yet we demonstrate here that it can drive aberrant self-renewal in AML. Remarkably, these same players contribute to the generation of iPS cells by the Yamanaka factors: $p53^{R172H}$ enhances iPS cell formation beyond p53 loss (Yi et al., 2012) and Foxh1 cooperates with p53-deficiency to achieve a similar effect (Takahashi et al., 2014). Collectively, these observations point to a convergent action of p53 GOF on cellular plasticity and stemness, which can influence distinct cancer processes depending on context.

METHODS

Animal models

All mouse experiments were approved by the Institutional Animal Care and Use Committee at Memorial-Sloan Kettering Cancer Center. *$p53^{LSLR172H}$* and *$p53^{LoxP}$* mice were described previously (Olive et al., 2004). C57BL/6 (B6.SJL-*Ptprca Pepcb/BoyJ* (CD45.1) mice, thymectomized mice, *Vav1Cre* and *Mx1Cre mice* were purchased from Jackson Laboratory and bred in a mouse facility at MSKCC.

Primary cell culture

Total bone marrow cells from *$p53^{R172H/F}$;Vav1Cre, $p53^{F/F}$;Vav1Cre and $p53^{F/F}$ (WT) mice* (6-8 weeks) or purified bone marrow $cKit^+$ cells were transduced as described below with *sh.Ren or sh.p53* retrovirus and plated in methylcellulose medium (Methocult M3434, Stem Cell Technologies). Cells were seeded at 10,000 total bone marrow cells or 4,000 purified $cKit^+$ cells per replicate. Colony forming units were enumerated using a Zeiss Axio Observer microscope, and cells were re-plated (4,000 cells/replicate) every 7–10 days. Primary mouse PMN leukemias derived from *$p53^{R172H/F}$;Vav1Cre* and *$p53^{F/F}$;Vav1Cre mice* were cultured in 1:1 DMEM to IMDM with 10% FBS (Gibco), 100 U/mL penicillin, 100 μg/ml streptomycin, 50 μM 2-mercaptoethanol and recombinant mouse SCF (50 ng/ml), IL3 (10 ng/ml) and IL6 (10 ng/ml) at 37°C in 5% CO_2. Puro (puromycin) and Dox (doxycycline) were used at a final concentration of 1 μg/ml for all cell culture assays.

Cell lines

The human leukemia line KY821 (JCRB cell bank) was grown in RPMI 1640 and 20% FBS (Gibco). KL922 (*p53*$^{\Delta/\Delta}$), KL973 (*p53*$^{R172H/11B3}$) and KL974 (*p53*$^{R172H/\Delta}$) primary mouse cell lines (Chen et al., 2014; Liu et al., 2016) were cultured with RPMI, 10% FBS (Gibco) and recombinant mouse SCF (50 ng/ml), IL3 (10 ng/ml) and IL6 (10 ng/ml). PlatinumE (Morita et al., 2000) cells were a gift from Craig Thomson's lab and HEK293T were purchased from ATCC (CRL-3216) and were used for retroviral production while maintained in DMEM with 10% FBS. Media were supplemented with 100 U/mL penicillin, 100 μg/ml streptomycin and cultures were incubated at 37°C, 5% CO_2. All cells were tested negative for mycoplasma (MP0025-1KT) and were not maintained for longer than 10 passages in culture. For cell line authentication we confirmed TP53 expression by WB and Sanger sequencing confirmed the specific mutation.

Xenotransplantation

Experiments were carried out in accordance with institutional guidelines approved by MSKCC. Immune-deficient NSG mice (6-10 weeks-old) mice were bred under pathogen-free conditions. and were sub-lethally irradiated (200-250 cGy) 3-24 hours before transplantation. KY821 cells were injected by tail-vain injection. CBC analysis was performed on peripheral blood collected from submandibular bleeding using a Drew Hemavet Analyzer (Veterinary Diagnostics).

Histology and microscopy

Tissues were dissected from mice for fixation overnight in 10% formalin (Fisher). Bones were decalcified per manufacturer's instructions (IDEXX BioResearch), and fixed tissues were dehydrated and embedded in paraffin for sectioning. Paraffin sections (5 μm) were prepared and stained with hematoxylin and eosin (H&E) (Leica Autostainer XL).

Flow cytometry

Single cell suspensions were prepared from bone marrow, spleen or peripheral blood. Red blood cells were lysed with ammonium-chloride-potassium (ACK) buffer, and the remaining cells were resuspended in PBS with 3% FBS. Non-specific antibody binding was blocked by incubation with 20 μg/ml Rat IgG (Sigma-Aldrich) for 15 min, and cells were then incubated with the indicated primary antibodies for 30 min on ice. Stained cells were quantified using a Fortessa analyzer (BD Biosciences) or isolated with a FACSAria II (BD Biosciences). FlowJo software (TreeStar) was used to generate flow cytometry plots. More details on FACS antibodies found in Table S2.

Bone marrow competitive transplantation

Femurs and tibiae were isolated from donor $p53^{F/F}$ (WT), *$p53^{F/F}$;Mx1Cre* or *$p53^{R172H/F}$;Mx1Cre* (CD45.2), as well as *WT* (CD45.1) mice. Bones were flushed with PBS and the single-cell suspension was centrifuged (5 min, 0.5g, 4 °C) and treated with red cell ACK lysis buffer, as described above. Total nucleated bone marrow cells were re-suspended in PBS, passed through a 40 μM cell strainer and counted. Donor cells (1×10^6 per genotype, per mouse) were mixed 1:1 with support bone marrow cells (CD

45.1), and transplanted via retro-orbital injection into lethally irradiated (950 Rad) CD45.1 recipient mice. Chimerism was monitored by flow cytometry (anti-CD45.1 and anti-CD45.2, BD Bioscience) of peripheral blood at 4-week intervals post-transplant three weeks after last pIpC injection and for 16 weeks at which time mice were sacrificed and chimerism was assessed in other hematopoietic compartments (bone marrow).

Retroviral transduction

Hematopoietic stem and progenitor cells were isolated by sorting $Lin^{-}cKit^{+}Sca1^{+}$ cells or enriched using an autoMACS Pro separator (Miltenyi Biotec) using CD117 magnetic microbeads (Miltenyi Biotech, 130-091-224), then cultured in the presence of 50 ng/ml SCF, 10 ng/ml IL-3, and 10 ng/ml IL-6, and infected with concentrated supernatants of *LMNe-sh.Ren/sh.p53-BFP or MLPe sh.Ren/sh.p53/sh.FoxH1* retrovirus after 24 and 48 h (more details about the shRNAs in Table S2). Transduction efficiency was determined by reporter fluorescence at 48 h, and 5,000 sorted cells were injected into CD45.1 mice as described above.

Cell viability and DNA synthesis

Apoptosis assays were performed by staining with Annexin V (BD Pharmingen) according to the manufacturer's instructions, in combination with DAPI. For cell cycle studies, BrdU (BD Pharmingen) was used per manufacturer's instructions and stained with 2 μg/ml DAPI prior to flow cytometric analysis.

Quantitative RNA expression assays

Total RNA was extracted from cells using the RNeasy Plus Mini Kit (Qiagen). RNA quantity and quality were determined using an Agilent 2100 Bioanalyzer. RNA-seq libraries were prepared from total RNA by polyA selection using oligo-dT beads (Life Technologies) according to the manufacturer's instructions. The resulting poly-A+ RNA served as input for library construction using standard Illumina protocols. Sequencing was performed on an Illumina HiSeq 2500 sequencer using 50 bp pair-end reads. For mRNA quantification, total RNA was used for cDNA synthesis (Agilent). Real-time PCR reactions were carried out using SYBR Green Master Mix (QuantaBio) and a Via7 (AB Applied biosystems).

RNA sequencing analysis

RNA-Seq library construction and sequencing were performed at the integrated genomics operation (IGO) Core at MSKCC. Poly-A selection was performed. For sequencing, approximately 30 million 50bp paired-end reads were acquired per replicate condition. Resulting RNA-Seq data was analyzed by removing adaptor sequences using Trimmomatic (Bolger et al., 2014). RNA-Seq reads were then aligned to GRCh37.75 (hg19) with STAR (Dobin et al., 2013) and genome-wide transcript counting was performed by HTSeq (Anders et al., 2015) to generate a matrix of fragments per kilobase of exon per million fragments mapped (RPKM). Gene expressions of RNA-Seq data were managed by hierarchical clustering based on one minus Pearson correlation test using Morpheus (https://software.broadinstitute.org/morpheus/). All results from the RNA-Seq experiments can be found under GSE125097.

Gene set enrichment analysis

Gene set enrichment analysis was performed using gene set as permutation type, 1,000 permutations and log2 ratio of classes, or with gene set and Signal2Noise as metrics for ranking genes. Gene sets used in this study were identified from the Molecular Signatures Database (MSigDB Curated v4.0). Gene pathways and functions were assessed using Ingenuity Pathway Analysis (Qiagen Bioinformatics).

Expression of gene signatures in human AML and normal cells.

Visualization of gene signatures derived from transcriptional data as Log2 expression values for different karyotypes of AML patients described previously in GSE42519 (Rapin et al., 2014). For normal hematopoietic cells values were averaged over all genes in each signature and visualized by using Sinaplot. Student's t-test was performed using the R programming language (https://www.R-project.org/).

Quantification and Statistical Analysis

All p-values were calculated using unpaired two-tailed Student's *t* test with Graphpad Prism software, unless otherwise described in the methods or figure legends. No specific randomization or blinding protocol was used for these analyses. Statistically significant differences are indicated with asterisks in figures with the accompanying p-values in the legend. Error bars in figures indicate standard deviation (SD) or standard error of the mean (SEM) for the number of replicates, as indicated in the figure legend.

Plasmids and viral production

All vectors were derived from the Murine Stem Cell Virus (MSCV, Clontech) retroviral vector backbone. miRE-based shRNAs were designed and cloned as previously described (Zuber et al., 2011a) into the LT3GEPIR (TRE3G-GFP-miRE-PGK-PuroR-IRES-rtTA3) vector (Fellmann et al., 2013). The mouse Foxh1 cDNA was cloned in a pVXL-hygromycin-mFoxh1 vector (provided by Yilong Zou, Massagué lab, MSKCC). All constructs were verified by sequencing. Lentiviruses were produced by co-transfection of 293T cells with 10 ug LT3GEPIR construct and helper vectors (3.75 ug psPAX2 and 1.25 ugVSV-G). For retroviral infection PlatinumE cells were plated in 15 cm diameter dishes each transfected with 54 ug of MSCV vectors and 2.7ug of VSV-G and 8.1ug of pCl-eco. Transfection of packaging cells was performed using HBS and CaCl2 or Mirus transfection reagent (MIR 2304). Viral supernatants were passed through a 0.45 um filter (Millipore) and concentrated with Centrifugal Filter units (Millipore) to obtain high virus titer. Concentrated virus was supplemented with 8 ug/ml of polybrene (Sigma) before adding to target cells.

Immunoblotting. For protein lysates, cells were incubated with RIPA buffer supplemented with protease inhibitors (Protease inhibitor tablets, Roche) for 30 min and cleared by centrifugation (15 min 14.000 rpms 4C). Protein was quantified using the DC protein assay (BioRad). The following antibodies were used for immunoblotting: β-ACTIN (ac-15, Sigma), mTP53 (CM5, Leica microsystems), hTP53 (DO-1, Santa Cruz), mFoxh1 (Abcam 49133) and hFOXH1 (Abcam 102590).

Chromatin immunoprecipitation (ChIP). Chromatin immunoprecipitation was performed as previously described (Banito et al., 2018). Briefly, KL974 ($p53^{R172H/\Delta}$) cells were fixed with 1% formaldehyde for 15 min, and the cross-linking reaction was stopped by adding 125mM glycine. Cells were washed twice with cold PBS and lysed in buffer (150 mM NaCl, 1%v/v Nonidet P-40, 0.5% w/v deoxycholate, 0.1% w/v SDS, 50 mM Tris pH8, 5m M EDTA) supplemented with protease inhibitors. Cell lysates were sonicated using a *Covaris E220 Sonicator* to generate fragments less than 400 bp. Sonicated lysates were centrifuged, and incubated overnight at 4^{o}C with specific antibodies (Foxh1 Abcam 49133;). Immunocomplexes were recovered by incubation with 30 ul protein A/G magnetic beads (Thermofisher) for 2h at 4^{o}C. Beads were sequentially washed twice with RIPA buffer, increasing stringency ChIP wash buffers (150 mM NaCl, 250 mM NaCl, 250 mM LiCl) and finally TE buffer. Immunocomplexes were eluted using elution buffer (1% SDS, 100mM $NaHCO_3$), and cross-linking was reverted by addition of 300 mM NaCl and incubation at 65^{o}C overnight. DNA was purified using a PCR purification kit (Qiagen). Input chromatin was used for estimation of relative enrichment. The results for the ChIP-seq experiments can be found under GSE125097.

ChIP-Seq Library Preparation, Illumina Data Analysis and Peak Detection. ChIP-Seq libraries were prepared at the Center for Epigenetic Research (MSKCC) using the NEBNext® ChIP-Seq Library Prep Master Mix Set for Illumina® (New England

BioLabs) following the manufacture's instructions. Reads were trimmed for quality and Illumina adapter sequences using 'trim_galore' before aligning to mouse assembly mm9 with bowtie2 using the default parameters. Aligned reads with the same start site and orientation were removed using the Picard tool MarkDuplicates (http://broadinstitute.github.io/picard/). Density profiles were created by extending each read to the average library fragment size and then computing density using the BEDTools suite (http://bedtools.readthedocs.io). Enriched regions were discovered using MACS2 and scored against matched input libraries (fold change > 2 and p-value < 0.005). Dynamic regions between two conditions were discovered using a similar method, with the second ChIP library replacing input. Peaks were then filtered against genomic 'blacklisted' regions (http://mitra.stanford.edu/kundaje/akundaje/release/blacklists/mm9-mouse/mm9blacklist.bed.gz) and those within 500 bp were merged. All genome browser tracks and read density tables were normalized to a sequencing depth of ten million mapped reads. Dynamic peaks were annotated using linear genomic distance and motif signatures were obtained using the 'de novo' approach with Homer v4.5 (http://homer.ucsd.edu/).

CHAPTER II: Functional contribution of members of the PRC2 complex in Complex Karyotype Acute Myeloid Leukemia

SUMMARY

Recurring deletions of chromosomes 7 and 17 (7/del(7q) and 17/del(17p)) occur in myelodysplastic syndromes and acute myeloid leukemia (AML) and are associated with poor prognosis. However, the presence of functionally relevant tumor suppressors at these sites is largely unexplored. Using RNAi we show that reduction in gene dosage of *Ezh2* and *Suz12*, located on 7q36.1 and 17q11.2 respectively, cooperate with loss of p53 and Mll3, a previously shown tumor suppressive gene on chromosome 7q36.1 to promote leukemogenesis. Ezh2 and Suz12 suppression enhance self-renewal of HSPCs and similarly to the human 7/del(7q) and 17/del(17p) AMLs, the derived leukemias are refractory to conventional chemotherapy. Hence, our mouse model suggests that Ezh2 and Suz12 are putative tumor suppressive genes in p53-deficient AML and can contribute to leukemia without being mutated but rather lost via chromosomal aberrations.

INTRODUCTION

Acute myeloid leukemia (AML) is a heterogenous disease in terms of its clinical and genetic presentation. It is thought to be caused by mutations that can increase the proliferative capacity of the cells but also impair their ability to respond to

differentiation signals (Kelly and Gilliland, 2002). With the advent of next-generation sequencing, genomic studies revealed a number of genes that are recurrently mutated in different AML subtypes, which not only led to greater understanding of the disease but has also allowed for new drug target discovery (Patel et al., 2012).

However, some subsets of AML harbor large chromosomal deletions that beyond the impact they have on the prognosis of patients their biological and molecular significance is very poorly understood. For example, monosomy 7 or large deletions of 7q (7/del(7q)) are found in patients with myelodysplastic syndrome (MDS) as well as in patients with AML, and often co-occur with monosomy on 5/del(5q) and/or del(17p) in the subtype of patients classified as complex karyotype AML (CK-AML) (Mrozek, 2008). These cytogenetic characteristics are also found in patients with therapy-related myeloid neoplasms arising after treatment with alkylating agents for a different malignancy (Qian et al., 2010). More than any other type of AML, these types of myeloid disorders are chemoresistant and leave these patients with very few treatment options (Dohner et al., 2010).

TP53 which is a well-established tumor suppressor gene (TSG), resides on chromosome 17p which is the most commonly deleted chromosomal region in human cancers (Beroukhim et al., 2010). It has also been shown recently that a *TP53* mutation ($p53^{R172H}$) has GOF effects and can mediate enhanced self-renewal, supporting a new role for at least some of these mutations that are the most common genetic event in complex-karyotype and therapy-related AML (Loizou et al., 2019). In addition to *TP53* other putative tumor suppressors have been proposed for CK-AML at other chromosomal regions that include α-catenin (*CTNNA1*) on 5q31 (Liu et al., 2007), *NF1*

on 17q11 (Rucker et al., 2006), *SPRY4* on 5q31.3 (Zhao et al., 2015), *MLL3 (KMT2C)* on 7q36.1 (Chen et al., 2014) and *EGR1* on 5q31.2 (Joslin et al., 2007).

Despite the fact that AML is a disease driven by epigenetic dysregulation (Ntziachristos et al., 2013), the contribution of these chromosomal abnormalities in inactivating epigenetic modifiers is largely unknown with the exception of histone methyl-transferase MLL3 that was shown to act as a functionally relevant tumor suppressor within 7q (Chen et al., 2014).

The PRC2 complex which deposits repressive marks on histones has been described to be a target of mutations in different tumor types (Conway et al., 2015). More specifically, two members of the PRC2 complex, EZH2 that has the catalytic activity to mediate H3K27 methylation, and SUZ12 that is part of the core complex, have been shown to be mutated in leukemia (Conway et al., 2015). We reasoned that loss of *EZH2,* which is located on chromosome 7q36.1 and *SUZ12* that resides on chromosome 17q11.2 can contribute to leukemogenesis by acquired chromosomal breaks. Here we employed RNAi technology that allows for intermediate gene dosage, and showed that downregulation of these genes contributes to leukemia by enhancing the self-renewal properties of HSPCs and also leads to increased chemoresistance of leukemic cells.

RESULTS

Analysis of Co-occurring Alterations in Human Myeloid Neoplasms

We reasoned that there is a possibility for more tumor suppressor genes to exist on these frequent chromosomal aberrations and inside the minimally deleted regions (MDRs) that encompass other functional AML tumor suppressors such as *MLL3* and *NF1* (Chen

et al., 2014). We observed that *EZH2* and *SUZ12* encoding for key components of PRC2 complexes, were located proximal to *MLL3* and *NF1* on chromosomes 7 and 17 respectively (Figure 9A). Analysis of the AML TCGA dataset (Cancer Genome Atlas Research et al., 2013) showed that in the vast majority of AML cases both *EZH2* and *SUZ12* were concomitantly deleted along with the neighboring *MLL3* and *NF1* genes (Figure 9B). Notably, these aberrations frequently co-occurred with inactivation or deletion of *TP53* (Figure 9B). Based on these data and given the known interplay of Polycomp (PRC2) and trithorax (MLL3) complexes in development and cancer (Piunti and Shilatifard, 2016), we speculated that PRC2-deficiency might cooperate with p53 inactivation and *MLL3* loss in myeloid leukemogenesis. Notably, *NF1* and *TP53* alterations were the most significantly co-occurring genetic events in PRC2-deficient (*EZH2* or *SUZ12 loss*) AML patients (Figure 9C) and were associated with a significant decrease in overall survival either alone (dark blue line) or in combination with TP53 alterations (red line) (Figure 9D).

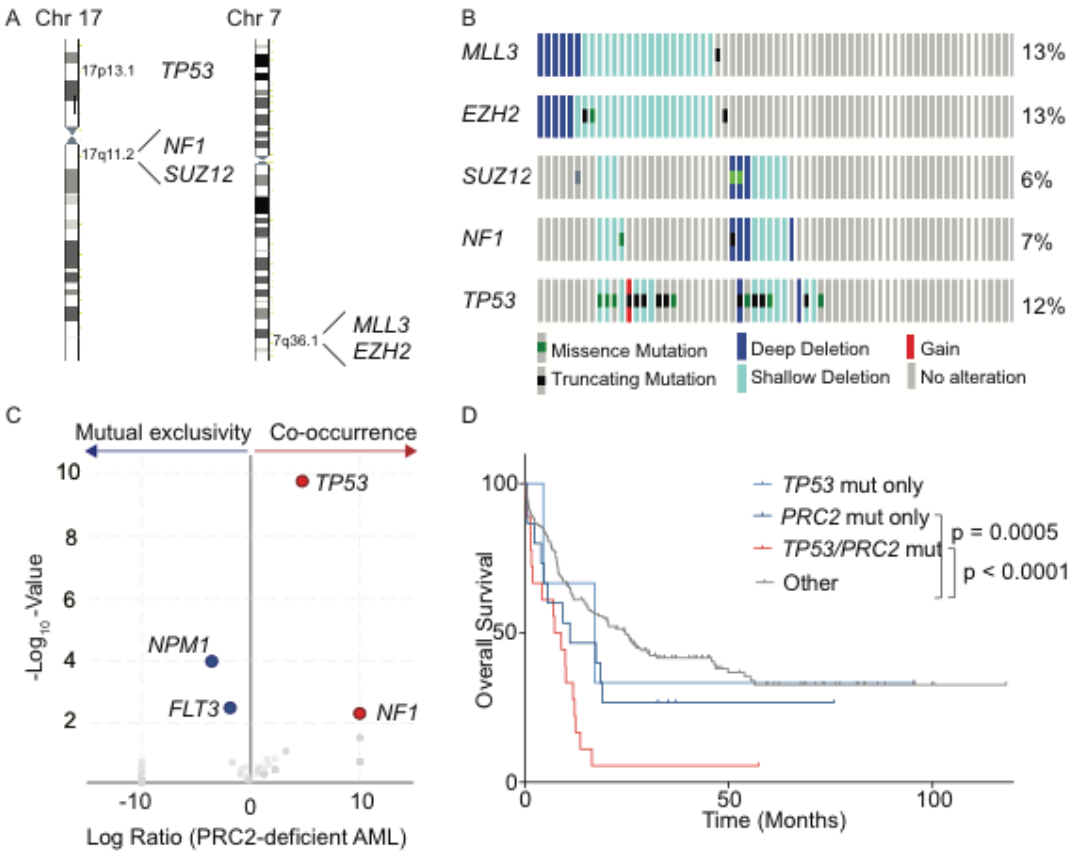

Figure 9 Co-deleted genes in AML

(A) Schematic representation of chromosomes depicting the minimally deleted regions that encompass NF1 and SUZ12 on chromosome 17 and MLL3 and EZH2 on chromosome 7. (B) Oncoprint showing the mutually inclusivity of MLL3 with EZH2 and SUZ12 with NF1 all of which can occur with TP53 mutations. (C) Volcano plot of the significantly occurring (red) and mutually exclusive genes (blue) in PRC2-deficient AML. (D) Overall Survival curve of patients with AML that are TP53-mutant (light blue), PRC2-mutant (dark blue) or exhibit both alterations (red) or neither (grey). P value calculated by log-rank test is indicated. (cBioPortal, TCGA).

PRC2 Suppression Cooperates with Other Lesions to Drive Leukemogenesis

To study the effect of PRC2 suppression during leukemogenesis, we used a transplantation-based mouse modeling approach that has been used to study the effects of genes in AML (Chen et al., 2014; Zhao et al., 2015; Zhao et al., 2010). This approach requires that HSPCs are retrovirally-transduced with vectors that express the desired genetic events producing ‘‘chimeric’’ mice after transplantation of these cells into syngeneic wild-type but also thymectomized mice for avoiding the occurrence of thymic lymphomas (Donehower et al., 1992; Loizou et al., 2019). Here we used shRNAs, which can model the impact of inactivation of genes as well as model haploinsufficient tumor suppressors (Chen et al., 2014; Hemann et al., 2003). We utilized shRNAs targeting Nf1 or Renilla luciferase (control) together with shRNAs for either Ezh2 or Suz12 or both into $p53^{F/F}$;$Mll3^{F/+}$; Vav1CRE HSPCs. This allowed us to study the effect of decreased expression of these genes while

eliminating the requirement for generating a multi-allelic genetically engineered mouse model.

To study the impact of PRC2 deficiency on leukemia we produced multiple shRNAs (n=5-6) for both Ezh2 and Suz12, capable of decreasing expression of these genes to various degrees aiming that the shRNA with the most suited knock-down would be selected *in vivo*. To access the independent and combined loss of function effect for each of these genes (*Ezh2, Suz12, Nf1*) in the $p53^{\Delta/\Delta}$;$Mll3^{\Delta/+}$ genetic background, we generated various shRNA vectors. The shRNAs were linked to either GFP or mCherry, so that the donor HSPCs were fluorescently labelled, allowing tracking of each shRNA independently in the recipient animals. This experimental strategy led to seven different shRNA combinations, yielding a mix of single or double positive GFP and mCherry HSPCs for each condition: PM ($p53^{\Delta/\Delta}$;$Mll3^{\Delta/+}$; shRen/Ren), PMN ($p53^{\Delta/\Delta}$;$Mll3^{\Delta/+}$; shRen/Nf1), PMN-E ($p53^{\Delta/\Delta}$;$Mll3^{\Delta/+}$; shNf1/Ezh2), PMN-S($p53^{\Delta/\Delta}$;$Mll3^{\Delta/+}$; shNf1/Suz12), PM-E ($p53^{\Delta/\Delta}$;$Mll3^{\Delta/+}$; shRen/Ezh2), PM-S ($p53^{\Delta/\Delta}$;$Mll3^{\Delta/+}$; shRen/Suz12) and PM-ES ($p53^{\Delta/\Delta}$;$Mll3^{\Delta/+}$; shEzh2/Suz12)(Figure 10A).

Following bone marrow transplantation, we monitored the chimeric thymectomized BM recipient mice over time for signs of disease and sacrificed the moribund mice for subsequent analysis. We observed the previously characterized cooperation of Nf1 in the $p53^{\Delta/\Delta}$; $Mll3^{\Delta/+}$ cells (Chen et al., 2014), whereas the Ren;Ren group ($p53^{\Delta/\Delta}$; $Mll3^{\Delta/+}$ alone) gave rise to leukemias with a later onset and with low penetrance (Figure 10B). Despite our initial observations that shEzh2 and shSuz12 shortened the survival in mice (data not shown), a second biological replicate showed no additional

effect on survival compared to mice transduced with Nf1 and Ren shRNA (shRen; shNf1: median survival = 83 days versus shNf1; Ezh2: median survival = 92.5 days, p = 0.5 versus shNf1; shSuz12: median survival = 85, p = 0.52) (Figure 10B). We did however observe a reproducible significant decrease in survival when we depleted Ezh2 (shRen; shEzh2) compared to the shRen; shRen group (p=0.03) (Figure 10B). This suggested that loss of Ezh2 accelerates leukemia initiation and progression on the $p53^{\Delta/\Delta}$;$Mll3^{\Delta/+}$ background.

We also observed features of leukemia in all the groups, such as elevated white blood cell (WBC) counts (Figure 10C), anemia as observed by low red blood cells (RBC) (Figure 10D), splenomegaly (Figure 10E) and hepatomegaly (not shown).

In addition to these pathognomonic features of leukemia, isolation of DNA from the BM of the leukemic mice and subsequent low pass DNA sequencing revealed that these cells had characteristics of chromosomal losses and gains recapitulating a key feature of CK-AML in patients (Figure 11A-D). Furthermore, in vitro culture of the leukemic bone marrow cells allowed the generation of cell lines from these models. When treated with cytarabine (AraC), the standard of care for AML, these PRC2-deficient leukemias were more refractory to treatment compared to AML lines driven by ML-AF9 or other PMN cell lines (Figure 11E). Further examination of the bone marrow and spleens of transplanted mice showed that these were filled with leukemic blasts that expressed the fluorescent markers of the shRNAs as well as myeloid lineage markers, verifying that these genetic aberrations lead to a myeloid leukemia in mice (Figure 12). Hence, our results suggest that PRC2 deficiency reproducibly

leads to a disease that recapitulates key features of human CK-AML in the context of p53/Mll3 inactivation. Further experiments will be needed to determine if there is an additional advantage on leukemia onset when combined with p53/Mll3/NF1 inactivation.

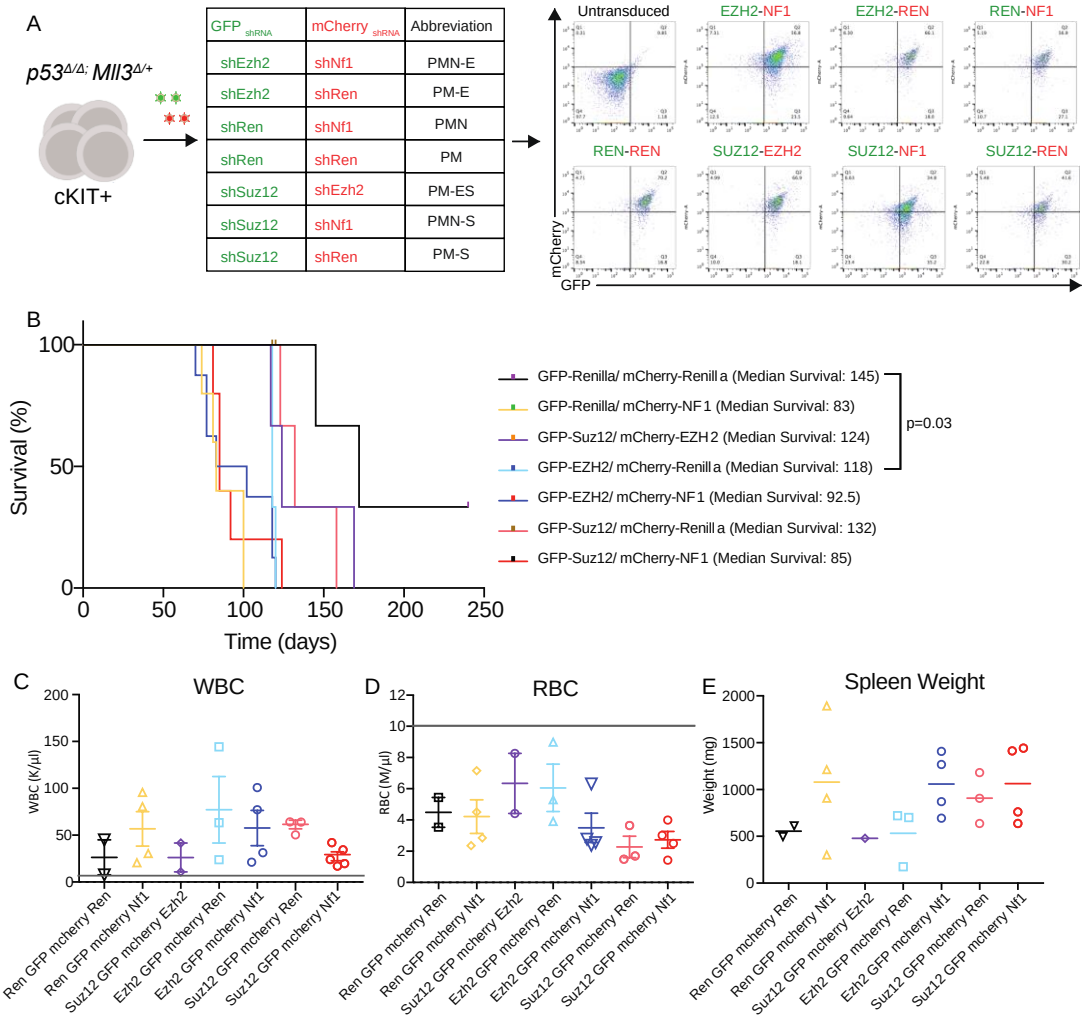

Figure 10 Mouse model of PRC2 deficient CK-AML

(A) cKIT^{+} HSPCs from p53$^{\Delta/\Delta}$;Mll3$^{\Delta/+}$ were co-transduced with shRNAs against different genes and were GFP and mCherry positive 2 days post-infection. (B) Survival curve of mice transplanted with cKIT+ cells. (C) WBC, (D) RBC and (E) Spleen weights from moribund mice. (vertical lines depict normal threshholds)

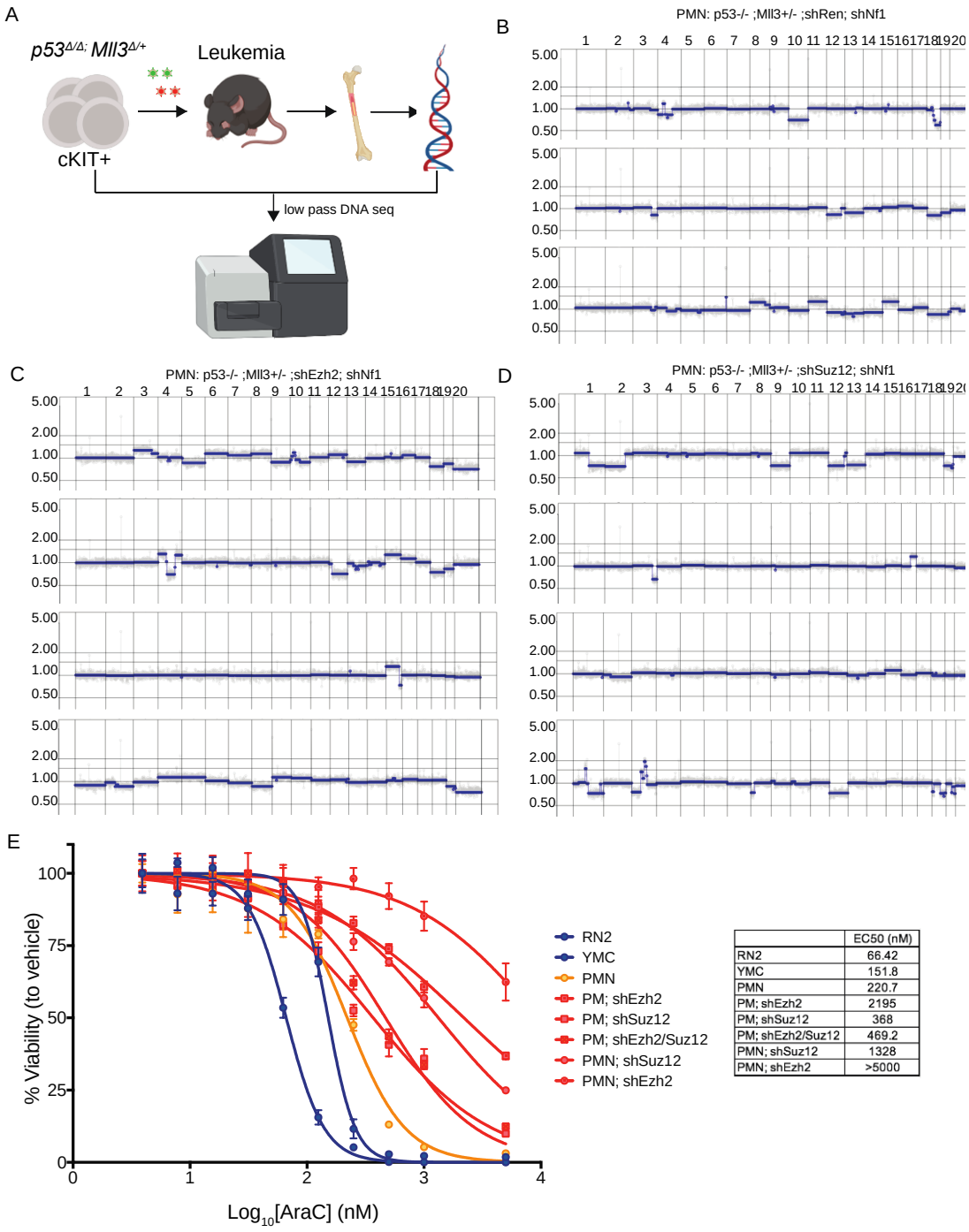

	EC50 (nM)
RN2	66.42
YMC	151.8
PMN	220.7
PM; shEzh2	2195
PM; shSuz12	368
PM; shEzh2/Suz12	469.2
PMN; shSuz12	1328
PMN; shEzh2	>5000

Figure 11 Murine PRC2 deficient CK-AML cells show complex CNVs and chemoresistance.

(A) Primary leukemias from the BM of mice were used to isolate genomic DNA (gDNA) which was subjected to sparse sequencing. (B) Profile of gDNA from 3 independent mice from $p53^{\Delta/\Delta}$;$Mll3^{\Delta/+}$; shRen; shNf1. (C) Profile of gDNA from 4 independent mice from $p53^{\Delta/\Delta}$;$Mll3^{\Delta/+}$; shEzh2; shNf1. (D) Profile of gDNA from 4 independent mice from $p53^{\Delta/\Delta}$;$Mll3^{\Delta/+}$; shSuz12; shNf1. (E) Percentage of viability after AraC treatment in leukemia cell lines from the different genotypes. Leukemic lines: RN2: Mll-Af9;NRASG12D, YMC: Mll-Af9, PMN: $p53^{\Delta/\Delta}$;$Mll3^{\Delta/+}$; shRen;shNf1, PM;Ezh2: $p53^{\Delta/\Delta}$;$Mll3^{\Delta/+}$; shEzh2, PM;Suz12: $p53^{\Delta/\Delta}$;$Mll3^{\Delta/+}$; shSuz12, PM;Ezh2;shSuz12: $p53^{\Delta/\Delta}$;$Mll3^{\Delta/+}$; shEzh2;shSuz12, PMN;Suz12: $p53^{\Delta/\Delta}$;$Mll3^{\Delta/+}$; shNf1;shSuz12, PMN;Ezh2: $p53^{\Delta/\Delta}$;$Mll3^{\Delta/+}$; shNf1;shEzh2.

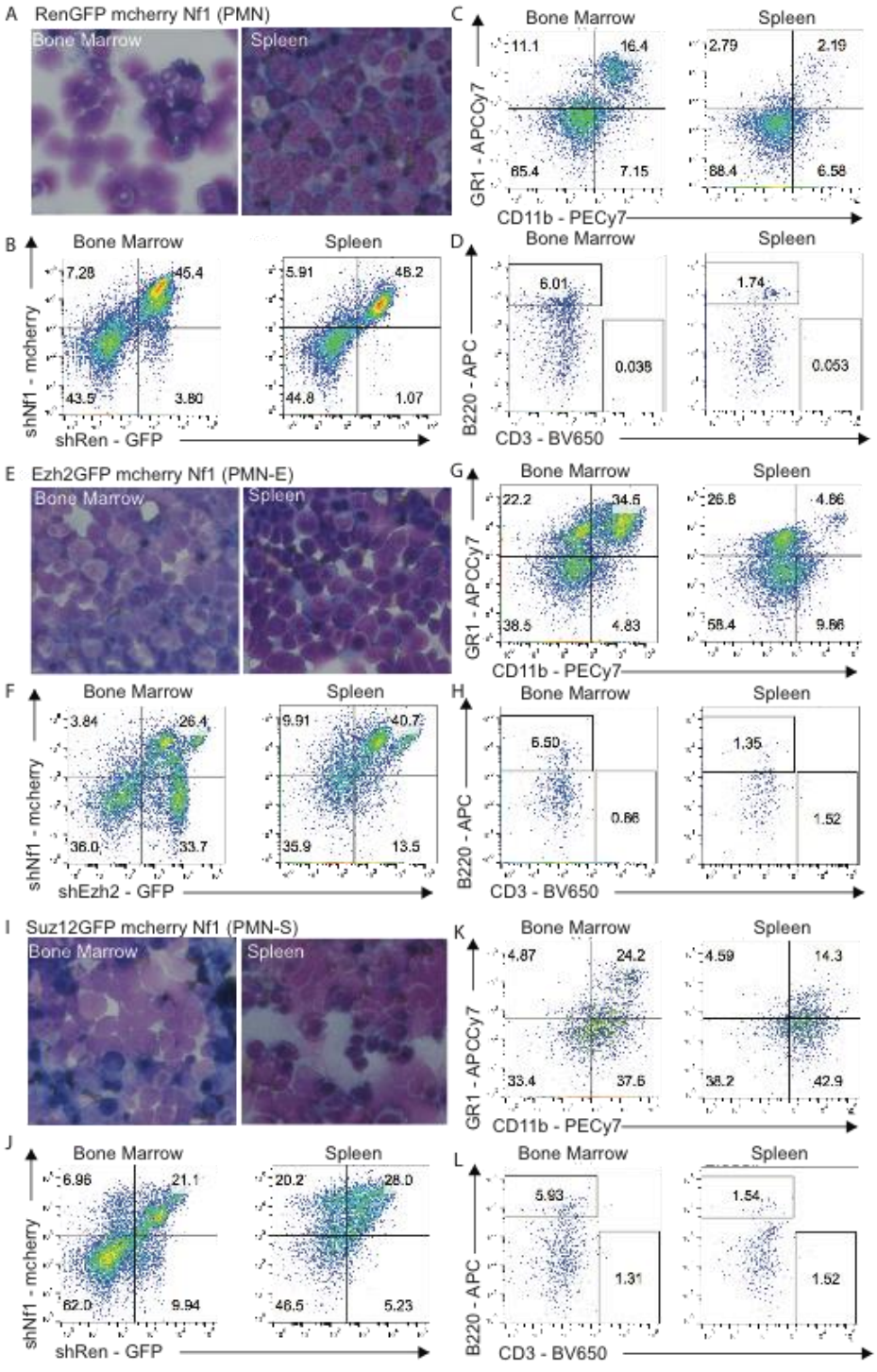

Figure 12 Morphologic and FACS analysis of leukemic cells.

Moribund mice from each group were analyzed by FACS and gates were determined based on unstained controls for each experiment (A)(E)(I) Bone marrow and Spleen cytospins stained with Wright-Giemsa staining. (B)(F)(J) GFP and mCherry percentage of cells in the bone marrow and spleens of mice. (C)(G)(K) GR1 and CD11b expression of cells from the bone marrow and spleens of mice. (D)(H)(L) B220 and CD3 expression of cells from the bone marrow and spleen of mice.

EZH2 and SUZ12 Suppression increases self-renewal of HSPCs

In parallel to the transplants we decided to assess if there was a difference in the self-renewal of HSPCs transduced with the different shRNAs mentioned above and so we plated transduced HSPCs from the seven genotypes described above in single-cell confluency and measured their ability to form colonies. We observed a significant increase in the self-renewal properties of $p53^{\Delta/\Delta}$;$Mll3^{\Delta/+}$ HSPCs transduced with shRNAs against Ezh2 (PM-E and PMN-E) and Suz12 (PM-S and PMN-S) that was not seen in the shRen group (PM) or shNf1 group (PMN) (Figure 13A). Over time and even though we started with a heterogenous population of cells expressing different percentages of the shRNAs, those targeting Ezh2, Suz12 or both were dramatically selected in culture suggesting that they influenced the self-renewal capacity of these cells and were therefore expanded in these culturing conditions (Figure 13 B,C,D). At passage 6 (P6) the morphology of the cells still replating was assessed by cytospins and Wright-Giemsa staining which showed a population of cells with increased nuclear to cytoplasmic ratio indicative of stem-like cells (Figure 13E). This was further supported

by FACS analysis of these cells which stained positive for the stem cell markers cKIT and to varying degrees they were also positive for another stem cell marker SCA-1 (Figure 13F).

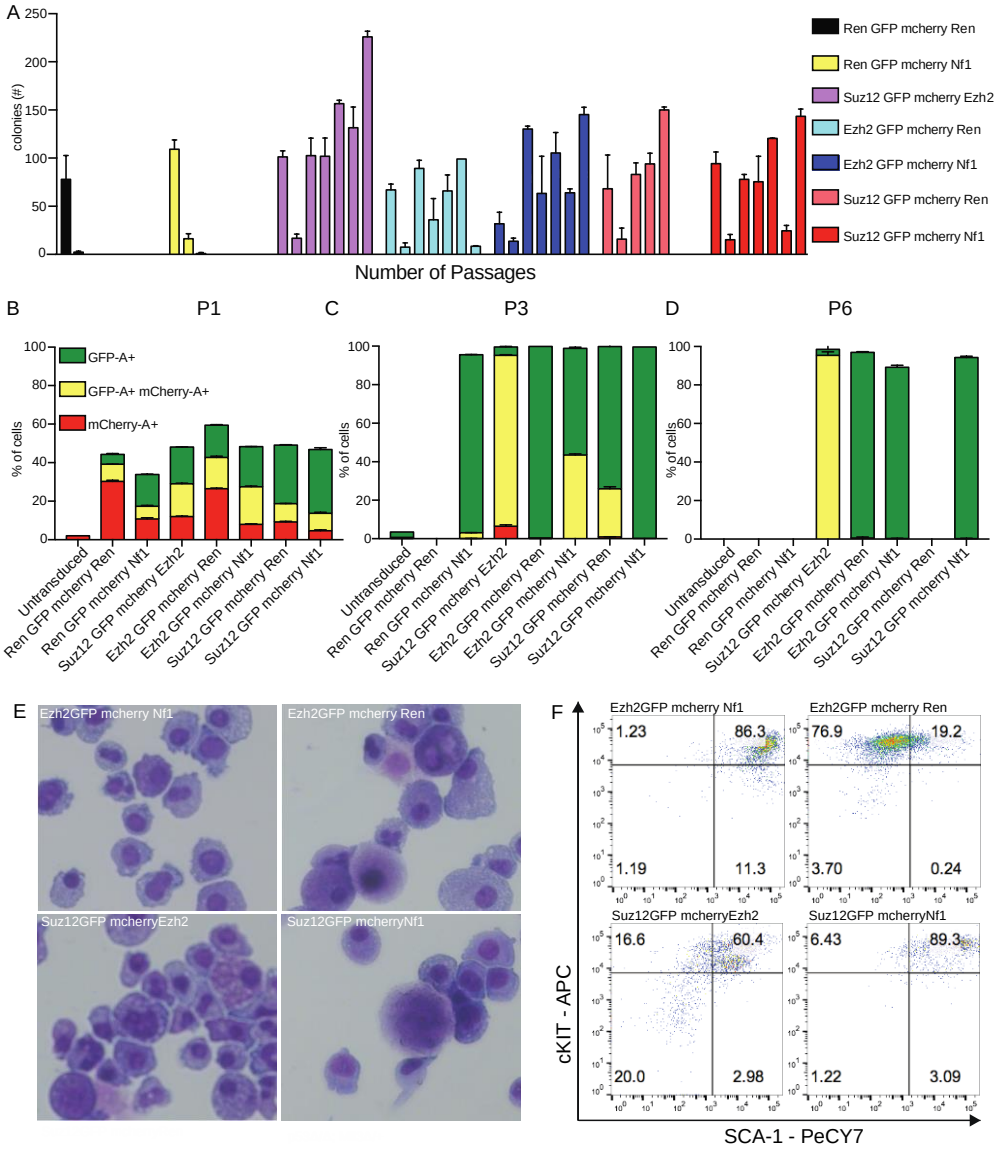

Figure 13 CFU assay from PRC2 deficient HSPCs.

(A) Number of colonies per passage (different bars) per genotype (different colors). (B) Percentage of GFP+ (green), mCherry+ (red) and double positive (yellow) colonies at passage P1 (C) P3 and (P6). (E) Cytospins of colonies at P6 from different genotypes stained with Wright-Giemsa staining. (F) FACS analysis for cKIT and SCA-1 expression of CFU colonies at P6 from different genotypes.

Ezh2 and Suz12 Suppression Produces a Transcriptional Profile Linked to Human 5q/7q AML

As a first step toward understanding the molecular mechanism whereby Ezh2 and Suz12 suppression impairs differentiation and contributes to AML, we analyzed the transcriptional profile of $p53^{\Delta/\Delta}$;$Mll3^{\Delta/+}$;shNf1;shEzh2 (PMN-E) and $p53^{\Delta/\Delta}$;$Mll3^{\Delta/+}$; shNf1;shSuz12 (PMN-S) as well as $p53^{\Delta/\Delta}$;$Mll3^{\Delta/+}$;shNf1 (PMN) driven leukemias (Figure 14A). To link this data to human PRC2-deficient AML, we initially compared gene expression levels of chr5(q)/7(q)-deleted AML patients (these are usually enriched in TP53 mutations and features of complex karyotype) versus AML types with normal karyotype. We generated a signature of 105 genes that were significantly upregulated in chr5(q)/7(q)leukemias. Gene set enrichment analysis based on differential gene expression comparisons of PMN-E versus PMN as well as PMN-S versus PMN leukemias showed a significant enrichment of the captured human chr5(q)/7(q) signature in genes upregulated in PRC2-depleted AML cells (Figueroa et al., 2010) (Figure 14B). This suggested that the transcriptional output of PCR2-loss in our model closely reflects the transcriptional profile observed in the human disease. In addition, many of these upregulated targets may reflect direct PRC2 target genes.

A more detailed compatison of the genes that are up-regulated in patients that have lost 5q/7q, (Figure 14C), with our murine dataset (Figure 14D) lead us to identify *Cd34* as one of the common, top upregulated genes. *Cd34* was not only upregulated significantly in our PMN-E and PMN-S murine leukemias (Figure 14E and F) but ectopic transduction of PMN leukemias with additional shRNAs targeting Ezh2 and shSuz12 leads to the same effect (Figure 14G). This suggested that *Cd34* could be a conserved target of the PRC2 complex normally suppressed but aberrantly activated in some leukemias that have impaired PRC2 function. Using chromatin immunoprecipitation (ChIP), we found a significant enrichment of Suz12 binding of the Cd34 promoter with two different Suz12 antibodies (Figure 15).

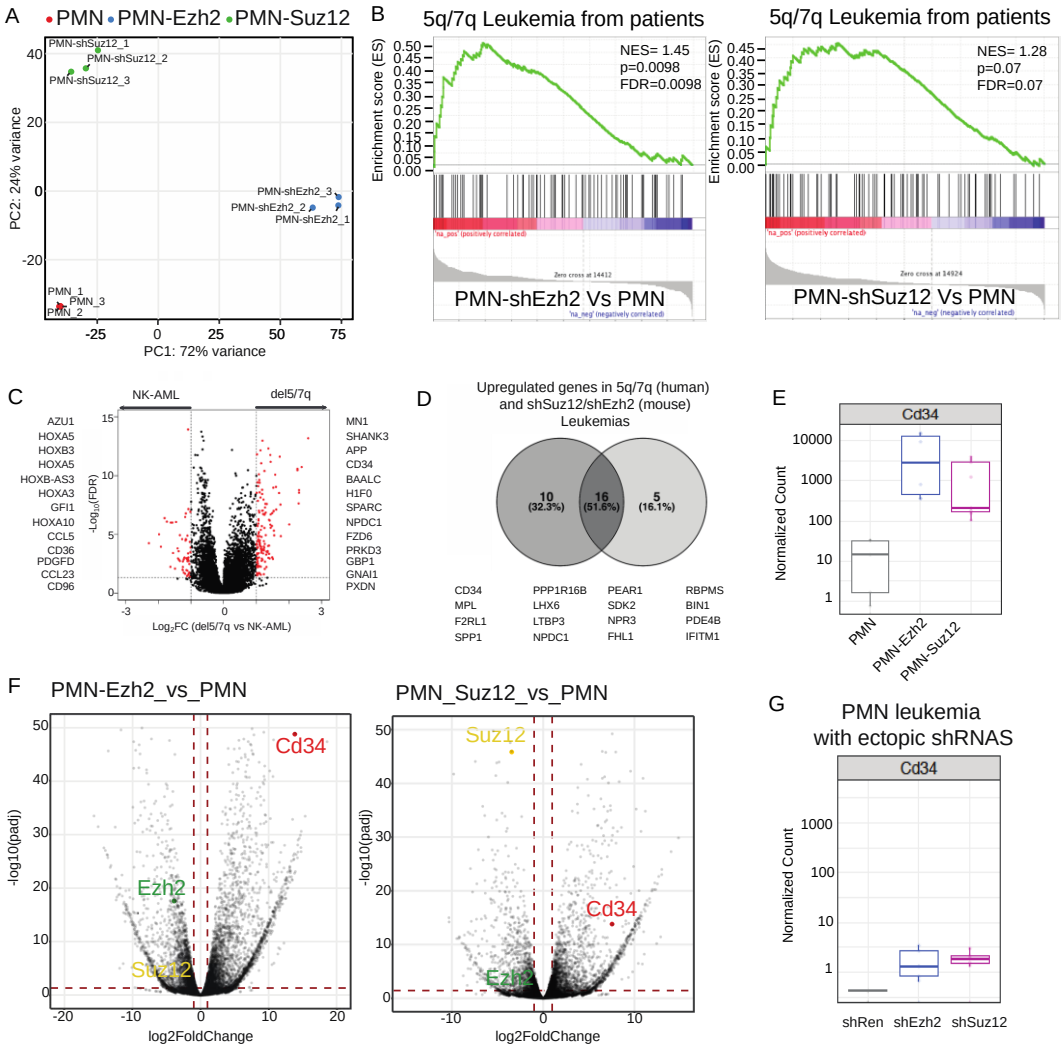

Figure 14 Transcriptional overlap between human and mouse PRC2 deficient leukemias.

(A) PCA from RNA-seq expression derived from mice with PMN (red), PMN-shEzh2 (blue) and PMN-shSuz12 (green) leukemias. (B) GSEA profiles of PMN-shEzh2 and PMN-shSuz12 leukemias compared to the differentially expressed genes from leukemias of patients with deletions on 5q and 7q. (C) Volcano plot of the differentially expressed genes in patients with a normal karyotype (NK) compared to those with deletions on 5q and 7q. (D) Common upregulated genes between human 5q/7q leukemias and murine PMN-E and PMN-S compared to Normal-Karyotype AML (NK-AML) and PMN leukemias, respectively. (E) Normalized counts of expression of Ezh2, Suz12 and Cd34 in PMN, PMN-E and PMN-S leukemias. (F) Volcano plots of the differentially expressed genes comparing PMN to PMN-E leukemias (left) and PMN to PMN-S leukemias (right). (G) Normalized counts of expression for Cd34 upon Ezh2 (blue) and Suz12 (magenta) KD in PMN leukemias.

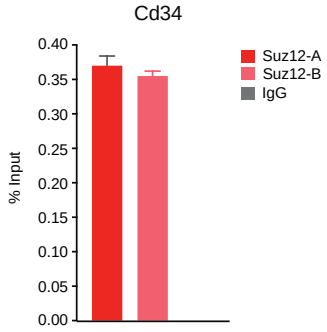

Figure 15 Suz12 binds at the *Cd34* locus.

Chromatin Immunoprecipitation with two different Suz12 antibodies coupled to amplification by qRT-PCR specific primers at the Cd34 locus.

Taken together these results suggested that *Cd34* is a direct target of the

PRC2 repressive complex leading to reduced CD34 expression. Large chromosomal deletions in the leukemic setting can lead to PRC2 loss followed by a significant increase in *Cd34* expression which is a known marker of hematopoietic stem cells and mediates self-renewal (Matsuoka et al., 2001).

DISCUSSION

Our studies identify Ezh2 and Suz12 as a tumor suppressor genes on chromosomes 7 and 17 respectively the attenuation of which contributes to AML by enhancing self-renewal and inducing chemoresistance. Although PRC2 members are frequently mutated in cancer its role in AML is contradictory as there are studies supporting that it's needed for disease progression (Shi et al., 2013) and others report it to be lost suggesting it might function as a tumor suppressor (Jerez et al., 2012). Here we propose that these genes are important for controlling self-renewal in HSPCs which it has been linked to chemoresistance in leukemia (Yu et al., 2019).

In AML, Ezh2 and Suz12 are contained within large hemizygous deletions that encompass all or part of chromosome 7 and 17 and are common in treatment-associated myeloid neoplasms and complex karyotype AML with evidence for homozygous inactivation of Ezh2 in almost half of the cases (Jerez et al., 2012). For Suz12 the results are similar suggesting that it can be both a haploinsufficient gene but also completely inactivated in patients (Score et al., 2012) (Miro et al., 2009).

Although our experimental system doesn't allow us to distinguish between haploinsufficiency versus complete loss of function, reduction in expression of Ezh2 and Suz12 leads to gene expression changes that we show play a role in controlling

normal differentiation of HSPCs. Suppression of Suz12 or Ezh2 alone is not sufficient to drive leukemogenesis but instead can cooperate with p53 loss and heterozygous loss of Mll3 to impair the differentiation of hematopoietic stem and progenitor cells, resulting in leukemia.

Our murine model showed a high degree of transcriptional overlap with RNA-seq analysis of leukemias from patients with 5(q) or 7(q) deletions, implying that PRC2 is an important mediator of this disease, and further supports the relevance of our model to the human disease. Nonetheless, the potential failure of Ezh2 and Suz12 to accelerate disease when Nf1 is also compromised suggests that when the disease is already aggressive these genes don't contribute at the initiation stage. This however needs to be confirmed as the results were different between the two replicates and a third time will be essential in confirming the involvement of these genes at this stage of the disease. Despite this, transcriptionally our murine leukemias show a big overlap with the human disease, also seem to develop complex karyotypes and show marked chemoresistance validating our model as an accurate one in studying this disease.

More work is clearly needed to further understand the role of these genes in this context which would require genome-wide studies of the histone mark deposited by PRC2, H3K27me3 as well as its competing mark H3K27ac. Furthermore, it would be crucial to extend our ChIP-qRT PCR of the Cd34 locus more globally in order to unravel a pattern in the genes affect upon PRC2 loss.

We have created here a murine model that recapitulates the genetics, transcriptional output and chemotherapy response of a disease that lacks good models and therapies. Thus, we propose that this model may serve as a preclinical system to test new drug

treatments against these particularly aggressive forms of AML. Understanding of the complex interactions between these genes that are lost because of the deletions in AML may lead to more rational approaches for patients with leukemia harboring chromosomal abnormalities.

METHODS

Animal models

All mouse experiments were approved by the Institutional Animal Care and Use Committee at Memorial-Sloan Kettering Cancer Center. $p53^{LoxP}$ mice were described previously (Olive et al., 2004) and the $Mll3^{LoxP}$ have not been published and were generated by the Hsieh lab. C57BL/6 (B6.SJL-*Ptprca Pepcb/BoyJ* (CD45.1) mice, thymectomized mice and *Vav1Cre mice* were purchased from Jackson Laboratory and bred in a mouse facility at MSKCC.

Primary cell culture

Total bone marrow cells from $p53^{F/F}$;$Mll3^{F/+}$; *Vav1Cre mice* (6-8 weeks) or purified bone marrow $cKit^+$ cells were transduced with the different shRNAS and were plated in methylcellulose medium (Methocult M3434, Stem Cell Technologies). Cells were seeded at 4,000 purified $cKit^+$ cells per replicate. Colony forming units were enumerated using a Zeiss Axio Observer microscope, and cells were re-plated (4,000 cells/replicate) every 7–10 days. Primary mouse PMN leukemias derived from mice were cultured in RPMI 1640 with 10% FBS (Gibco), 100 U/mL penicillin, 100 μg/ml streptomycin,

50 μM 2-mercaptoethanol and recombinant mouse SCF (50 ng/ml), IL3 (10 ng/ml) and IL6 (10 ng/ml) at 37°C in 5% CO_2.

Cell lines

PMN murine leukemic cells KL922 (*p53$^{\Delta/\Delta}$;Mll3$^{\Delta/+}$)* (Chen et al., 2014; Liu et al., 2016) were cultured with RPMI 1640, 10% FBS (Gibco) and recombinant mouse SCF (50 ng/ml), IL3 (10 ng/ml) and IL6 (10 ng/ml). PlatinumE (Morita et al., 2000) cells were a gift from Craig Thomson's lab and HEK293T were purchased from ATCC (CRL-3216) and were used for retroviral production while maintained in DMEM with 10% FBS. Media were supplemented with 100 U/mL penicillin, 100 μg/ml streptomycin and cultures were incubated at 37°C, 5% CO_2. All cells were tested negative for mycoplasma (MP0025-1KT) and were not maintained for longer than 10 passages in culture. For cell line authentication we confirmed TP53 expression by WB and Sanger sequencing confirmed the deletion.

Histology and microscopy

Tissues were dissected from mice for fixation overnight in 10% formalin (Fisher). Bones were decalcified per manufacturer's instructions (IDEXX BioResearch), and fixed tissues were dehydrated and embedded in paraffin for sectioning. Paraffin sections (5 μm) were prepared and stained with hematoxylin and eosin (H&E) (Leica Autostainer XL).

Flow cytometry

Single cell suspensions were prepared from bone marrow, spleen or peripheral blood. Red blood cells were lysed with ammonium-chloride-potassium (ACK) buffer, and the remaining cells were resuspended in PBS with 3% FBS. Non-specific antibody binding was blocked by incubation with 20 μg/ml Rat IgG (Sigma-Aldrich) for 15 min, and cells were then incubated with the indicated primary antibodies for 30 min on ice. Stained cells were quantified using a Fortessa analyzer (BD Biosciences) or isolated with a FACSAria II (BD Biosciences). FlowJo software (TreeStar) was used to generate flow cytometry plots. More details on FACS antibodies found in Table S2.

Bone marrow transplantation

Femurs and tibiae were isolated from donor mice $p53^{\Delta/\Delta};Mll3^{\Delta/+}$ and bones were flushed with PBS and the single-cell suspension was centrifuged (5 min, 0.5g, 4 °C) and treated with red cell ACK lysis buffer, as described above. Total nucleated bone marrow cells were re-suspended in PBS, passed through a 40 μM cell strainer and counted. Donor cells (1×10^6 per genotype, per mouse) were mixed 1:1 with support bone marrow cells (CD 45.1), and transplanted via retro-orbital injection into lethally irradiated (850 Rad) theymectomized recipient mice. Chimerism was monitored by flow cytometry of peripheral blood.

Retroviral transduction

Hematopoietic stem and progenitor cells were isolated by sorting $Lin^{-}cKit^{+}Sca1^{+}$ cells or enriched using an autoMACS Pro separator (Miltenyi Biotec) using CD117 magnetic

microbeads (Miltenyi Biotech, 130-091-224), then cultured in the presence of 50 ng/ml SCF, 10 ng/ml IL-3, and 10 ng/ml IL-6, and infected with concentrated supernatants of *MLSe-sh.Ren/Nf1/Ezh2/Suz12-mCherry or MLSe-sh.Ren/Ezh2/Suz12-GFP* retrovirus after 24 and 48 h. Transduction efficiency was determined by reporter fluorescence at 48 h, and cells were injected into lethally irradiated thymectomized mice as described above.

Quantitative RNA expression assays

Total RNA was extracted from cells using the RNeasy Plus Mini Kit (Qiagen). RNA quantity and quality were determined using an Agilent 2100 Bioanalyzer. RNA-seq libraries were prepared from total RNA by polyA selection using oligo-dT beads (Life Technologies) according to the manufacturer's instructions. The resulting poly-A+ RNA served as input for library construction using standard Illumina protocols. Sequencing was performed on an Illumina HiSeq 2500 sequencer using 50 bp pair-end reads. For mRNA quantification, total RNA was used for cDNA synthesis (Agilent). Real-time PCR reactions were carried out using SYBR Green Master Mix (QuantaBio) and a Via7 (AB Applied biosystems).

RNA sequencing analysis

RNA-Seq library construction and sequencing were performed at the integrated genomics operation (IGO) Core at MSKCC. Poly-A selection was performed. For sequencing, approximately 30 million 50bp paired-end reads were acquired per replicate condition. Resulting RNA-Seq data was analyzed by removing adaptor sequences using

Trimmomatic (Bolger et al., 2014). RNA-Seq reads were then aligned to GRCh37.75 (hg19) with STAR (Dobin et al., 2013) and genome-wide transcript counting was performed by HTSeq (Anders et al., 2015) to generate a matrix of fragments per kilobase of exon per million fragments mapped (RPKM). Gene expressions of RNA-Seq data were managed by hierarchical clustering based on one minus Pearson correlation test using Morpheus (https://software.broadinstitute.org/morpheus/). All results from the RNA-Seq experiments can be found under GSE125097.

Gene set enrichment analysis

Gene set enrichment analysis was performed using gene set as permutation type, 1,000 permutations and log2 ratio of classes, or with gene set and Signal2Noise as metrics for ranking genes. Gene sets used in this study were identified from the Molecular Signatures Database (MSigDB Curated v4.0). Gene pathways and functions were assessed using Ingenuity Pathway Analysis (Qiagen Bioinformatics).

Expression of gene signatures in human AML and normal cells.

Visualization of gene signatures derived from transcriptional data as Log2 expression values for different karyotypes of AML patients described previously in GSE42519 (Rapin et al., 2014). For normal hematopoietic cells values were averaged over all genes in each signature and visualized by using Sinaplot. Student's t-test was performed using the R programming language (https://www.R-project.org/).

Quantification and Statistical Analysis

All p-values were calculated using unpaired two-tailed Student's *t* test with Graphpad Prism software, unless otherwise described in the methods or figure legends. No specific randomization or blinding protocol was used for these analyses. Statistically significant differences are indicated with asterisks in figures with the accompanying p-values in the legend. Error bars in figures indicate standard deviation (SD) or standard error of the mean (SEM) for the number of replicates, as indicated in the figure legend.

Plasmids and viral production

All vectors were derived from the Murine Stem Cell Virus (MSCV, Clontech) retroviral vector backbone. miRE-based shRNAs were designed and cloned as previously described **(Zuber et al., 2011a)**. All constructs were verified by sequencing. For retroviral infection PlatinumE cells were plated in 15 cm diameter dishes each transfected with 54 ug of MSCV vectors and 2.7ug of VSV-G and 8.1ug of pCl-eco. Transfection of packaging cells was performed using HBS and $CaCl_2$ or Mirus transfection reagent (MIR 2304). Viral supernatants were passed through a 0.45 um filter (Millipore) and concentrated with Centrifugal Filter units (Millipore) to obtain high virus titer. Concentrated virus was supplemented with 8 ug/ml of polybrene (Sigma) before adding to target cells.

Immunoblotting. For protein lysates, cells were incubated with RIPA buffer supplemented with protease inhibitors (Protease inhibitor tablets, Roche) for 30 min and cleared by centrifugation (15 min 14.000 rpms 4C). Protein was quantified using the

DC protein assay (BioRad). The following antibodies were used for immunoblotting: β-ACTIN (ac-15, Sigma).

Chromatin immunoprecipitation (ChIP). Chromatin immunoprecipitation was performed as previously described (Banito et al., 2018). Briefly, cells were fixed with 1% formaldehyde for 15 min, and the cross-linking reaction was stopped by adding 125mM glycine. Cells were washed twice with cold PBS and lysed in buffer (150 mM NaCl, 1%v/v Nonidet P-40, 0.5% w/v deoxycholate, 0.1% w/v SDS, 50 mM Tris pH8, 5m M EDTA) supplemented with protease inhibitors. Cell lysates were sonicated using a *Covaris E220 Sonicator* to generate fragments less than 400 bp. Sonicated lysates were centrifuged, and incubated overnight at 4ºC with specific antibodies (Foxh1 Abcam 49133;). Immunocomplexes were recovered by incubation with 30 ul protein A/G magnetic beads (Thermofisher) for 2h at 4ºC. Beads were sequentially washed twice with RIPA buffer, increasing stringency ChIP wash buffers (150 mM NaCl, 250 mM NaCl, 250 mM LiCl) and finally TE buffer. Immunocomplexes were eluted using elution buffer (1% SDS, 100mM $NaHCO_3$), and cross-linking was reverted by addition of 300 mM NaCl and incubation at 65ºC overnight. DNA was purified using a PCR purification kit (Qiagen). Input chromatin was used for estimation of relative enrichment. The results for the ChIP-seq experiments can be found under GSE125097.

ChIP-Seq Library Preparation, Illumina Data Analysis and Peak Detection. ChIP-Seq libraries were prepared at the Center for Epigenetic Research (MSKCC) using the NEBNext® ChIP-Seq Library Prep Master Mix Set for Illumina® (New England

BioLabs) following the manufacture's instructions. Reads were trimmed for quality and Illumina adapter sequences using 'trim_galore' before aligning to mouse assembly mm9 with bowtie2 using the default parameters. Aligned reads with the same start site and orientation were removed using the Picard tool MarkDuplicates (http://broadinstitute.github.io/picard/). Density profiles were created by extending each read to the average library fragment size and then computing density using the BEDTools suite (http://bedtools.readthedocs.io). Enriched regions were discovered using MACS2 and scored against matched input libraries (fold change > 2 and p-value < 0.005). Dynamic regions between two conditions were discovered using a similar method, with the second ChIP library replacing input. Peaks were then filtered against genomic 'blacklisted' regions (http://mitra.stanford.edu/kundaje/akundaje/release/blacklists/mm9-mouse/mm9blacklist.bed.gz) and those within 500 bp were merged. All genome browser tracks and read density tables were normalized to a sequencing depth of ten million mapped reads. Dynamic peaks were annotated using linear genomic distance and motif signatures were obtained using the 'de novo' approach with Homer v4.5 (http://homer.ucsd.edu/).

DISCUSSION

Despite the plethora of scientific papers on the functions of p53 we still manage to identify novel functions of this gene in different and unpredicted contexts which poses the question: Is it because it's the biggest driver in cancer or is it because more laboratories have focused on studying this gene? Perhaps the fact that it is the most highly mutated gene in cancer suggests that at least to some extend the former must be true.

Mutations in genes are selected for their ability to enhance cellular fitness and follow the fundamental Darwinian rules of evolution as these genetic events alter biological processes and increase fitness. Cancer-related mutations have been described to affect one or more key biological processes that can lead to cancer when perturbed. These biological capabilities acquired during the multistep development of human tumors, have also been termed "Hallmarks of Cancer" and include functions like sustained proliferative capacity, evasion of apoptosis and growth arrest, replicative immortality and ability to metastasize (Hanahan and Weinberg, 2000). It is for this reason that p53 has been one of the most successful drivers in cancer; when perturbed and in one hit can contribute to cancer through all these functions.

The ancient Greeks believed cancer to be caused by an imbalance of humors, specifically, an excess of black bile a mechanism believed for many centuries. The hypothesis that cancers could arise from stem cells appeared much later in the late 1800s and it was proposed as the embryonal rest theory of cancer. This theory proposed that adult organs retained embryonic tissue which could in the presence of an extrinsic

stimulus resume cell proliferation and produce tumors. This theory however was generally discredited by the 20th century. Nowadays, tissue stem cells are perceived as the cell of origin in a lot of tumor types, which as a hypothesis is used to explain the fact that only a small population of cells can propagate the tumor in transplantation assays and explain how relapse occurs after treatment (Visvader, 2011). Our results support the hypothesis that one possible mechanism by which p53 mutations are so highly selected in tumors is because by promoting aberrant self-renewal they push the cells in a stem-like state perfectly malleable for transformation. Whether our results extend to other tumor types remains to be proven but it has been shown that hotspot *TP53* mutations are associated with embryonic stem cell signatures in various solid tumors (Koifman et al., 2018).

There are several theories as to how cancer-related mutations lead to the formation of tumors and several ones might be true. For instance, it is not clear whether mutations occur only in the tissue stem cells and because these cells are long-lived with self-renewal properties can acquire other mutations that will eventually lead to transformation. Another hypothesis is that these mutations can occur in more differentiated cells, like progenitors, that render these cells with self-renewal properties and can then also accumulate more mutations which will transform these cells into cancer cells. In leukemias, the tissue hierarchy is – to a big extent – delineated and the different types of cells can be sorted based on their self-surface markers and studied *ex vivo*. Scott A. Armstrong's group used this model to sort out the hematopoietic stem cells and the progenitors and transformed both with the same oncogene – *Mll-Af9* to show that both these cells could be transformed supporting that progenitors could be

transcriptionally reprogrammed to resemble stem cells in the presence of a strong oncogene (Krivtsov et al., 2006). Our unpublished data support that *TP53* mutations can perhaps do both: when expressed in HSCs they increase their self-renewal properties but when present in downstream progenitors such as GMPs, can endow them with aberrant self-renewal properties both *in vitro (CFU assay)* as well as *in vivo* (in transplants).

This aberrant self-renewal phenotype in the presence of oncogenes or mutated tumor suppressors is a strong theme in leukemia biology with the most common mutations to be shown to promote enhanced stem cell capacity in HSCs. The most common mutations include *DNMT3a* (Challen et al., 2011), *TET2* (Moran-Crusio et al., 2011), *IDH1/2* (Sasaki et al., 2012), *ASXL1* (Abdel-Wahab et al., 2013). In line with this we were able to show that the advantage of $p53^{R172H}$ mutations in the hematopoietic compartment was because of their ability to mediate a continuous self-renewal effect in HSPCs which was not there in p53 null cells (Loizou et al., 2019). The implications of these results go beyond our work in leukemia and suggest an early, pre-leukemic advantage of these *TP53* mutations that can be relevant in patients with clonal hematopoiesis.

Even though the p53 mutation we were studying is the most common one in patients with AML, the question still remains if other mutations have the same effect. We performed experiments assessing the self-renewal properties of HSPCs derived from $p53^{R270H}$ (Olive et al., 2004) and $p53^{R248Q}$ (Schulz-Heddergott et al., 2018) and we did not observe the effect we saw with $p53^{R172H}$ mutant HSPCs (data not shown). It is unclear whether this is because of the limiting expression of FOXH1 in these mutants

or it is more of a general transcriptional output that it is different. As the commonality between *TP53* mutants is still elusive, in order to test this a more high-throughput experimental setting needs to be implored to elucidate this in the future.

Furthermore, the fact that these two additional hotspot mutations did not exhibit enhanced self-renewal *in vitro* as assessed by their CFU ability, it does not mean that these mutants do not have GOF effects pertinent to other functions such as chemoresistance. It is possible that each mutation has unique capabilities and the hotspot mutations do not have convergent functions in the tumors that harbor these.

Regardless of the fact we have focused on studying the most common genetic configuration of *TP53* mutations which is its hemizygous state, some tumors retain the second wild-type allele (Liu et al., 2016). To which extend the wild-type allele is functional is unknown as the locus could be methylated and inactivated epigenetically. However, the dominant-negative (DN) effect that mutant p53 can exert on the wild-type is well described (Willis et al., 2004) and a group recently proposed that the major effect of the hotspot mutations in AML is to inactivate the wild-type allele (Boettcher et al., 2019). The authors introduced the most common hotspot mutations found in patients, in two established human AML cell line models using CRISPR-Cas9 genome editing. These engineered cells did not respond to chemotherapeutic drugs differently than their *TP53* deficient counterparts and were more efficient at inhibiting induction of p21 from the other *WT* allele than any other *TP53* mutation. This lead the authors to propose that the DN effect is what is driving the acquisition of these mutations in AML.

Even though we do not exclude that the DN effect is a strong pressure for these mutations to occur, we have seen that at least in one experimental setting – the CFU

assay – when we assessed the self-renewal effect of $p53^{R172H/+}$ HSPCs they behaved similarly to WT, whereas the $p53^{R172H/\Delta}$ showed indefinitely self-renewal properties. Furthermore the cells used for the majority of the experiments in the Boettcher paper were established human cell lines driven by diverse genetic and other events where exogenous engineering of the different TP53 mutations, albeit from the endogenous locus, might not have the same effect as leukemic cells generated on a *TP53* mutant background.

Both from our *TP53* mutant studies as well as using *TP53* deficient HSPCs for studying the role of the PRC2 complex in leukemia, we were able to generate a series of murine leukemia models that recapitulated key features of the disease such as the complex karyotype as assessed by sparse genome sequencing. It would be of great interest to study if the chromosomal losses and gains are recurrent and if within those sites there are syntenic regions in the human patients that encompass additional drivers. As CK-AML is devoid of other mutations besides *TP53* these re-occurring events might contain the cooperating events that lead to AML.

Despite the fact our murine models are a great proxy to the human disease they still have limitations. These limitations are produced because the models rely on the utilization of multiple shRNAs linked to fluorescent proteins that are unstable and are prone to stochastic silencing. Furthermore studies have suggested that fluorescent proteins can be immunogenic and therefore might influence the evolution of the disease in the mouse as a result of constant immunoediting. To avoid this we have made a GEMM that is $p53^{F/F}$; $Nf1^{F/+}$; $Mll3^{F/+}$ driven by an inducible (Mx1CRE) or constitutive (Vav1CRE) hematopoietic specific CRE Recombinase. With the use of this multi-allelic mouse

model we want to assess *in vivo* in non-transplant conditions, the evolution of the disease from the early initiation stages (few weeks after recombination) until the later stages (moribund mice) and track the genomic changes that occur at each step. Furthermore this model allows us to layer other putative cooperating events on this leukemia-prone background and assess their role in the disease.

Nevertheless, and despite generating a model of CK-AML with impaired PRC2 function, we still do not understand the broader implication of the chromatin architecture upon Ezh2 and Suz12 KD. Optimization of our ChIP-seq protocols for Ezh2, Suz12 and H3K27me3 in these murine CK-AML cell lines will shed light into the biochemical and broader molecular implications of PRC2 deficiency. Additionally, we have observed varying degrees of KD for both Ezh2 and Suz12 from the derived leukemias suggesting that these genes can indeed be haploinsufficient tumor suppressor genes. In order to validate this we have crossed the $p53^{F/F}$; $Mll3^{F/+}$; Vav1Cre mice and the $p53^{F/F}$; $Nf1^{F/+}$; Vav1Cre mice to $Ezh2^{F/+}$ and plan to do the same for $Suz12^{F/+}$ so we can determine the dosage requirement for both these genes in the development of AML.

CONCLUDING REMARKS

While in the 30 years of studying p53 we have realized the tremendous complexity of the p53 pathway and the detrimental consequences it can have when lost in cells, it is still an impossible therapeutic target. However efforts to restore some of these *TP53* mutations with GOF and/or DN effects into their wild-type conformation and restore their tumor suppressive functions, give great hope to the astounding morbidity associated with TP53 mutant tumors.

As complex-karyotype AML has dismal prognosis new preclinical models such as the ones we developed here, together with our ever-increasing understanding of the complexity of p53 action and its effects in different contexts (genetic, metabolic or others), will hopefully lead to more robust clinical advances in the years to come.

BIBLIOGRAPHY

Abdel-Wahab, O., Gao, J., Adli, M., Dey, A., Trimarchi, T., Chung, Y.R., Kuscu, C., Hricik, T., Ndiaye-Lobry, D., Lafave, L.M.*, et al.* (2013). Deletion of Asxl1 results in myelodysplasia and severe developmental defects in vivo. J Exp Med *210*, 2641-2659.

Abelson, S., Collord, G., Ng, S.W.K., Weissbrod, O., Mendelson Cohen, N., Niemeyer, E., Barda, N., Zuzarte, P.C., Heisler, L., Sundaravadanam, Y.*, et al.* (2018). Prediction of acute myeloid leukaemia risk in healthy individuals. Nature *559*, 400-404.

Alexandrova, E.M., Yallowitz, A.R., Li, D., Xu, S., Schulz, R., Proia, D.A., Lozano, G., Dobbelstein, M., and Moll, U.M. (2015). Improving survival by exploiting tumour dependence on stabilized mutant p53 for treatment. Nature *523*, 352-356.

Anders, S., Pyl, P.T., and Huber, W. (2015). HTSeq--a Python framework to work with high-throughput sequencing data. Bioinformatics *31*, 166-169.

Armstrong, S.A., Staunton, J.E., Silverman, L.B., Pieters, R., den Boer, M.L., Minden, M.D., Sallan, S.E., Lander, E.S., Golub, T.R., and Korsmeyer, S.J. (2002). MLL translocations specify a distinct gene expression profile that distinguishes a unique leukemia. Nat Genet *30*, 41-47.

Attisano, L., Silvestri, C., Izzi, L., and Labbe, E. (2001). The transcriptional role of Smads and FAST (FoxH1) in TGFbeta and activin signalling. Mol Cell Endocrinol *180*, 3-11.

Bagger, F.O., Kinalis, S., and Rapin, N. (2019). BloodSpot: a database of healthy and malignant haematopoiesis updated with purified and single cell mRNA sequencing profiles. Nucleic Acids Res *47*, D881-D885.

Baker, S.J., Markowitz, S., Fearon, E.R., Willson, J.K., and Vogelstein, B. (1990a). Suppression of human colorectal carcinoma cell growth by wild-type p53. Science *249*, 912-915.

Baker, S.J., Preisinger, A.C., Jessup, J.M., Paraskeva, C., Markowitz, S., Willson, J.K., Hamilton, S., and Vogelstein, B. (1990b). p53 gene mutations occur in combination with 17p allelic deletions as late events in colorectal tumorigenesis. Cancer Res *50*, 7717-7722.

Banito, A., Li, X., Laporte, A.N., Roe, J.S., Sanchez-Vega, F., Huang, C.H., Dancsok, A.R., Hatzi, K., Chen, C.C., Tschaharganeh, D.F.*, et al.* (2018). The SS18-SSX Oncoprotein Hijacks KDM2B-PRC1.1 to Drive Synovial Sarcoma. Cancer Cell *33*, 527-541 e528.

Banito, A., Rashid, S.T., Acosta, J.C., Li, S., Pereira, C.F., Geti, I., Pinho, S., Silva, J.C., Azuara, V., Walsh, M.*, et al.* (2009). Senescence impairs successful reprogramming to pluripotent stem cells. Genes Dev *23*, 2134-2139.

Bartek, J., Bartkova, J., Vojtesek, B., Staskova, Z., Rejthar, A., Kovarik, J., and Lane, D.P. (1990a). Patterns of expression of the p53 tumour suppressor in human breast tissues and tumours in situ and in vitro. Int J Cancer *46*, 839-844.

Bartek, J., Iggo, R., Gannon, J., and Lane, D.P. (1990b). Genetic and immunochemical analysis of mutant p53 in human breast cancer cell lines. Oncogene *5*, 893-899.

Ben-Porath, I., Thomson, M.W., Carey, V.J., Ge, R., Bell, G.W., Regev, A., and Weinberg, R.A. (2008). An embryonic stem cell-like gene expression signature in poorly differentiated aggressive human tumors. Nat Genet *40*, 499-507.
Bennett, J.M., Catovsky, D., Daniel, M.T., Flandrin, G., Galton, D.A., Gralnick, H.R., and Sultan, C. (1976). Proposals for the classification of the acute leukaemias. French-American-British (FAB) co-operative group. Br J Haematol *33*, 451-458.
Beroukhim, R., Mermel, C.H., Porter, D., Wei, G., Raychaudhuri, S., Donovan, J., Barretina, J., Boehm, J.S., Dobson, J., Urashima, M.*, et al.* (2010). The landscape of somatic copy-number alteration across human cancers. Nature *463*, 899-905.
Boettcher, S., Miller, P.G., Sharma, R., McConkey, M., Leventhal, M., Krivtsov, A.V., Giacomelli, A.O., Wong, W., Kim, J., Chao, S.*, et al.* (2019). A dominant-negative effect drives selection of TP53 missense mutations in myeloid malignancies. Science *365*, 599-604.
Bolger, A.M., Lohse, M., and Usadel, B. (2014). Trimmomatic: a flexible trimmer for Illumina sequence data. Bioinformatics *30*, 2114-2120.
Bouaoun, L., Sonkin, D., Ardin, M., Hollstein, M., Byrnes, G., Zavadil, J., and Olivier, M. (2016). TP53 Variations in Human Cancers: New Lessons from the IARC TP53 Database and Genomics Data. Hum Mutat *37*, 865-876.
Bougeard, G., Sesboue, R., Baert-Desurmont, S., Vasseur, S., Martin, C., Tinat, J., Brugieres, L., Chompret, A., de Paillerets, B.B., Stoppa-Lyonnet, D.*, et al.* (2008). Molecular basis of the Li-Fraumeni syndrome: an update from the French LFS families. J Med Genet *45*, 535-538.
Brecqueville, M., Cervera, N., Adelaide, J., Rey, J., Carbuccia, N., Chaffanet, M., Mozziconacci, M.J., Vey, N., Birnbaum, D., Gelsi-Boyer, V.*, et al.* (2011). Mutations and deletions of the SUZ12 polycomb gene in myeloproliferative neoplasms. Blood Cancer J *1*, e33.
Brennan, J., Lu, C.C., Norris, D.P., Rodriguez, T.A., Beddington, R.S., and Robertson, E.J. (2001). Nodal signalling in the epiblast patterns the early mouse embryo. Nature *411*, 965-969.
Brummelkamp, T.R., Bernards, R., and Agami, R. (2002). A system for stable expression of short interfering RNAs in mammalian cells. Science *296*, 550-553.
Burnett, A.K., Russell, N.H., Hills, R.K., Hunter, A.E., Kjeldsen, L., Yin, J., Gibson, B.E., Wheatley, K., and Milligan, D. (2013). Optimization of chemotherapy for younger patients with acute myeloid leukemia: results of the medical research council AML15 trial. J Clin Oncol *31*, 3360-3368.
Cancer Genome Atlas Research, N., Ley, T.J., Miller, C., Ding, L., Raphael, B.J., Mungall, A.J., Robertson, A., Hoadley, K., Triche, T.J., Jr., Laird, P.W.*, et al.* (2013). Genomic and epigenomic landscapes of adult de novo acute myeloid leukemia. N Engl J Med *368*, 2059-2074.
Caulin, C., Nguyen, T., Lang, G.A., Goepfert, T.M., Brinkley, B.R., Cai, W.W., Lozano, G., and Roop, D.R. (2007). An inducible mouse model for skin cancer reveals distinct roles for gain- and loss-of-function p53 mutations. J Clin Invest *117*, 1893-1901.
Cerami, E., Gao, J., Dogrusoz, U., Gross, B.E., Sumer, S.O., Aksoy, B.A., Jacobsen, A., Byrne, C.J., Heuer, M.L., Larsson, E.*, et al.* (2012). The cBio cancer genomics portal:

an open platform for exploring multidimensional cancer genomics data. Cancer Discov *2*, 401-404.
Challen, G.A., Sun, D., Jeong, M., Luo, M., Jelinek, J., Berg, J.S., Bock, C., Vasanthakumar, A., Gu, H., Xi, Y.*, et al.* (2011). Dnmt3a is essential for hematopoietic stem cell differentiation. Nat Genet *44*, 23-31.
Charney, R.M., Forouzmand, E., Cho, J.S., Cheung, J., Paraiso, K.D., Yasuoka, Y., Takahashi, S., Taira, M., Blitz, I.L., Xie, X.*, et al.* (2017). Foxh1 Occupies cis-Regulatory Modules Prior to Dynamic Transcription Factor Interactions Controlling the Mesendoderm Gene Program. Dev Cell *40*, 595-607 e594.
Chen, C., Liu, Y., Rappaport, A.R., Kitzing, T., Schultz, N., Zhao, Z., Shroff, A.S., Dickins, R.A., Vakoc, C.R., Bradner, J.E.*, et al.* (2014). MLL3 is a haploinsufficient 7q tumor suppressor in acute myeloid leukemia. Cancer Cell *25*, 652-665.
Chiu, W.T., Charney Le, R., Blitz, I.L., Fish, M.B., Li, Y., Biesinger, J., Xie, X., and Cho, K.W. (2014). Genome-wide view of TGFbeta/Foxh1 regulation of the early mesendoderm program. Development *141*, 4537-4547.
Conway, E., Healy, E., and Bracken, A.P. (2015). PRC2 mediated H3K27 methylations in cellular identity and cancer. Curr Opin Cell Biol *37*, 42-48.
Cullen, P. (1811). Case of Splenitis Acutus. Edinb Med Surg J *7*, 169-171.
De Kouchkovsky, I., and Abdul-Hay, M. (2016). 'Acute myeloid leukemia: a comprehensive review and 2016 update'. Blood Cancer J *6*, e441.
DeLeo, A.B., Jay, G., Appella, E., Dubois, G.C., Law, L.W., and Old, L.J. (1979). Detection of a transformation-related antigen in chemically induced sarcomas and other transformed cells of the mouse. Proc Natl Acad Sci U S A *76*, 2420-2424.
Di Agostino, S., Strano, S., Emiliozzi, V., Zerbini, V., Mottolese, M., Sacchi, A., Blandino, G., and Piaggio, G. (2006). Gain of function of mutant p53: the mutant p53/NF-Y protein complex reveals an aberrant transcriptional mechanism of cell cycle regulation. Cancer Cell *10*, 191-202.
Dittmer, D., Pati, S., Zambetti, G., Chu, S., Teresky, A.K., Moore, M., Finlay, C., and Levine, A.J. (1993). Gain of function mutations in p53. Nat Genet *4*, 42-46.
Do, P.M., Varanasi, L., Fan, S., Li, C., Kubacka, I., Newman, V., Chauhan, K., Daniels, S.R., Boccetta, M., Garrett, M.R.*, et al.* (2012). Mutant p53 cooperates with ETS2 to promote etoposide resistance. Genes Dev *26*, 830-845.
Dobin, A., Davis, C.A., Schlesinger, F., Drenkow, J., Zaleski, C., Jha, S., Batut, P., Chaisson, M., and Gingeras, T.R. (2013). STAR: ultrafast universal RNA-seq aligner. Bioinformatics *29*, 15-21.
Dohner, H., Estey, E.H., Amadori, S., Appelbaum, F.R., Buchner, T., Burnett, A.K., Dombret, H., Fenaux, P., Grimwade, D., Larson, R.A.*, et al.* (2010). Diagnosis and management of acute myeloid leukemia in adults: recommendations from an international expert panel, on behalf of the European LeukemiaNet. Blood *115*, 453-474.
Dohner, H., Weisdorf, D.J., and Bloomfield, C.D. (2015). Acute Myeloid Leukemia. N Engl J Med *373*, 1136-1152.
Dombret, H., Seymour, J.F., Butrym, A., Wierzbowska, A., Selleslag, D., Jang, J.H., Kumar, R., Cavenagh, J., Schuh, A.C., Candoni, A.*, et al.* (2015). International phase

3 study of azacitidine vs conventional care regimens in older patients with newly diagnosed AML with >30% blasts. Blood *126*, 291-299.
Donehower, L.A., Harvey, M., Slagle, B.L., McArthur, M.J., Montgomery, C.A., Jr., Butel, J.S., and Bradley, A. (1992). Mice deficient for p53 are developmentally normal but susceptible to spontaneous tumours. Nature *356*, 215-221.
Donehower, L.A., Harvey, M., Vogel, H., McArthur, M.J., Montgomery, C.A., Jr., Park, S.H., Thompson, T., Ford, R.J., and Bradley, A. (1995). Effects of genetic background on tumorigenesis in p53-deficient mice. Mol Carcinog *14*, 16-22.
Duan, W., Gao, L., Jin, D., Otterson, G.A., and Villalona-Calero, M.A. (2008). Lung specific expression of a human mutant p53 affects cell proliferation in transgenic mice. Transgenic Res *17*, 355-366.
el-Deiry, W.S., Harper, J.W., O'Connor, P.M., Velculescu, V.E., Canman, C.E., Jackman, J., Pietenpol, J.A., Burrell, M., Hill, D.E., Wang, Y.*, et al.* (1994). WAF1/CIP1 is induced in p53-mediated G1 arrest and apoptosis. Cancer Res *54*, 1169-1174.
Eliyahu, D., Raz, A., Gruss, P., Givol, D., and Oren, M. (1984). Participation of p53 cellular tumour antigen in transformation of normal embryonic cells. Nature *312*, 646-649.
Ernst, T., Chase, A.J., Score, J., Hidalgo-Curtis, C.E., Bryant, C., Jones, A.V., Waghorn, K., Zoi, K., Ross, F.M., Reiter, A.*, et al.* (2010). Inactivating mutations of the histone methyltransferase gene EZH2 in myeloid disorders. Nat Genet *42*, 722-726.
Estey, E.H. (2014). Acute myeloid leukemia: 2014 update on risk-stratification and management. Am J Hematol *89*, 1063-1081.
Fellmann, C., Hoffmann, T., Sridhar, V., Hopfgartner, B., Muhar, M., Roth, M., Lai, D.Y., Barbosa, I.A., Kwon, J.S., Guan, Y.*, et al.* (2013). An optimized microRNA backbone for effective single-copy RNAi. Cell Rep *5*, 1704-1713.
Figueroa, M.E., Lugthart, S., Li, Y., Erpelinck-Verschueren, C., Deng, X., Christos, P.J., Schifano, E., Booth, J., van Putten, W., Skrabanek, L.*, et al.* (2010). DNA methylation signatures identify biologically distinct subtypes in acute myeloid leukemia. Cancer Cell *17*, 13-27.
Finlay, C.A., Hinds, P.W., and Levine, A.J. (1989). The p53 proto-oncogene can act as a suppressor of transformation. Cell *57*, 1083-1093.
Freed-Pastor, W.A., Mizuno, H., Zhao, X., Langerod, A., Moon, S.H., Rodriguez-Barrueco, R., Barsotti, A., Chicas, A., Li, W., Polotskaia, A.*, et al.* (2012). Mutant p53 disrupts mammary tissue architecture via the mevalonate pathway. Cell *148*, 244-258.
Freed-Pastor, W.A., and Prives, C. (2012). Mutant p53: one name, many proteins. Genes Dev *26*, 1268-1286.
Gao, J., Aksoy, B.A., Dogrusoz, U., Dresdner, G., Gross, B., Sumer, S.O., Sun, Y., Jacobsen, A., Sinha, R., Larsson, E.*, et al.* (2013). Integrative analysis of complex cancer genomics and clinical profiles using the cBioPortal. Sci Signal *6*, pl1.
Genovese, G., Jaiswal, S., Ebert, B.L., and McCarroll, S.A. (2015). Clonal hematopoiesis and blood-cancer risk. N Engl J Med *372*, 1071-1072.
Giacomelli, A.O., Yang, X., Lintner, R.E., McFarland, J.M., Duby, M., Kim, J., Howard, T.P., Takeda, D.Y., Ly, S.H., Kim, E.*, et al.* (2018). Mutational processes shape the landscape of TP53 mutations in human cancer. Nat Genet.

Goldberg, A.D., Allis, C.D., and Bernstein, E. (2007). Epigenetics: a landscape takes shape. Cell *128*, 635-638.
Gong, Q., Zhou, L., Xu, S., Li, X., Zou, Y., and Chen, J. (2015). High Doses of Daunorubicin during Induction Therapy of Newly Diagnosed Acute Myeloid Leukemia: A Systematic Review and Meta-Analysis of Prospective Clinical Trials. PLoS One *10*, e0125612.
Guglielmelli, P., Biamonte, F., Score, J., Hidalgo-Curtis, C., Cervantes, F., Maffioli, M., Fanelli, T., Ernst, T., Winkelman, N., Jones, A.V.*, et al.* (2011). EZH2 mutational status predicts poor survival in myelofibrosis. Blood *118*, 5227-5234.
Gurdon, J.B. (1973). Nuclear transplantation and regulation of cell processes. Br Med Bull *29*, 259-263.
Hanahan, D., and Weinberg, R.A. (2000). The hallmarks of cancer. Cell *100*, 57-70.
Hanel, W., Marchenko, N., Xu, S., Yu, S.X., Weng, W., and Moll, U. (2013). Two hot spot mutant p53 mouse models display differential gain of function in tumorigenesis. Cell Death Differ *20*, 898-909.
Hemann, M.T., Fridman, J.S., Zilfou, J.T., Hernando, E., Paddison, P.J., Cordon-Cardo, C., Hannon, G.J., and Lowe, S.W. (2003). An epi-allelic series of p53 hypomorphs created by stable RNAi produces distinct tumor phenotypes in vivo. Nat Genet *33*, 396-400.
Hong, H., Takahashi, K., Ichisaka, T., Aoi, T., Kanagawa, O., Nakagawa, M., Okita, K., and Yamanaka, S. (2009). Suppression of induced pluripotent stem cell generation by the p53-p21 pathway. Nature *460*, 1132-1135.
Humpton, T.J., Hock, A.K., Maddocks, O.D.K., and Vousden, K.H. (2018). p53-mediated adaptation to serine starvation is retained by a common tumour-derived mutant. Cancer Metab *6*, 18.
Jain, A.K., Allton, K., Iacovino, M., Mahen, E., Milczarek, R.J., Zwaka, T.P., Kyba, M., and Barton, M.C. (2012). p53 regulates cell cycle and microRNAs to promote differentiation of human embryonic stem cells. PLoS Biol *10*, e1001268.
Jerez, A., Sugimoto, Y., Makishima, H., Verma, A., Jankowska, A.M., Przychodzen, B., Visconte, V., Tiu, R.V., O'Keefe, C.L., Mohamedali, A.M.*, et al.* (2012). Loss of heterozygosity in 7q myeloid disorders: clinical associations and genomic pathogenesis. Blood *119*, 6109-6117.
Joslin, J.M., Fernald, A.A., Tennant, T.R., Davis, E.M., Kogan, S.C., Anastasi, J., Crispino, J.D., and Le Beau, M.M. (2007). Haploinsufficiency of EGR1, a candidate gene in the del(5q), leads to the development of myeloid disorders. Blood *110*, 719-726.
Kandoth, C., McLellan, M.D., Vandin, F., Ye, K., Niu, B., Lu, C., Xie, M., Zhang, Q., McMichael, J.F., Wyczalkowski, M.A.*, et al.* (2013). Mutational landscape and significance across 12 major cancer types. Nature *502*, 333-339.
Kantarjian, H.M., Thomas, X.G., Dmoszynska, A., Wierzbowska, A., Mazur, G., Mayer, J., Gau, J.P., Chou, W.C., Buckstein, R., Cermak, J.*, et al.* (2012). Multicenter, randomized, open-label, phase III trial of decitabine versus patient choice, with physician advice, of either supportive care or low-dose cytarabine for the treatment of older patients with newly diagnosed acute myeloid leukemia. J Clin Oncol *30*, 2670-2677.

Kastan, M.B., Onyekwere, O., Sidransky, D., Vogelstein, B., and Craig, R.W. (1991). Participation of p53 protein in the cellular response to DNA damage. Cancer Res *51*, 6304-6311.
Kastenhuber, E.R., and Lowe, S.W. (2017). Putting p53 in Context. Cell *170*, 1062-1078.
Kawamura, T., Suzuki, J., Wang, Y.V., Menendez, S., Morera, L.B., Raya, A., Wahl, G.M., and Izpisua Belmonte, J.C. (2009). Linking the p53 tumour suppressor pathway to somatic cell reprogramming. Nature *460*, 1140-1144.
Kelly, L.M., and Gilliland, D.G. (2002). Genetics of myeloid leukemias. Annu Rev Genomics Hum Genet *3*, 179-198.
Koifman, G., Shetzer, Y., Eizenberger, S., Solomon, H., Rotkopf, R., Molchadsky, A., Lonetto, G., Goldfinger, N., and Rotter, V. (2018). A Mutant p53-Dependent Embryonic Stem Cell Gene Signature Is Associated with Augmented Tumorigenesis of Stem Cells. Cancer Res *78*, 5833-5847.
Kotler, E., Shani, O., Goldfeld, G., Lotan-Pompan, M., Tarcic, O., Gershoni, A., Hopf, T.A., Marks, D.S., Oren, M., and Segal, E. (2018). A Systematic p53 Mutation Library Links Differential Functional Impact to Cancer Mutation Pattern and Evolutionary Conservation. Mol Cell *71*, 178-190 e178.
Krivtsov, A.V., Twomey, D., Feng, Z., Stubbs, M.C., Wang, Y., Faber, J., Levine, J.E., Wang, J., Hahn, W.C., Gilliland, D.G.*, et al.* (2006). Transformation from committed progenitor to leukaemia stem cell initiated by MLL-AF9. Nature *442*, 818-822.
Kuhn, R., Schwenk, F., Aguet, M., and Rajewsky, K. (1995). Inducible gene targeting in mice. Science *269*, 1427-1429.
Kuo, Y.H., Zaidi, S.K., Gornostaeva, S., Komori, T., Stein, G.S., and Castilla, L.H. (2009). Runx2 induces acute myeloid leukemia in cooperation with Cbfbeta-SMMHC in mice. Blood *113*, 3323-3332.
Lane, D.P., and Crawford, L.V. (1979). T antigen is bound to a host protein in SV40-transformed cells. Nature *278*, 261-263.
Lang, G.A., Iwakuma, T., Suh, Y.A., Liu, G., Rao, V.A., Parant, J.M., Valentin-Vega, Y.A., Terzian, T., Caldwell, L.C., Strong, L.C.*, et al.* (2004). Gain of function of a p53 hot spot mutation in a mouse model of Li-Fraumeni syndrome. Cell *119*, 861-872.
Laptenko, O., and Prives, C. (2006). Transcriptional regulation by p53: one protein, many possibilities. Cell Death Differ *13*, 951-961.
Le Beau, M.M., Espinosa, R., 3rd, Davis, E.M., Eisenbart, J.D., Larson, R.A., and Green, E.D. (1996). Cytogenetic and molecular delineation of a region of chromosome 7 commonly deleted in malignant myeloid diseases. Blood *88*, 1930-1935.
Lee, K.S., Kim, H.J., Li, Q.L., Chi, X.Z., Ueta, C., Komori, T., Wozney, J.M., Kim, E.G., Choi, J.Y., Ryoo, H.M.*, et al.* (2000). Runx2 is a common target of transforming growth factor beta1 and bone morphogenetic protein 2, and cooperation between Runx2 and Smad5 induces osteoblast-specific gene expression in the pluripotent mesenchymal precursor cell line C2C12. Mol Cell Biol *20*, 8783-8792.
Lessard, J., Schumacher, A., Thorsteinsdottir, U., van Lohuizen, M., Magnuson, T., and Sauvageau, G. (1999). Functional antagonism of the Polycomb-Group genes eed and Bmi1 in hemopoietic cell proliferation. Genes Dev *13*, 2691-2703.

Li, X., Xu, S., Tan, Y., and Chen, J. (2015). The effects of idarubicin versus other anthracyclines for induction therapy of patients with newly diagnosed leukaemia. Cochrane Database Syst Rev, CD010432.
Linzer, D.I., and Levine, A.J. (1979). Characterization of a 54K dalton cellular SV40 tumor antigen present in SV40-transformed cells and uninfected embryonal carcinoma cells. Cell *17*, 43-52.
Liu, T.X., Becker, M.W., Jelinek, J., Wu, W.S., Deng, M., Mikhalkevich, N., Hsu, K., Bloomfield, C.D., Stone, R.M., DeAngelo, D.J.*, et al.* (2007). Chromosome 5q deletion and epigenetic suppression of the gene encoding alpha-catenin (CTNNA1) in myeloid cell transformation. Nat Med *13*, 78-83.
Liu, Y., Chen, C., Xu, Z., Scuoppo, C., Rillahan, C.D., Gao, J., Spitzer, B., Bosbach, B., Kastenhuber, E.R., Baslan, T.*, et al.* (2016). Deletions linked to TP53 loss drive cancer through p53-independent mechanisms. Nature *531*, 471-475.
Liu, Y., Elf, S.E., Miyata, Y., Sashida, G., Liu, Y., Huang, G., Di Giandomenico, S., Lee, J.M., Deblasio, A., Menendez, S.*, et al.* (2009). p53 regulates hematopoietic stem cell quiescence. Cell Stem Cell *4*, 37-48.
Loizou, E., Banito, A., Livshits, G., Ho, Y.J., Koche, R.P., Sanchez-Rivera, F.J., Mayle, A., Chen, C.C., Kinalis, S., Bagger, F.O.*, et al.* (2019). A Gain-of-Function p53-Mutant Oncogene Promotes Cell Fate Plasticity and Myeloid Leukemia through the Pluripotency Factor FOXH1. Cancer Discov *9*, 962-979.
Lowe, S.W., Ruley, H.E., Jacks, T., and Housman, D.E. (1993). p53-dependent apoptosis modulates the cytotoxicity of anticancer agents. Cell *74*, 957-967.
Margueron, R., and Reinberg, D. (2011). The Polycomb complex PRC2 and its mark in life. Nature *469*, 343-349.
Marion, R.M., Strati, K., Li, H., Murga, M., Blanco, R., Ortega, S., Fernandez-Capetillo, O., Serrano, M., and Blasco, M.A. (2009). A p53-mediated DNA damage response limits reprogramming to ensure iPS cell genomic integrity. Nature *460*, 1149-1153.
Marzo, I., Brenner, C., Zamzami, N., Jurgensmeier, J.M., Susin, S.A., Vieira, H.L., Prevost, M.C., Xie, Z., Matsuyama, S., Reed, J.C.*, et al.* (1998). Bax and adenine nucleotide translocator cooperate in the mitochondrial control of apoptosis. Science *281*, 2027-2031.
Matsuoka, S., Ebihara, Y., Xu, M., Ishii, T., Sugiyama, D., Yoshino, H., Ueda, T., Manabe, A., Tanaka, R., Ikeda, Y.*, et al.* (2001). CD34 expression on long-term repopulating hematopoietic stem cells changes during developmental stages. Blood *97*, 419-425.
Miro, X., Zhou, X., Boretius, S., Michaelis, T., Kubisch, C., Alvarez-Bolado, G., and Gruss, P. (2009). Haploinsufficiency of the murine polycomb gene Suz12 results in diverse malformations of the brain and neural tube. Dis Model Mech *2*, 412-418.
Mizuno, H., Spike, B.T., Wahl, G.M., and Levine, A.J. (2010). Inactivation of p53 in breast cancers correlates with stem cell transcriptional signatures. Proc Natl Acad Sci U S A *107*, 22745-22750.
Moran-Crusio, K., Reavie, L., Shih, A., Abdel-Wahab, O., Ndiaye-Lobry, D., Lobry, C., Figueroa, M.E., Vasanthakumar, A., Patel, J., Zhao, X.*, et al.* (2011). Tet2 loss leads to increased hematopoietic stem cell self-renewal and myeloid transformation. Cancer Cell *20*, 11-24.

Morita, S., Kojima, T., and Kitamura, T. (2000). Plat-E: an efficient and stable system for transient packaging of retroviruses. Gene Ther *7*, 1063-1066.
Morton, J.P., Timpson, P., Karim, S.A., Ridgway, R.A., Athineos, D., Doyle, B., Jamieson, N.B., Oien, K.A., Lowy, A.M., Brunton, V.G.*, et al.* (2010). Mutant p53 drives metastasis and overcomes growth arrest/senescence in pancreatic cancer. Proc Natl Acad Sci U S A *107*, 246-251.
Mrozek, K. (2008). Cytogenetic, molecular genetic, and clinical characteristics of acute myeloid leukemia with a complex karyotype. Semin Oncol *35*, 365-377.
Muller, P.A., and Vousden, K.H. (2013). p53 mutations in cancer. Nat Cell Biol *15*, 2-8.
Muller, P.A., and Vousden, K.H. (2014). Mutant p53 in cancer: new functions and therapeutic opportunities. Cancer Cell *25*, 304-317.
Nakahata, T., and Ogawa, M. (1982). Identification in culture of a class of hemopoietic colony-forming units with extensive capability to self-renew and generate multipotential hemopoietic colonies. Proc Natl Acad Sci U S A *79*, 3843-3847.
Nikoloski, G., Langemeijer, S.M., Kuiper, R.P., Knops, R., Massop, M., Tonnissen, E.R., van der Heijden, A., Scheele, T.N., Vandenberghe, P., de Witte, T.*, et al.* (2010). Somatic mutations of the histone methyltransferase gene EZH2 in myelodysplastic syndromes. Nat Genet *42*, 665-667.
Nowak, D., Stewart, D., and Koeffler, H.P. (2009). Differentiation therapy of leukemia: 3 decades of development. Blood *113*, 3655-3665.
Ntziachristos, P., Mullenders, J., Trimarchi, T., and Aifantis, I. (2013). Mechanisms of epigenetic regulation of leukemia onset and progression. Adv Immunol *117*, 1-38.
Ogilvy, S., Elefanty, A.G., Visvader, J., Bath, M.L., Harris, A.W., and Adams, J.M. (1998). Transcriptional regulation of vav, a gene expressed throughout the hematopoietic compartment. Blood *91*, 419-430.
Ohashi, S., Natsuizaka, M., Wong, G.S., Michaylira, C.Z., Grugan, K.D., Stairs, D.B., Kalabis, J., Vega, M.E., Kalman, R.A., Nakagawa, M.*, et al.* (2010). Epidermal growth factor receptor and mutant p53 expand an esophageal cellular subpopulation capable of epithelial-to-mesenchymal transition through ZEB transcription factors. Cancer Res *70*, 4174-4184.
Olive, K.P., Tuveson, D.A., Ruhe, Z.C., Yin, B., Willis, N.A., Bronson, R.T., Crowley, D., and Jacks, T. (2004). Mutant p53 gain of function in two mouse models of Li-Fraumeni syndrome. Cell *119*, 847-860.
Olivier, M., Hollstein, M., and Hainaut, P. (2010). TP53 mutations in human cancers: origins, consequences, and clinical use. Cold Spring Harb Perspect Biol *2*, a001008.
Pant, V., Quintas-Cardama, A., and Lozano, G. (2012). The p53 pathway in hematopoiesis: lessons from mouse models, implications for humans. Blood *120*, 5118-5127.
Papaemmanuil, E., Dohner, H., and Campbell, P.J. (2016a). Genomic Classification in Acute Myeloid Leukemia. N Engl J Med *375*, 900-901.

Papaemmanuil, E., Gerstung, M., Bullinger, L., Gaidzik, V.I., Paschka, P., Roberts, N.D., Potter, N.E., Heuser, M., Thol, F., Bolli, N.*, et al.* (2016b). Genomic Classification and Prognosis in Acute Myeloid Leukemia. N Engl J Med *374*, 2209-2221.
Parada, L.F., Land, H., Weinberg, R.A., Wolf, D., and Rotter, V. (1984). Cooperation between gene encoding p53 tumour antigen and ras in cellular transformation. Nature *312*, 649-651.
Passegue, E., Jamieson, C.H., Ailles, L.E., and Weissman, I.L. (2003). Normal and leukemic hematopoiesis: are leukemias a stem cell disorder or a reacquisition of stem cell characteristics? Proc Natl Acad Sci U S A *100 Suppl 1*, 11842-11849.
Patel, J.P., Gonen, M., Figueroa, M.E., Fernandez, H., Sun, Z., Racevskis, J., Van Vlierberghe, P., Dolgalev, I., Thomas, S., Aminova, O.*, et al.* (2012). Prognostic relevance of integrated genetic profiling in acute myeloid leukemia. N Engl J Med *366*, 1079-1089.
Pietras, E.M., Reynaud, D., Kang, Y.A., Carlin, D., Calero-Nieto, F.J., Leavitt, A.D., Stuart, J.M., Gottgens, B., and Passegue, E. (2015). Functionally Distinct Subsets of Lineage-Biased Multipotent Progenitors Control Blood Production in Normal and Regenerative Conditions. Cell Stem Cell *17*, 35-46.
Piunti, A., and Shilatifard, A. (2016). Epigenetic balance of gene expression by Polycomb and COMPASS families. Science *352*, aad9780.
Prives, C., and Hall, P.A. (1999). The p53 pathway. J Pathol *187*, 112-126.
Qian, Z., Joslin, J.M., Tennant, T.R., Reshmi, S.C., Young, D.J., Stoddart, A., Larson, R.A., and Le Beau, M.M. (2010). Cytogenetic and genetic pathways in therapy-related acute myeloid leukemia. Chem Biol Interact *184*, 50-57.
Qin, H., Yu, T., Qing, T., Liu, Y., Zhao, Y., Cai, J., Li, J., Song, Z., Qu, X., Zhou, P.*, et al.* (2007). Regulation of apoptosis and differentiation by p53 in human embryonic stem cells. J Biol Chem *282*, 5842-5852.
Rapin, N., Bagger, F.O., Jendholm, J., Mora-Jensen, H., Krogh, A., Kohlmann, A., Thiede, C., Borregaard, N., Bullinger, L., Winther, O.*, et al.* (2014). Comparing cancer vs normal gene expression profiles identifies new disease entities and common transcriptional programs in AML patients. Blood *123*, 894-904.
Rollig, C., Bornhauser, M., Thiede, C., Taube, F., Kramer, M., Mohr, B., Aulitzky, W., Bodenstein, H., Tischler, H.J., Stuhlmann, R.*, et al.* (2011). Long-term prognosis of acute myeloid leukemia according to the new genetic risk classification of the European LeukemiaNet recommendations: evaluation of the proposed reporting system. J Clin Oncol *29*, 2758-2765.
Rotter, V. (1983). p53, a transformation-related cellular-encoded protein, can be used as a biochemical marker for the detection of primary mouse tumor cells. Proc Natl Acad Sci U S A *80*, 2613-2617.
Rucker, F.G., Bullinger, L., Schwaenen, C., Lipka, D.B., Wessendorf, S., Frohling, S., Bentz, M., Miller, S., Scholl, C., Schlenk, R.F.*, et al.* (2006). Disclosure of candidate genes in acute myeloid leukemia with complex karyotypes using microarray-based molecular characterization. J Clin Oncol *24*, 3887-3894.
Rucker, F.G., Schlenk, R.F., Bullinger, L., Kayser, S., Teleanu, V., Kett, H., Habdank, M., Kugler, C.M., Holzmann, K., Gaidzik, V.I.*, et al.* (2012). TP53 alterations in acute

myeloid leukemia with complex karyotype correlate with specific copy number alterations, monosomal karyotype, and dismal outcome. Blood *119*, 2114-2121.
Sabapathy, K., Klemm, M., Jaenisch, R., and Wagner, E.F. (1997). Regulation of ES cell differentiation by functional and conformational modulation of p53. EMBO J *16*, 6217-6229.
Sarig, R., Rivlin, N., Brosh, R., Bornstein, C., Kamer, I., Ezra, O., Molchadsky, A., Goldfinger, N., Brenner, O., and Rotter, V. (2010). Mutant p53 facilitates somatic cell reprogramming and augments the malignant potential of reprogrammed cells. J Exp Med *207*, 2127-2140.
Sasaki, M., Knobbe, C.B., Munger, J.C., Lind, E.F., Brenner, D., Brustle, A., Harris, I.S., Holmes, R., Wakeham, A., Haight, J.*, et al.* (2012). IDH1(R132H) mutation increases murine haematopoietic progenitors and alters epigenetics. Nature *488*, 656-659.
Sashida, G., Harada, H., Matsui, H., Oshima, M., Yui, M., Harada, Y., Tanaka, S., Mochizuki-Kashio, M., Wang, C., Saraya, A.*, et al.* (2014). Ezh2 loss promotes development of myelodysplastic syndrome but attenuates its predisposition to leukaemic transformation. Nat Commun *5*, 4177.
Schuler, A., Schwieger, M., Engelmann, A., Weber, K., Horn, S., Muller, U., Arnold, M.A., Olson, E.N., and Stocking, C. (2008). The MADS transcription factor Mef2c is a pivotal modulator of myeloid cell fate. Blood *111*, 4532-4541.
Schulz-Heddergott, R., Stark, N., Edmunds, S.J., Li, J., Conradi, L.C., Bohnenberger, H., Ceteci, F., Greten, F.R., Dobbelstein, M., and Moll, U.M. (2018). Therapeutic Ablation of Gain-of-Function Mutant p53 in Colorectal Cancer Inhibits Stat3-Mediated Tumor Growth and Invasion. Cancer Cell *34*, 298-314 e297.
Score, J., Hidalgo-Curtis, C., Jones, A.V., Winkelmann, N., Skinner, A., Ward, D., Zoi, K., Ernst, T., Stegelmann, F., Dohner, K.*, et al.* (2012). Inactivation of polycomb repressive complex 2 components in myeloproliferative and myelodysplastic/myeloproliferative neoplasms. Blood *119*, 1208-1213.
Seita, J., and Weissman, I.L. (2010). Hematopoietic stem cell: self-renewal versus differentiation. Wiley Interdiscip Rev Syst Biol Med *2*, 640-653.
Serrano, M., Lin, A.W., McCurrach, M.E., Beach, D., and Lowe, S.W. (1997). Oncogenic ras provokes premature cell senescence associated with accumulation of p53 and p16INK4a. Cell *88*, 593-602.
Shen, X., Liu, Y., Hsu, Y.J., Fujiwara, Y., Kim, J., Mao, X., Yuan, G.C., and Orkin, S.H. (2008). EZH1 mediates methylation on histone H3 lysine 27 and complements EZH2 in maintaining stem cell identity and executing pluripotency. Mol Cell *32*, 491-502.
Shi, J., Wang, E., Zuber, J., Rappaport, A., Taylor, M., Johns, C., Lowe, S.W., and Vakoc, C.R. (2013). The Polycomb complex PRC2 supports aberrant self-renewal in a mouse model of MLL-AF9;Nras(G12D) acute myeloid leukemia. Oncogene *32*, 930-938.
Shibue, T., and Weinberg, R.A. (2017). EMT, CSCs, and drug resistance: the mechanistic link and clinical implications. Nat Rev Clin Oncol *14*, 611-629.
Shih, A.H., Abdel-Wahab, O., Patel, J.P., and Levine, R.L. (2012). The role of mutations in epigenetic regulators in myeloid malignancies. Nat Rev Cancer *12*, 599-612.

Sneeringer, C.J., Scott, M.P., Kuntz, K.W., Knutson, S.K., Pollock, R.M., Richon, V.M., and Copeland, R.A. (2010). Coordinated activities of wild-type plus mutant EZH2 drive tumor-associated hypertrimethylation of lysine 27 on histone H3 (H3K27) in human B-cell lymphomas. Proc Natl Acad Sci U S A *107*, 20980-20985.
Somervaille, T.C., and Cleary, M.L. (2006). Identification and characterization of leukemia stem cells in murine MLL-AF9 acute myeloid leukemia. Cancer Cell *10*, 257-268.
Spittau, B., and Krieglstein, K. (2012). Klf10 and Klf11 as mediators of TGF-beta superfamily signaling. Cell Tissue Res *347*, 65-72.
Steensma, D.P., Bejar, R., Jaiswal, S., Lindsley, R.C., Sekeres, M.A., Hasserjian, R.P., and Ebert, B.L. (2015). Clonal hematopoiesis of indeterminate potential and its distinction from myelodysplastic syndromes. Blood *126*, 9-16.
Su, I.H., Basavaraj, A., Krutchinsky, A.N., Hobert, O., Ullrich, A., Chait, B.T., and Tarakhovsky, A. (2003). Ezh2 controls B cell development through histone H3 methylation and Igh rearrangement. Nat Immunol *4*, 124-131.
Tadokoro, Y., Ema, H., Okano, M., Li, E., and Nakauchi, H. (2007). De novo DNA methyltransferase is essential for self-renewal, but not for differentiation, in hematopoietic stem cells. J Exp Med *204*, 715-722.
Takahashi, K., Tanabe, K., Ohnuki, M., Narita, M., Sasaki, A., Yamamoto, M., Nakamura, M., Sutou, K., Osafune, K., and Yamanaka, S. (2014). Induction of pluripotency in human somatic cells via a transient state resembling primitive streak-like mesendoderm. Nat Commun *5*, 3678.
Takahashi, K., and Yamanaka, S. (2006). Induction of pluripotent stem cells from mouse embryonic and adult fibroblast cultures by defined factors. Cell *126*, 663-676.
Takahashi, S. (2011). Current findings for recurring mutations in acute myeloid leukemia. J Hematol Oncol *4*, 36.
Tamada, H., Suzuki, Y., and Tamura, G. (1994). [Analysis of loss of heterozygosity (LOH) at the p53 and Rb suppressor genes in urinary bladder carcinoma]. Nihon Hinyokika Gakkai Zasshi *85*, 722-730.
Thein, M.S., Ershler, W.B., Jemal, A., Yates, J.W., and Baer, M.R. (2013). Outcome of older patients with acute myeloid leukemia: an analysis of SEER data over 3 decades. Cancer *119*, 2720-2727.
Tomita, N., Monden, M., Kikkawa, N., Imamura, M., Ohtoshi, M., Ohhashi, S., Sakamoto, T., Tanigawa, N., Nakano, H., Hioki, K.*, et al.* (2004). [Analysis of microsatellite instability and p53 LOH in advanced colorectal cancers--first report of the No. 3 protocol]. Gan To Kagaku Ryoho *31*, 367-372.
Utikal, J., Polo, J.M., Stadtfeld, M., Maherali, N., Kulalert, W., Walsh, R.M., Khalil, A., Rheinwald, J.G., and Hochedlinger, K. (2009). Immortalization eliminates a roadblock during cellular reprogramming into iPS cells. Nature *460*, 1145-1148.
Vire, E., Brenner, C., Deplus, R., Blanchon, L., Fraga, M., Didelot, C., Morey, L., Van Eynde, A., Bernard, D., Vanderwinden, J.M.*, et al.* (2006). The Polycomb group protein EZH2 directly controls DNA methylation. Nature *439*, 871-874.
Visvader, J.E. (2011). Cells of origin in cancer. Nature *469*, 314-322.

Vogelstein, B., Papadopoulos, N., Velculescu, V.E., Zhou, S., Diaz, L.A., Jr., and Kinzler, K.W. (2013). Cancer genome landscapes. Science *339*, 1546-1558.
Wang, T., Yu, H., Hughes, N.W., Liu, B., Kendirli, A., Klein, K., Chen, W.W., Lander, E.S., and Sabatini, D.M. (2017). Gene Essentiality Profiling Reveals Gene Networks and Synthetic Lethal Interactions with Oncogenic Ras. Cell *168*, 890-903 e815.
Weissmueller, S., Manchado, E., Saborowski, M., Morris, J.P.t., Wagenblast, E., Davis, C.A., Moon, S.H., Pfister, N.T., Tschaharganeh, D.F., Kitzing, T.*, et al.* (2014). Mutant p53 drives pancreatic cancer metastasis through cell-autonomous PDGF receptor beta signaling. Cell *157*, 382-394.
Weisz, L., Oren, M., and Rotter, V. (2007). Transcription regulation by mutant p53. Oncogene *26*, 2202-2211.
Willis, A., Jung, E.J., Wakefield, T., and Chen, X. (2004). Mutant p53 exerts a dominant negative effect by preventing wild-type p53 from binding to the promoter of its target genes. Oncogene *23*, 2330-2338.
Wolf, D., Admon, S., Oren, M., and Rotter, V. (1984). Abelson murine leukemia virus-transformed cells that lack p53 protein synthesis express aberrant p53 mRNA species. Mol Cell Biol *4*, 552-558.
Wong, T.N., Ramsingh, G., Young, A.L., Miller, C.A., Touma, W., Welch, J.S., Lamprecht, T.L., Shen, D., Hundal, J., Fulton, R.S.*, et al.* (2015). Role of TP53 mutations in the origin and evolution of therapy-related acute myeloid leukaemia. Nature *518*, 552-555.
Woods, B.A., and Levine, R.L. (2015). The role of mutations in epigenetic regulators in myeloid malignancies. Immunol Rev *263*, 22-35.
Xie, M., Lu, C., Wang, J., McLellan, M.D., Johnson, K.J., Wendl, M.C., McMichael, J.F., Schmidt, H.K., Yellapantula, V., Miller, C.A.*, et al.* (2014). Age-related mutations associated with clonal hematopoietic expansion and malignancies. Nat Med *20*, 1472-1478.
Xu, B., On, D.M., Ma, A., Parton, T., Konze, K.D., Pattenden, S.G., Allison, D.F., Cai, L., Rockowitz, S., Liu, S.*, et al.* (2015). Selective inhibition of EZH2 and EZH1 enzymatic activity by a small molecule suppresses MLL-rearranged leukemia. Blood *125*, 346-357.
Yamamoto, M., Meno, C., Sakai, Y., Shiratori, H., Mochida, K., Ikawa, Y., Saijoh, Y., and Hamada, H. (2001). The transcription factor FoxH1 (FAST) mediates Nodal signaling during anterior-posterior patterning and node formation in the mouse. Genes Dev *15*, 1242-1256.
Yi, L., Lu, C., Hu, W., Sun, Y., and Levine, A.J. (2012). Multiple roles of p53-related pathways in somatic cell reprogramming and stem cell differentiation. Cancer Res *72*, 5635-5645.
Yu, Z., Liu, L., Shu, Q., Li, D., and Wang, R. (2019). Leukemia stem cells promote chemoresistance by inducing downregulation of lumican in mesenchymal stem cells. Oncol Lett *18*, 4317-4327.
Zehir, A., Benayed, R., Shah, R.H., Syed, A., Middha, S., Kim, H.R., Srinivasan, P., Gao, J., Chakravarty, D., Devlin, S.M.*, et al.* (2017). Mutational landscape of metastatic cancer revealed from prospective clinical sequencing of 10,000 patients. Nat Med *23*, 703-713.

Zhang, J., Ding, L., Holmfeldt, L., Wu, G., Heatley, S.L., Payne-Turner, D., Easton, J., Chen, X., Wang, J., Rusch, M.*, et al.* (2012). The genetic basis of early T-cell precursor acute lymphoblastic leukaemia. Nature *481*, 157-163.
Zhao, Z., Chen, C.C., Rillahan, C.D., Shen, R., Kitzing, T., McNerney, M.E., Diaz-Flores, E., Zuber, J., Shannon, K., Le Beau, M.M.*, et al.* (2015). Cooperative loss of RAS feedback regulation drives myeloid leukemogenesis. Nat Genet *47*, 539-543.
Zhao, Z., Zuber, J., Diaz-Flores, E., Lintault, L., Kogan, S.C., Shannon, K., and Lowe, S.W. (2010). p53 loss promotes acute myeloid leukemia by enabling aberrant self-renewal. Genes Dev *24*, 1389-1402.
Zhu, J., Sammons, M.A., Donahue, G., Dou, Z., Vedadi, M., Getlik, M., Barsyte-Lovejoy, D., Al-awar, R., Katona, B.W., Shilatifard, A.*, et al.* (2015). Gain-of-function p53 mutants co-opt chromatin pathways to drive cancer growth. Nature *525*, 206-211.
Zuber, J., McJunkin, K., Fellmann, C., Dow, L.E., Taylor, M.J., Hannon, G.J., and Lowe, S.W. (2011a). Toolkit for evaluating genes required for proliferation and survival using tetracycline-regulated RNAi. Nat Biotechnol *29*, 79-83.
Zuber, J., Radtke, I., Pardee, T.S., Zhao, Z., Rappaport, A.R., Luo, W., McCurrach, M.E., Yang, M.M., Dolan, M.E., Kogan, S.C.*, et al.* (2009). Mouse models of human AML accurately predict chemotherapy response. Genes Dev *23*, 877-889.
Zuber, J., Rappaport, A.R., Luo, W., Wang, E., Chen, C., Vaseva, A.V., Shi, J., Weissmueller, S., Fellmann, C., Taylor, M.J.*, et al.* (2011b). An integrated approach to dissecting oncogene addiction implicates a Myb-coordinated self-renewal program as essential for leukemia maintenance. Genes Dev *25*, 1628-1640.